Structural Basis and Functional Consequences of Alternative ATF2-Jun Heterodimer Orientations at the Interferon-β Enhancer

by

Veronica Elizabeth Burns

A dissertation submitted in partial fulfillment
of the requirements for the degree of
Doctor of Philosophy
(Biological Chemistry)
in The University of Michigan
2011

Doctoral Committee:

Professor Tom K. W. Kerppola, Chair
Professor David Engelke
Professor Ari Gafni
Professor Nils G. Walter
Associate Professor Raymond Trievel

TABLE OF CONTENTS

LIST OF FIGURES

Figure

LIST OF ABBREVIATIONS

AP-1	activating protein 1
ATF2	activating transcription factor 2
ATF2-Jun	heterodimeric transcription factor composed of ATF2 and Jun
AX	Alexa Fluor 568 dye
bp	base pairs
bZIP	basic-region leucine-zipper
bATF2	amino acid residues 322-397 of human ATF2
bJun	amino acid residues 240-315 of human Jun
CBP	CREB-binding protein
cDNA	complementary cDNA
CRE	cAMP response element
DNA	deoxyribonucleic acid
DTT	dithiolthrietol
EDTA	Ethylenediaminetetraacetic acid
6-FAM	6-carboxyfluorescein dye
Fos	c-fos transcription factor
Fos-Jun	heterodimeric transcription factor composed of Fos and Jun
FRET	fluorescence resonance energy transfer
GAPDH	glyceraldehyde-3 phosphatase dehydrogenase

gelFRET	gel-based fluorescence resonance energy transfer assay
GFP	green fluorescent protein
HeLa	immortalized cervical carcinoma cells from Henrietta Lacks
His	hexa histidine(6xHis)-tag
HMGI	high-mobility group I protein
IFNb	oligonucleotide duplex containing the PRDIV-III element
iIRF3	amino acid residues 1-111 of human IRF3
IRF3	interferon regulatory factor 3
IRF7	interferon regulatory factor 7
ITC	isothermal titration calorimetry
Jun	c-Jun transcription factor
LEPREL1	leprecan-like 1 gene
LEPREL1-T1	non-protein-coding transcript transcribed upstream of LEPREL1
mRNA	messenger ribonucleic acid
NFAT	nuclear factor of activated T-cells transcription factor
PAGE	polyacrylamide gel electrophoresis
PBS	phosphate-buffered saline
PCAF	p300/CBP-associated factor
PCR	polymerase chain reaction
PDB	protein data bank
PRD	positive regulatory domain within the interferon-β enhancer
pH	potential hydrogen ion concentration
Pol II	RNA polymerase II

poly(dI-dC)	alternating copolymer of deoxyguanine and deoxycytosine
qRT-PCR	quantitative real-time PCR
RANTES	regulated upon activation, normal T-cell expressed, and secreted
RPL9	60S ribosomal protein L9
SDS	sodium dodecyl sulfate
SNP	single nucleotide polymorphism
SUMO	small ubiquitin-like modifier protein
TCEP	tris(2-carboxyethyl) phosphine
TPA	tissue plasminogen activator
TR	Texas red C_5 bromoacetamide dye
ULP1	ubiquitin-like protein 1
UPA	urokinase-type plasminogen activator
UV	ultraviolet

ABSTRACT

The selective activation of genes is essential for diverse biological processes such as growth, development, and responses to environmental cues. Unlike lower organisms that often use individual proteins to control gene activation, transcription regulation in higher organisms generally requires cooperation among multiple proteins. Cooperation can be achieved via interactions between DNA-binding proteins that bind to adjoining DNA sequences. Such interactions can stabilize DNA binding by these proteins. Many eukaryotic transcription factors form heterodimers that can bind to DNA in two opposite orientations. Because of the asymmetry of such heterodimers, cooperative DNA binding has been predicted, and in some cases observed, to require a specific orientation of heterodimer binding.

Interferon regulatory factor 3 (IRF3) and a heterodimer containing activating transcription factor 2 and c-Jun (ATF2-Jun) bind cooperatively to the human interferon-β enhancer, and opposite orientations of ATF2-Jun binding have been observed using different experimental approaches. High mobility group protein I (HMGI) binds to sequences overlapping the ATF2-Jun-IRF3 site within the interferon-β enhancer and facilitates DNA-binding and synergistic transcriptional activation by components of the enhancer complex, yet its effects on ATF2-Jun-IRF3 complex formation have not been investigated. This thesis presents the identification of the structural determinants of ATF2-Jun heterodimer orientation at the interferon-β enhancer *in vitro* as well as

functional characterization in cells. Using gel-based fluorescence resonance energy transfer analysis, I found that ATF2-Jun binds to the interferon-β enhancer in both orientations alone and in association with IRF3 and HMGI. Two symmetry-related sets of amino acid residues in ATF2 and Jun facilitated the opposite orientations of heterodimer interactions with IRF3 at the interferon-β enhancer. Expression of ATF2 and Jun variants that bound the interferon-β enhancer in opposite orientations together with IRF3 produced distinct levels of interferon-β transcription in Sendai-virus infected Hela cells. Expression of these proteins resulted in different relative levels of transcription of different genes regulated by ATF2 and Jun. Collectively, this work illustrates a novel mode of cooperative DNA-binding by transcription factors and suggests that alternative nucleoprotein arrangements can influence transcriptional activity through distinct mechanisms at different genes.

CHAPTER 1: INTRODUCTION

I. LITERATURE BACKGROUND

I.A. Cooperative DNA-binding by adjacent transcription factors

The regulation of gene activation is essential for diverse biological processes such as growth, development, and responses to environmental cues. One of the central problems in understanding the regulation of gene activation is to explain how specific genes are selected for activation. In lower organisms, the specification of gene activation is largely dependent on sequence-specific transcription factors which bind to gene-specific DNA sequences in response to environmental cues. Despite the enormous expansion of genome size during evolution, however, the sequence-specificity of transcription factors has not increased on average (4, 46). In higher organisms, multiple transcription factors must cooperate to specify gene activation.

There are numerous mechanisms whereby transcription factors can cooperate. Transcription factors that bind adjacent sites can interact with each other in order to increase the specificity of DNA binding. This cooperative specification of DNA-binding can involve either direct or indirect interactions between transcription factors. Direct interactions, such as those between dimerizing transcription factors, can be obligatory for DNA binding. Autonomous DNA-binding factors can also engage in interactions, such

as those required for cooperative ternary complex formation. In all cases, interactions between adjacent transcription factors appear to be largely dependent on the spatial relationship between their cognate DNA recognition elements, allowing variations in the regulatory sequences of different genes to specify a particular transcription factor complex with distinct physical and functional attributes. Although these facets of transcription factor cooperativity are certainly not the only ones governing the specificity of eukaryotic gene regulation, they represent an important aspect of how multiple transcription factor can come together to exert diverse functional effects.

I.A.i. Pair-wise interactions

The formation of large families of dimerizing transcription factors is one way in which a wide variety of DNA motifs can be recognized in higher organisms. Members of these families can interact directly or indirectly with related or unrelated proteins in order to create homo- and heterodimeric complexes with unique DNA-binding specificities. Direct interactions often involve so-called "coiled-coil" interactions which mediate the coiling of one alpha helix around another. Proteins which ulitize this interaction interface typically cannot otherwise bind to DNA as monomers. Dimerizing interactions between transcription factors can involve many other types of interfaces as well, including other types of direct protein-protein interactions as well as mutually favorable distortions in the DNA structure. These interactions give rise to complexes that recognize a larger repertoire of DNA sequences and regulatory proteins. Pair-wise interactions among transcription factors are therefore a simple mechanism of increasing the specificity of DNA recognition by a limited group of proteins.

I.A.i.a. Direct dimerization interactions

The nuclear receptor superfamily of transcription factors illustrates the regulatory power of dimerization interactions among a related group of proteins. Nuclear receptors bind to hormone response elements composed of two hexad repeats. The individual hexamers can exist in different relative orientations with variable spacing between them, creating different types of hormone response element motifs (93). One member of the nuclear receptor family, the retinoid X receptor, can dimerize with many other members of the nuclear receptor family to form different heterodimers which preferentially interact with direct hexad repeats spaced by a different number of nucleotides (39, 44, 85, 96) [Fig. 1.1]. A change in one nucleotide in the spacer region requires the heterodimerization partner to be rotated by approximately 36° around relative to the retinoid X receptor and translated by 3.4 Å along the double helix in order for dimerization and binding to occur (39, 44, 85, 94, 96). Thus, the recognition of different hormone response element variants by different nuclear receptor heterodimers exemplifies how transcription factor dimerization can contribute to the increased specificity of DNA recognition in higher organisms.

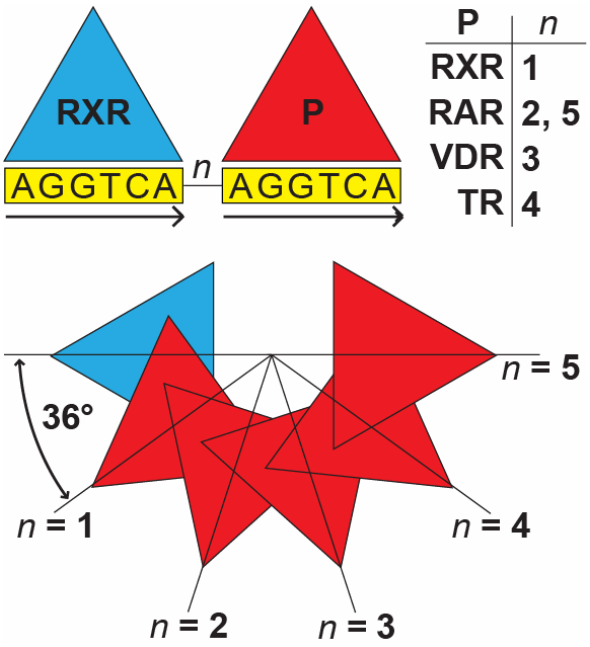

Fig. 1.1. Binding of nuclear hormone receptor heterodimers to hormone response elements. The retinoid X receptor (RXR, blue) dimerizes with itself, retinoic acid receptor (RAR), vitamin D receptor (VDR), and thyroid hormone receptor (TR) at hormone response elements (5'-AGGTCA-3', yellow) spaced by a variable number of nucleotides (n). A change in one nucleotide in the spacer region requires the heterodimerization partner (red) to be rotated by approximately 36° around relative to the retinoid X receptor and translated by 3.4 Å along the double helix in order for dimerization and binding to occur Retinoid X receptor and its partner, therefore, requires a succession of interaction surfaces or contortions in order for recognition of hexad repeats spaced by a progressively greater number of nucleotides.

Rules that determine transcription factor pairing in other heterodimeric complexes, however, are more complex. Sox proteins are known to interact with various POU proteins, and their genes are involved in the determination of cell fate (5, 53). The highly conserved DNA-binding region of Sox proteins have a limited ability to bind to specific target sites, and heterodimerization with POU proteins provides a potential basis for how they can distinguish their targets. Heterodimers formed by the Sox-2 and the POU family protein Oct-4 can interact at two distinct recognition elements, FGF4 and UTF1, with different degrees of cooperativity. The FGF4 enhancer contains a three base-pair spacer between the POU- and Sox-binding sites, whereas the UTF1 enhancer contains no spacer.

Comparison of the structures of Oct-4-Sox-2-FGF4 complex with an Oct1-Sox-2-UTF1 complex has revealed the distinct modes of POU-Sox interaction. In particular, the different protein-protein interaction interfaces are formed by different Sox surfaces which interact with the same surface of Oct proteins (89, 103). These divergent cooperative DNA-binding mechanisms have been proposed to allow different subsets of genes to respond differentially to the cellular levels of Oct-4 and Sox-2. Thus, distinct modes of POU-Sox dimerization can contribute to the selective regulation of different genes by the same transcription factor complex.

I.A.i.b. Indirect interactions

The formation of transcription factor dimers can require interactions in addition to direct protein-protein contacts. Heterodimers composed of the hematopoietic-specific Ets family transcription factor PU.1 and the lymphoid-restricted transcription factor interferon regulatory factor 4 (IRF4) bind to the enhancers of several light chain genes in B cells (29, 79). Whereas PU.1 potentiates the binding of IRF4 or the related protein, IRF8, to DNA, it exhibits an anti-cooperative interaction with IRF1 and IRF2 (31). A significant part of the cooperativity between PU.1 and IRF4 is mediated by the DNA-binding domains. Electrophoretic mobility shift assay and quantitative hydroxyl radical footprinting studies have shown that the binding affinity of the IRF4 DNA binding domain increases between 5- and 40-fold in the presence of the PU.1 DNA-binding domain (31, 42, 104). The structure of the DNA binding domains of PU.1 and IRF4 on a composite DNA element revealed that DNA-bending by PU.1 and IRF4 contribute to PU.1-IRF4 cooperativity such that the binding of one transcription factor will aid the binding of the other by helping to configure the DNA around it (31). Furthermore, this

configuration positions PU.1 and IRF4 for interactions involving amino acids specific to IRF4 and IRF8 (31). Together, protein-protein and indirect DNA-bending interactions contribute to the basis of selective cooperativity between PU.1 and IRF transcription factors.

I.A.ii. Ternary complex formation

Higher-order complexes formed by adjacent DNA-binding proteins can further increase the selectivity of transcription factor-dependent transcription regulation. A handful of crystal structures of multiprotein transcription factor complexes at composite regulatory elements have been solved including the MAT-α-MCM, SAP-1-SRF, and Fos-Jun-NFAT complexes (15, 45, 70, 98). Several features common to these complexes may also apply to other higher-order complexes and can explain cooperative DNA binding by transcription factors at composite regulatory elements. The interactions between cooperating DNA-binding proteins frequently involve regions in a close proximity to DNA. Thus, the DNA binding domains alone can be sufficient for cooperative complex formation at composite regulatory elements. Transcription factor binding to adjacent sites can create an uninterrupted protein-DNA interface extending across both recognition elements, thereby increasing the specificity and affinity of DNA binding. The DNA and protein conformations are often altered to form the protein-protein and protein-DNA interaction interfaces. These conformational rearrangements may contribute to the selectivity of multiprotein complex formation.

Multiprotein transcription factor complexes at composite recognition elements can have a significant role in human disease states. The formation of fusion proteins composed of the amino terminus of EWS (Ewing's sarcoma) protein attached to the

DNA-binding and carboxy-terminal region of Ets family proteins correlate with the unchecked control of gene expression during Ewing's sarcoma (67). Some EWS-Ets target genes, such as uridine phosphorylase, contain adjacent binding sites for Ets and AP-1 proteins. It has been shown that Ets family proteins that participate in Ewing's sarcoma, including Fli1, ERG, and ETV1, cooperatively bind these tandem elements with Fos-Jun while other Ets family members do not (56). Analysis of cooperativity between Fos-Jun and EWS-Fli1 fusion proteins *in vitro* showed that the DNA-binding domains of Fos and Jun and Fli1 are important for cooperative DNA binding (56). Whereas EWS-Fli1 activates the expression of UPP mRNA, is directly bound to the UPP promoter, and transforms 3T3 fibroblasts, a truncated form of EWS-Fli1 that cannot cooperatively bind DNA with Fos-Jun is defective in all of these properties (56). Thus, the ability of EWS-Ets proteins to cooperatively bind DNA with Fos-Jun mediates to the functional activities of these proteins and potentially the pathogenesis of Ewing's sarcoma.

I.B. Enhanceosomes

Interactions among adjacent transcription factors which are required for cooperative DNA-binding tend to require a specific arrangement of transcription factors at enhancer sequences. This arrangement may serve a purpose beyond merely permitting interactions among the transcription factors themselves. Specifically, the stereo-specific arrangement of transcription factors at enhancers is thought to act as a "docking" surface for co-activator proteins that can modify chromatin or recruit of general transcription machinery to the promoter. These higher-order nucleoprotein structures have been referred to as "enhanceosomes." Whereas some enhancer sequences specify a compact

and precise organization of transcription factors characteristic of the classical enhanceosome, others have been proposed to include an extended arrangement with a variable group of proteins.

Enhanceosomes that embody both of these models have been identified and characterized. The interferon-β and T-cell receptor-α enhanceosomes, for example, activates transcription only in response to stimuli that activate a specific group of transcription factors which must be organized in a specific arrangement at the enhancer (6, 21, 58, 68). Architectural proteins high mobility group I (HMGI) and lymphoid enhancer-binding factor 1 (LEF-1) influence the assembly of transcription factors at the interferon-β and T-cell receptor-α enhanceosome, respectively (9, 21, 58, 106). In contrast, the tumor necrosis factor-α enhanceosome can activate transcription in response to multiple signals through different sets of transcription factors which bind to the enhancer in different arrangements in response to different signals (33, 101, 102). However, inducer-specific enhanceosomes that are formed have different helical phasing requirements, indicating that the three-dimensional structure of these enhanceosomes is distinct (7, 102). Therefore, flexible enhanceosome arrangements do not necessarily obviate a role for nucleoprotein architecture in cooperative interactions with co-activator proteins and general transcription machinery.

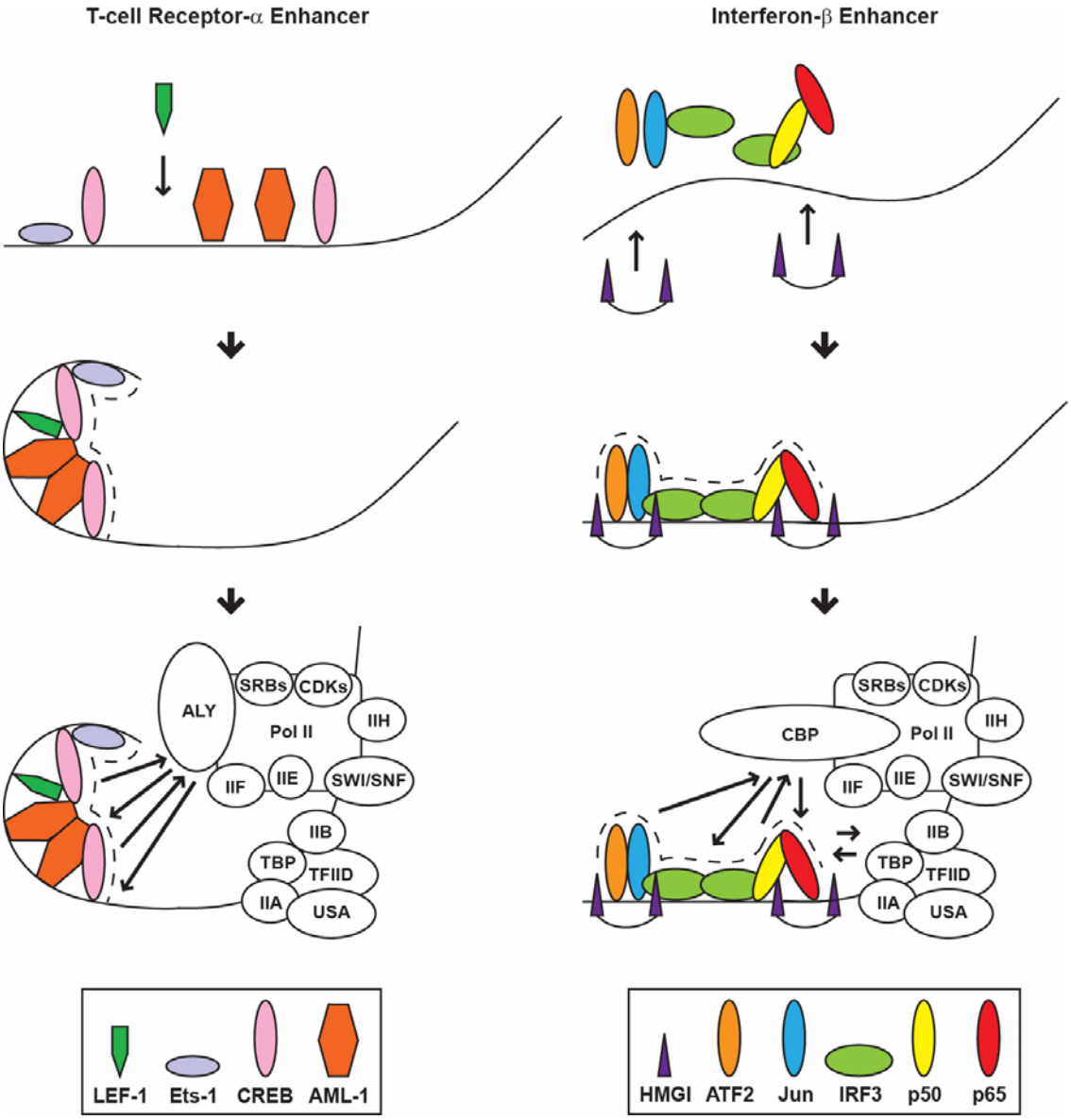

Fig. 1.2. Comparison of the formation of enhanceosome complexes at the T-cell receptor-α versus interferon-β enhancers. *Left panel:* The binding of the architectural protein LEF-1 to the T-cell receptor-α enhancer results in a 120° bend that is required for the assembly of an enhanceosome structure. The specific three-dimensional surface of the enhanceosome (dotted line) is required for efficient recruitment of the co-activator protein ALY along with the RNA Pol II holoenzyme. *Right panel:* The binding of the architectural protein HMGI to the interferon-β enhancer reduces an intrinsic 20° bend that is required for the assembly of an enhanceosome structure. The specific three-dimensional surface of the enhanceosome (dotted line) is required for efficient recruitment of the co-activator protein CBP along with RNA Pol II as well as reciprocal cooperative-DNA binding interactions with a sub-complex composed of TFIIA (IIA), TFIIB (IIB), TFIID (IID), TATA-binding protein (TBP), and the USA co-activator.

I.B.i. Role of architectural proteins

Although many of the sequence-specific transcription factors comprising the enhanceosome are traditional activator proteins, DNA-bending or "architectural" proteins can also contribute to transcriptional activation by facilitating interactions between activator proteins that bind to separate recognition elements (9, 87, 95). The interferon-β and the T-cell receptor-α enhanceosomes employ architectural proteins HMGI and LEF-1, respectively, to mediate cooperative binding of activators. HMGI and LEF-1 are sequence-specific DNA-bending proteins from two distinct classes of chromatin-associated high mobility group (HMG) proteins. Unlike LEF-1, which contains an activation domain, HMGI does not participate directly in stimulation but does facilitate cooperative assembly of the enhanceosome (58).

HMGI protein contains three repeated basic DNA-binding domains separated by short linkers. At least two of the domains simultaneously interact with the minor groove of different AT-rich sequences in the enhancer (105). The current idea is that the HMGI reverses a mild, yet inhibitory, 20° DNA bend toward the minor groove and facilitating the binding of transcription factors with an intrinsic preference for un-bent DNA (35, 55, 106). LEF-1 contains a conserved HMG domain, also found in the ubiquitous HMG-1 and -2 proteins, which binds in the minor groove and intercalates a hydrophobic amino acid between adjacent base pairs in the site (87). The HMG domain bends and untwists the DNA, molding the minor groove to fit the contour of the protein (38, 65). The resulting 120° bend permits cooperative interactions between other transcription factors at the T-cell receptor-α enhancer (37).

Specific regions of HMGI can undergo conformational changes upon interactions with proteins and DNA (88). This flexibility permits HMGI to participate in diverse biological processes ranging from transcription regulation to DNA recombination (19, 86, 88). In addition, phosphorylation and acetylation can modulate interactions involving HMGI (19). For example, in the context of the interferon-β enhanceosome, lysine acetylation of HMGI by the co-activator PCAF enhances the affinity of HMGI for other transcription factors and induces enhanceosome assembly (71). By contrast, acetylation by CBP on a distinct lysine residue results in detachment of the protein from the DNA leading to enhanceosome disruption and subsequent termination of interferon-β transcription (71, 72). These observations suggest that architectural proteins can function as the sensitive molecular switch required for both enhanceosome assembly and disassembly. Examination of the roles played by LEF-1 and HMGI in different enhanceosomes will determine whether their functions can be generalized or are context specific.

I.B.ii. Cooperative interactions with general factors

In addition to cooperative DNA-binding interactions among transcription factors, enhanceosomes utilize additional mechanisms of cooperativity to enrich the specificity of transcriptional activation. Numerous studies have revealed interactions between enhancer-bound transcription factors and the general factors (1, 7, 12, 57, 62, 63, 68, 107). In certain contexts, cooperative DNA-binding among these complexes facilitates the recruitment of general factors to specific genes, which also further stabilizes the enhanceosome itself (7, 57). The concerted association of multiple transcription factors with either co-activators or general factors has been proposed to underlie additional

mechanisms enhanceosome cooperativity, directly facilitating the recruitment of chromatin-modifying proteins and RNA polymerase II to nearby promoters. A specific activation surface has been proposed to mediate the cooperative recruitment of co-activator complexes by enhanceosomes (7, 10, 12, 58, 68, 102), although applicability of these architectural requirements to endogenous enhanceosomes for these and other genes remains to be determined.

I.B.ii.a. Reciprocal DNA-binding interactions

A model in which the enhanceosome engages in multiple, specific contacts with the general machinery predicts that those interactions will reciprocally stabilize the assembly of the enhanceosome. In vitro transcription experiments by Kim and Maniatis have demonstrated that, when the interferon-β enhanceosome was pre-incubated with TFIIA, TFIIB, TFIID, and the USA co-activators, a transcription complex resistant to the detergent sarkosyl as well as competitor oligonucleotides was formed (57). The TFIIE, TFIIF, TFIIH, and Pol II fractions, which apparently contain CBP, further increase the stability (57). A more direct reciprocal effect was observed with the co-activator ALY, which dramatically enhanced cooperative binding of LEF-1 and AML-1 to the T-cell receptor-α enhancer in DNase I footprinting experiments (12). Other studies have shown that the magnitude of the reciprocity is dependent upon the strengths of the activator–target interactions (99). This effect has been proposed to provide the additional specificity and energy necessary to drive the concerted formation of the final pre-initiation complex in the face of the large energetic obstacle posed by chromatin (59).

I.B.ii.b. Stereo-specific interactions

Transcription factors need not bind cooperatively to DNA in order to synergistically activate transcription. Experiments from the Maniatis lab using mammalian nuclear extracts depleted of endogenous interferon-β enhancer-binding proteins and supplemented with recombinant proteins have shown that the absence or repositioning of individual transcription factor binding sites within the interferon-β enhancer abolished cooperative activation of reporter gene plasmids even when the proteins were present at saturating concentrations (58). This type of cooperativity among multiple transcription factors has been portrayed as a specific activation surface that is chemically and spatially complementary to surfaces on co-activator and the general transcription machinery [Fig 1.2].

This model has been supported by other studies from the Maniatis lab which revealed that the activating surface of the interferon-beta enhanceosome displays a high specificity for the co-activator CBP (68). Removal of the individual transcription factor activation domains, replacement of activation domains with VP16, or altered helical phasing of the binding sites, abolished cooperative CBP-dependent transcriptional activation in vivo and the efficient assembly to the enhanceosome *in vitro* (68). Deletion analysis suggested that the p65 subunit of NF-kB contains specific domains which mediate interactions with either CBP or general transcription factors (33, 68). Studies have also shown a requirement for CBP in tumor necrosis factor-α transcription in the context of chromatin (33). A different co-activator called ALY interacts specifically with the combination of LEF-1 and AML-1 at the T-cell receptor-α enhancer (12). Taken together, these data suggest that specific identities and arrangements of transcription

factors can cooperatively increase the affinity of co-activators and general machinery for the enhanceosome through direct interactions.

Studies with other systems have also suggested that interactions between transcription factors and the general machinery can lead to cooperative activation of transcription. Multiple molecules of the Ebstein-Barr virus-specific transcription factor ZEBRA activate reporter gene transcription in a greater-than-additive fashion. ZEBRA-dependent activation, however, is highest with only two or three upstream binding sites, suggesting that recruitment of a limited set of auxillary regulatory proteins is sufficient for the effect (13). In contrast, Fos-Jun heterodimers fused to one or two GCN4 activation domains have been shown to activate reporter gene transcription equally well at sequences containing two tandem AP-1 sites (75), suggesting that the DNA-binding domains rather than the acidic activation regions are the principal determinant of transcriptional synergy.

The notion that contacting a limited repertoire of targets is sufficient for activation has derived support mainly from studies in yeast. The tethering of the DNA-binding protein LexA to any one of several different components of the general machinery (TBP, TFIIB, TAFs, or GAL11) was shown to be sufficient for transcriptional activation (80). These data imply that individual general factors, when recruited to a promoter, have the capacity to nucleate assembly of a functional transcription complex. Therefore, although the total mass of the complex in mammalian cells has been estimated to exceed 2.5 MDa and contain dozens of polypeptides, transcription factors may only interact with only a small portion of the overall surface, or a few targets within it, to stimulate transcription. However, unlike the case of LexA-co-activator fusions in yeast, the tethering of other co-

activators such as CBP or ALY to DNA-binding proteins does not bypass the function of transcription factors (12, 68). Therefore, the concept of "stereo-specificity" in transcription factor interactions with co-activators and the general transcription machinery requires further investigation.

I.B.iii. Context-dependent dynamics

The arrival and departure of various regulatory factors often occur at enhanceosomes during transcriptional activation, suggesting some form of dynamics. The T-cell receptor-α enhanceosome assembles early in T-cell differentiation but remains inactive until T-cells enter the double-positive stage (50). This suggests that the activity of the T-cell receptor-α enhanceosome is dynamically modulated by the recruitment of at least one stage-specific factor. Similarly, in B-cells, although RFX, NF-Y, and X2B transcription factors cooperatively bind MHC class II genes in a constitutive manner, activation occurs only when the class II transactivator protein is recruited to the preformed enhanceosome via a mechanism that is largely unknown (52, 66). At the interferon-β enhancer, key transcription factors have been found to associate sequentially rather than simultaneously after Sendai virus infection (1, 71). Comparisons of the biochemical details of enhanceosome formation in different contexts are required to reveal how enhanceosomes can be "adjusted" to accommodate alternate regulatory scenarios.

II. bZIP PROTEINS IN TRANSCRIPTIONAL ACTIVATION

Transcription regulation is thought to involve a myriad of nucleoprotein complexes in which the individual components play different roles in assembly and function of complexes at different genes. The basic region leucine zipper (bZIP) family of transcription factors functions in the assembly of these complexes. The bZIP family includes more than 70 proteins in humans that can cross-dimerize to potentially form hundreds of homo- and heterodimers expressed in a variety of cell types. The diversity of bZIP complex formation allows cells to respond to many different extra-cellular signals during a wide range of physiological and pathological processes.

The bZIP family has been subdivided into classes of proteins based on DNA-binding specificity or heterodimerization properties. Ternary complexes of bZIP homo- or heterodimers with other transcription factors allow responses to a variety of signals to which bZIP proteins alone do not respond. bZIP complexes can also exert their effects by binding components of the transcription machinery, including subunits of the TFIID and mediator complexes as well as by recruiting chromatin modifying complexes. Therefore, numerous mechanisms whereby bZIP family proteins influence transcriptional regulatory specificity likely exist.

II.A. Dimerization and DNA binding

bZIP proteins take their name from a highly conserved basic region required for DNA binding and a heptad repeat of leucine residues, the leucine zipper, required for dimerization (3, 60, 73). Since members of different bZIP protein subfamilies exhibit distinct DNA binding specificities, dimerization between different bZIP protein

subfamilies expands the repertoire of binding sites for bZIP family proteins to include sequences composed of different half-sites (43). Dimerization between different bZIP proteins at the same DNA sequence can further increases regulatory specificity by exerting different effects on transcriptional activation (20, 24).

Formation of homo- and heterodimeric bZIP complexes through the leucine zipper symmetrically juxtaposes the two basic regions to form a DNA-contact interface in which the dimer subunits interact in opposite relative directions with the major grooves of adjoining half-sites (40). Consequently, the DNA recognition sites for bZIP family proteins are all perfect or near-perfect palindromes. Six major categories of DNA-binding sites exist for bZIP proteins. In metazoans, these include the TPA responsive element (AP-1), cAMP responsive element (CRE), CAAT box, AF recognition element, CRE-like, and PAR binding sites (23). The bZIP family has been subdivided into classes of proteins based on their DNA-binding specificities and heterodimerization properties. Examples of such bZIP subfamilies include Fos/Jun, ATF/CREB, C/EBP, CNC, Maf, and Yap proteins (23).

The Fos/Jun/CREB/ATF families of bZIP proteins recognize a seven base-pair AP-1 site (5'-TGA(C/G)TCA-3') and an eight base-pair CRE site (TGACGTCA). Although mutational analysis of the basic regions of Fos and Jun have shown that corresponding mutations in the two basic regions have similar effects on DNA binding (84), contacts made with asymmetric base pair substitutions in the AP-1 site are not always identical between Fos and Jun (40). Even at recognition elements with symmetrical half-sites, UV-light crosslinking studies have suggested that there are some differences in the interaction of Fos and Jun with the left and right halves of the AP-1 site

(48, 90). Finally, binding-interference studies using base methylation and phosphate ethylation, as well as Fe^{2+}-methidiumpropyl -EDTA protection studies, have shown that, though there is an overall symmetry in the interference patterns, there are local differences that indicate that the individual contacts made at the two half sites are not identical even for homodimeric complexes (74). Thus, while the global structure of the dimeric DNA-binding complex is relatively symmetric, there are local variations in structure between the two halves of the recognition complexes.

The X-ray crystal structure of the Fos-Jun-AP-1 complex revealed that Fos-Jun heterodimers can bind the AP-1 site in two opposite orientations that are related by an approximately 180° rotation about the dimer axis [Fig. 1.3]. However, since not all Fos and Jun DNA-contacts are identical as described above, preferences for one orientation over the other can result from asymmetrical base substitutions within the core or flanking DNA recognition sequences (83). Consequently, Fos–Jun heterodimers bind to different AP-1 sites with different orientation preferences.

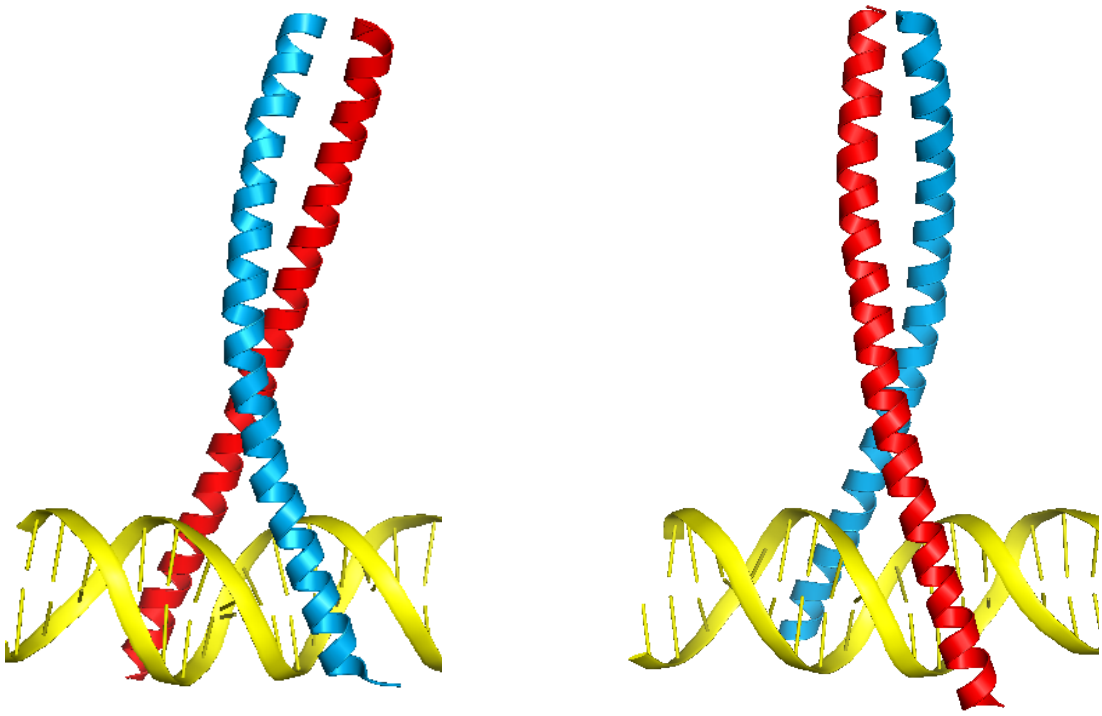

Fig. 1.3. Co-crystalization of Fos-Jun heterodimers bound to the canonical AP-1 recognition site in opposite orientations. Both Fos and Jun contact DNA, and the major DNA-contact sites are located within the major grooves of both halves of the recognition site. The amino-terminal ends of the basic regions of Fos and Jun are located in the major grooves approximately five base pairs from the center of the binding site. Upon binding to DNA, the previously unfolded basic regions become a-helical such that five conserved amino acid residues are positioned to contact specific base pairs in the target sites. The figure was created using the PyMOL Molecular Graphics System (22) and coordinates form the RCSB Protein Data Bank [www.pdb.org (8), PDB ID: 1FOS] in agreement with the published structure (40).

II.B. Interactions with other proteins

The selectivity of bZIP associations with unrelated proteins provides an additional mechanism for the specificity of transcriptional responses by bZIP proteins beyond that achieved by the heterodimerization properties of bZIP factors. Ternary complexes of the bZIP homo- and heterodimers with other transcription factors allow the transcriptional activation function of bZIP proteins to be used in response to a variety of signals to which bZIP proteins alone does not respond. The x-ray crystal structures of ternary complexes composed of the Fos-Jun heterodimer and nuclear factor of activated T-cells 1 (NFAT1)

at the interleukin-2 enhancer as well as the ATF2-Jun heterodimer and interferon regulator factor 3 (IRF3) at the interferon-β enhancer has been solved (15, 77). For other proteins, such general transcription factors, co-activators, histones, or transcription factors belonging to the Smad, Stat, bHLH, EWS, and nuclear hormone receptor families interactions with bZIP proteins have been reported (2, 17, 47, 54, 56, 64, 69, 81) but remain largely undefined at the structural level.

The co-activator paralogues p300 and CBP contain acetyltransferase domains (HAT) and catalyze the lysine acetylation of histones and other proteins as an important aspect of their functions. Prior studies revealed that ATF2 can interact with the CBP HAT domain (91). Examination of interaction between the bZIP domain of ATF2 with the HAT domain of p300 has shown that p300 HAT auto-acetylation can enhance the binding affinity (54). Pull-down assays revealed that hyper-acetylated p300 HAT is more efficiently retained by immobilized ATF2 bZIP domains than hypo-acetylated p300 HAT (54). Loop deleted p300 HAT lacking auto-acetylation was retained about as well as hyper-acetylated p300 HAT, suggesting that the loop and ATF2 compete for p300 HAT binding (54). While ATF-2 b-ZIP is a weak inhibitor of hypo-acetylated p300 HAT acetylation of a histone H4 peptide, hyper-acetylated p300 HAT is much more potently inhibited by the bZIP domain of ATF2 (54).

It has also been shown that the bZIP domain of ATF2 could serve as an acetylation substrate for p300. Using mass spectrometry, two p300 HAT lysine acetylation sites were mapped in ATF2 bZIP. Immunoprecipitation-Western blot analysis with anti-acetyl-lysine antibody revealed that ATF2 can undergo reversible acetylation *in vivo* (54). Mutational analysis of the two ATF2 bZIP acetylation sites revealed their

potential contributions to ATF2-mediated transcriptional activation (54). Taken together, these studies suggest multiple roles for protein acetylation in the regulation of transcription by p300/CBP and ATF2.

The transcriptional activation of CHOP (a CCAAT/ enhancer-binding protein-related gene) by amino acid deprivation involves ATF2 and ATF4 binding to the amino acid response element (AARE) within the promoter. Using a chromatin immunoprecipitation approach, it was reported that *in vivo* binding of phospho-ATF2 and ATF4 to CHOP AARE correlates with acetylation of histones H4 and H2B in response to amino acid starvation (11). A time course analysis reveals that ATF2 phosphorylation precedes histone acetylation, ATF4 binding and the increase in CHOP mRNA (11). It was also shown that ATF4 binding and histone acetylation are two independent events that are required for the CHOP induction upon amino acid starvation (11). Using ATF2-deficient mouse embryonic fibroblasts, it was demonstrated that ATF2 is essential in the acetylation of histone H4 and H2B at the endogenous CHOP locus (11). The role of ATF2 on histone H4 acetylation is dependent on its binding to the AARE and can be extended to other amino acid regulated genes (11). Thus, bZIP proteins can promote the modification of the chromatin structure to enhance transcriptional activation.

bZIP transcription factors can also interact with histone proteins during the maintenance of repressive chromatin states. Transcriptional activation of the interleukin-8 gene is restricted to specific cell types, although the transcriptional regulatory proteins controlling interleukin-8 gene expression are ubiquitous. In expressing epithelial cells the enhancer/promoter is nucleosome-free, whereas in non-expressing B-cells, a nucleosome containing the histone variant macroH2A is formed at the interleukin-8

regulatory region. Recruitment of the repressive macroH2A nucleosome requires direct interactions between ATF2 bound to the nearby AP1 site and macroH2A, and treatment with siRNA against ATF2 or macroH2A rescues IL-8 transcription in B cells (2). Substitution of the interleukin-8 enhancer ATF2 binding site with the IFN-b enhancer ATF2 binding site (PRDIV) abolishes macroH2A recruitment to the interleukin-8 enhancer and results in reporter gene activation in B-cells, whereas replacement of PRDIV with the interleukin-8 enhancer ATF2 binding site recruits macroH2A to the IFN-b enhancer and abolishes reporter gene activation in B-cells (2). Thus, interactions between ATF2 and different recognition sites can have differential effects on local chromatin architecture that may depend on conformational-specific interactions with histone variants.

I.C. Consequences of oriented heterodimer binding

Since interactions between bZIP proteins and other proteins often require a particular spatial arrangement of proteins on DNA, the relative positions of bZIP proteins and other proteins at individual regulatory regions can, in turn, influence their interactions. Differences in the conformation and positioning of DNA-bound bZIP proteins can be caused by differences in the sequence of the DNA recognition site. Asymmetric base substitutions in AP-1 sites which have opposite effects on the orientation of DNA-binding by Fos-Jun heterodimers have a potent effect on cooperative complex formation with NFAT1 and the efficiency of reporter gene activation (83). In this way, the efficiency of transcriptional activation by Fos-Jun-NFAT complexes can be modulated in a gene-specific manner.

The Fos-Jun-NFAT1 ternary complex bound to the ARRE2 site in the interleukin-2 enhancer contacts a 15 base pair recognition element in which all the base pairs are contacted by either Fos-Jun or NFAT1 (15). The cooperative interaction between Fos-Jun and NFAT1 induces a DNA bend of approximately 20° toward the interaction interface (15, 25), which is required to bring NFAT1 and Fos-Jun together. Both Fos-Jun and NFAT undergo conformational changes to form the interaction interface. The leucine zipper of the Fos-Jun heterodimer is tilted by approximately 15° toward NFAT1 [Fig. 1.4]. NFAT1 forms an extensive interaction interface with the Fos-Jun heterodimer involving one face of the leucine zipper. The conformation of NFAT in the ternary complex may also change relative to the binary complex. The interaction between NFAT1 and Fos-Jun is asymmetric and requires the binding of Jun to the half-site proximal to NFAT (15, 16, 25, 30, 78, 97). Thus, alternative orientations of bZIP heterodimer binding at different recognition elements can differentially accommodate cooperative interactions with adjacent proteins resulting in diverse transcriptional outputs.

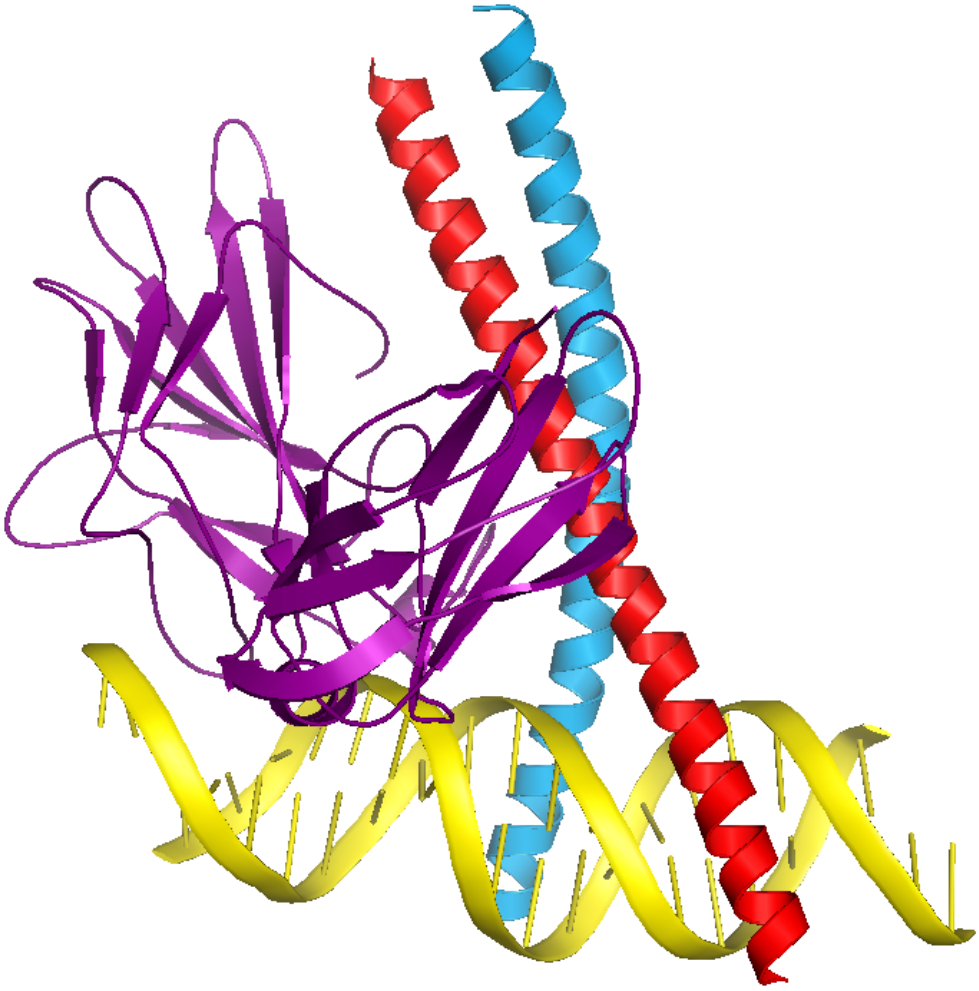

Fig. 1.4. Crystal structure of Fos-Jun-NFAT1-ARRE2 complex. The figure was created using the PyMOL Molecular Graphics System (22) and coordinates form the RCSB Protein Data Bank [www.pdb.org (8), PDB ID: 1A02] in agreement with the published structure (40).

Reversal of the orientation of bZIP heterodimer binding at any one recognition element can potentially influence genes in a stage-specific manner. In this scenario, the presence of either alternative DNA-binding proteins or post-translational modifications within an interaction interface could influence the architecture and function multi-protein complexes in a temporal- and cell-type specific manner. In support of the idea that the architecture of multi-protein complexes can influence transcriptional activation, repositioning of the activation domains of Fos-Jun heterodimers had a significant effect

on the efficiency of reporter gene activation in yeast independent of cooperation with NFAT1 (18). In a more recent study, pharmacologic inhibitors of Jun phosphorylation which do not affect recruitment of Fos, Jun, or NFAT to the endogenous interleukin-2 enhancer blocked a proposed "late phase" interleukin-2 enhancer activity including the binding of other transcription factors, the recruitment of CBP, and the acetylation of histone H3 at lysine 27 (51), indicating a potential role for regions outside of the DNA-binding domain of Jun in interleukin-2 enhancer dynamics.

Like Fos-Jun-NFAT1, only single bZIP heterodimer orientation was observed in the crystal structure of ATF2-Jun-IRF3 at the interferon-β enhancer (77) [Fig. 1.5]. By analogy to Fos-Jun and NFAT1, it was hypothesized that asymmetric interactions between ATF2-Jun and IRF3 at adjacent sites are the driving force for cooperative DNA-binding (77). However, the ATF2-Jun-IRF3 structure gives little support for this hypothesis. The only direct contact observed is between D45 of IRF3 (bound to 5' PRDIII half-site) and R345 of ATF2 (bound to the PRDIV half-site). R345A substitution in ATF2, however, had no detectable effect on complex formation with IRF3 at PRDIV-III as reveal by gel-shift analysis (77). Since Jun does not bind tightly to 3' nonconsensus PRDIV half-site and IRF3 bends the DNA toward itself and away from Jun, the authors attributed cooperative DNA-binding to complementary DNA conformations induced by the binding of ATF2-Jun and IRF3.

Previous photo-crosslinking analysis of ATF2-Jun-IRF3 complexes indicated that cooperativity between ATF2-Jun and IRF3 at the interferon-β enhancer required a heterodimer orientation opposite from that observed in the crystal structure (34). In a more recent study, comparison of the fluorescence polarization efficiency of end-labeled

oligonucleotides by ATF2 homodimers, Jun homodimers, versus ATF2-Jun heterodimers demonstrated that ATF2-Jun can bind to PRDIV in two orientations in the presence of IRF3 (26). Thus, ATF2-Jun-IRF3 represents a complex in which two alternative bZIP heterodimer orientations have been observed at the same enhancer element. Since the enhanceosome encompassing ATF2-Jun-IRF3 complexes has been described in detail, ATF2-Jun-IRF3 could provide a convenient model system to study the role of alternative bZIP heterodimer orientations in the dynamics of enhanceosome assembly and reorganization.

Fig. 1.5. Crystal structure of ATF2-Jun-IRF3-PRDIV-III complex. The figure was created using the PyMOL Molecular Graphics System (22) and coordinates form the RCSB Protein Data Bank [www.pdb.org (8), PDB ID: 1T2K] in agreement with the published structure (77).

III. ATF2, JUN, IRF3, HMGI INTERACTIONS ON DNA

III.A. Protein-DNA interactions

The interferon-β enhancer consists of four positive regulatory domains (PRDs) which are numbered according to the chronological order in which the domains were discovered to confer reporter plasmid virus-inducibility (27, 36, 41, 61) [Fig. 1.6]. IRF proteins bind to PRDI and PRDIII, the NF-κB heterodimer p50-p65 binds to PRDII, and ATF2-Jun binds to PRDIV. The downstream (3') PRDIV half-site overlaps PRDIII, which is recognized by two IRF molecules. PRDI is recognized by two additional IRF molecules. IRF3 preferentially recognizes the 5' PRDIII and PRDI half-sites, whereas either IRF3 or IRF7 recognize the 3' PRDIII and PRDI half-sites. PRDII, located immediately downstream of PRDI, is recognized by the p50-p65 NF-kB heterodimer. Flanking PRDIV and PRDII are two pairs of AT-rich sequences which are protected from DNase I digestion in the presence of HMGI (105). Whereas p50-p65 binds PRDII in a fixed orientation, ATF2-Jun heterodimers have been found to bind to PRDIV in two opposite orientations using different experimental approaches (26, 34). In an effort to identify factors that influence the orientation of ATF2-Jun at PRDIV, the binding of ATF2, Jun, IRF3, and HMGI at the PRDIV-III composite element have been the focus of several studies (14, 26, 28, 34, 77).

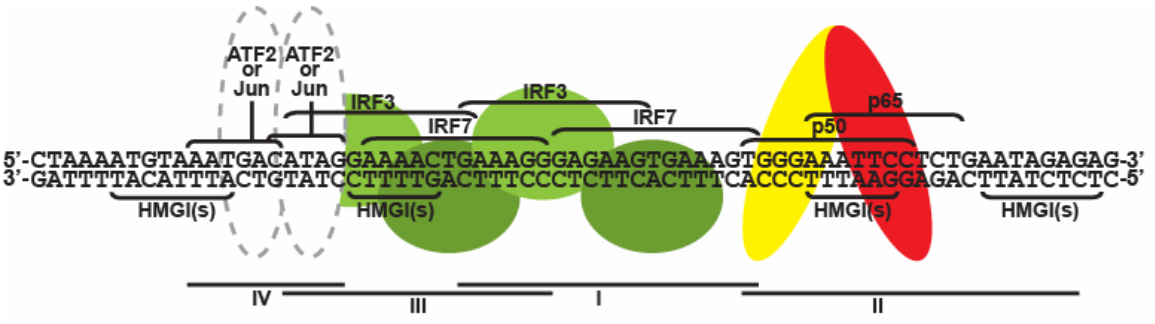

Fig. 1.6. Transcription factor binding sites within the interferon-β enhancer. Binding sites assignments for subunits of the ATF2-Jun heterodimer (dotted lines), IRF3 (light green), IRF7 (dark green), p50 (yellow), and p65 (red), indicated by brackets, are based on x-ray crystallographic structures. Binding sites assignments for an unknown number of HMGI molecules, indicated by brackets, are based on DNase I footprinting analysis. The positions of positive regulatory domain (PRD) IV, III, I, and II are indicated by lines.

X-ray crystallography has revealed that ATF2-Jun heterodimers adopt a structure similar to that of Fos-Jun heterodimers (77) [Fig. 1.5]. The two proteins dimerize through a C-terminal leucine zipper, and the N-terminal basic regions lie in the major grooves of PRDIV recognition element. ATF2-Jun binds to an 8-bp sequence (5′-TGACATAG-3′) in PRDIV which differs from the canonical CRE site (5'-TGACGTCA-3') by three base substitutions (underlined) in the 3' half-site. Consensus bZIP-DNA interactions are observed in the 5' half-site. An arginine-guanine contact, which is important for the binding of Fos-Jun heterodimers to the AP1 site (82), is observed in the consensus PRDIV half-site (77). In contrast, base substitutions in the nonconsensus 3' half-site appear to preclude optimal contacts between the basic region and the major groove. Non-optimal binding to the 3' half-site may be functionally important since the non-consensus recognition sequence is also observed in other organisms for which the surrounding the interferon-β enhancer sequence is strictly conserved with the exception

of several base pairs not included in enhancer binding-protein core recognition sequences (76).

Despite asymmetries in the sequence, ATF2-Jun heterodimers have been hypothesized to bind PRDIV in both orientations. Using a UV-light-crosslinking approach, Falvo *et al.* showed that ATF2-Jun binds to PRDIV in two orientations (34). In an independent study, measurement of the fluorescence polarization efficiencies of FAM fluorophores conjugated to one end of PRDIV oligonucleotides revealed that the binding of ATF2 and Jun homodimers have significantly different effects on tumbling time, with ATF2-Jun heterodimers yielding a tumbling time intermediate of the two homodimer complexes (26). Since these relative effects do not correlate with slight differences in the DNA binding affinities of these dimeric complexes at PRDIV as measured by isothermal titration calorimetry (14, 26), these results have been attributed to the binding of ATF2-Jun to PRDIV in both orientations.

Overlapping and adjacent to the 3' PRDIV half-site are two tandem IRF sites termed PRDIII. IRF7 expression is increased through a positive feedback by IFN stimulation, whereas IRF3 is constitutively expressed in most cell types (92). These properties suggested that the immediate early enhanceosome might only contain IRF3 and that IRF7 has a role in later stages of virus infection. Early work therefore focused on crystallizing the enhanceosome with IRF3 bound to the PRDIII region of enhancer. It then became clear, however, that IRF7 is constitutively expressed at high levels in plasmocytoid dendritic cells, the primary source of type I interferon in response to infection, and that it is essential for IRF7 expression (49). A challenge for structural studies was then to understand which of four IRF-binding sites in PRDIII–I would

accommodate IRF7 and IRF3 as their positioning might be crucial for enhanceosome assembly. A crystal structure suggests that IRF3 binds preferentially to the 5' half-sites of PRDIII and PRDI whereas IRF7 binds to the 3' half-site of PRDIII and PRDI [Fig. 1.6] (76).

In the ATF2-Jun-IRF3 crystal structure, two IRF3 molecules bind to the PRDIII region on opposite faces of the DNA. Although binding is cooperative, there are no direct protein–protein contacts between the domains (32, 77). The IRF3 DNA-binding domain contains a trihelical bundle (α1–α3) connected through three long loops (L1–L3) to a four-stranded antiparallel β-sheet. The recognition site is bipartite with the 3' PRDIII half-site (5'-AANNGAAA-3') being recognized by helix α3 in the major groove and the 5' PRDIII half-site (5'-AANNGAAA-3') by loop L1 in the minor groove. As the two binding sites overlap, the 3' PRDIII half-site has minor groove contacts through loop L1 that extend into the binding site of the 5' PRDIII half-site. In this configuration of the two binding sites, the DNA curvature stabilized by binding of one IRF-3 molecule is about optimal for binding of the other, explaining the cooperative binding behavior (32, 77). Since PRDIV and PRDIII also overlap, the 5' IRF3 molecule has similar minor groove interactions that extend into the 3' PRDIV half-site. The simultaneous interaction of the 3' heterodimer subunit with the major groove and the 5' IRF3 molecule with the minor groove has been proposed to induce a DNA conformation that mutually increases the affinities of ATF2-Jun and IRF3, thereby underlying cooperative DNA-binding (77).

DNase I footprinting analyses have suggested that two HMGI sites flank the PRDIV (nucleotides − 105 to − 98, and nucleotides − 91 to − 83) (105, 106). Since HMGI failed to co-crystalize with other components of the interferon-β enhancer, the

stoicheometry of HMGI binding to these sites in the functional enhanceosome is not known. In the absence of other proteins, however, a single molecule of HMGI has been proposed to utilize two of three DNA-binding domain modules to simultaneously recognize two sites that flank PRDIV (105). It has been proposed that ATF2-Jun and IRF3 sterically exclude the binding of individual HMGI molecules to each of these sites (77). However, it is possible that alternative HMGI-DNA interactions can exist in the presence of ATF2, Jun, and IRF3.

III.B. Heterodimer-IRF3 interactions

Virus-inducibility of reporter plasmids is strongly dependent on the helical phasing between PRDIV and PRDIII in reporter gene constructs (100), indicating that direct interactions between ATF2-Jun and IRF3 may contribute transcriptional activation. Since interactions with IRF3 could potentially influence the preferred orientation of DNA-binding by ATF2-Jun, Falvo *et al.* used UV-light-crosslinking to address this idea (34). Whereas ATF2-Jun alone had no detectable orientation preference, co-incubation with IRF3 was sufficient to fix the orientation of ATF2-Jun at PRDIV such that ATF2 favors the nonconsensus half-site (34). Since this effect was dependent on an intact IRF3 binding site (34), it was proposed that cooperative DNA-binding interactions between ATF2-Jun and IRF3 at PRDIV-III had a dominant effect on the orientation of ATF2-Jun binding.

In a subsequent study, Panne *et al* co-crystallized the minimal DNA-binding domains of ATF2, Jun, and IRF3 at PRDIV–PRDIII composite recognition element in an effort to explore the molecular details underlying cooperative DNA-binding interactions between ATF2-Jun and IRF3 (77). In the structural model, Jun rather than ATF2 is

bound to the PRDIV half-site proximal to IRF3. Based on the structure, it was apparent that the nucleotide used to derivatize the oligonucleotide with a photoactivatable group in the earlier UV-light-crosslinking experiments (34) is contacted by IRF3 rather than ATF2 or Jun. Therefore, the crystal structure was interpreted to more accurately reflect the configuration of ATF2-Jun-IRF3 complexes at PRDIV-III.

Despite the fixed orientation of ATF2-Jun at PRDIV in the crystal with IRF3, the structure reveals surprisingly few protein-protein interactions between ATF2-Jun and IRF3. The only direct contact observed is between D45 of IRF3 (bound to 5' PRDIII half-site) and R345 of ATF2 (bound to the PRDIV half-site). R345A substitution in ATF2, however, had no detectable effect on complex formation with IRF3 at PRDIV-III as reveal by gel-shift analysis (77). Since Jun does not bind tightly to 3' nonconsensus PRDIV half-site and IRF3 bends the DNA toward itself and away from Jun, the authors attributed cooperative DNA-binding to complementary DNA conformations induced by the binding of ATF2-Jun and IRF3. In support of this model, ATF2-Jun-IRF3 complex formation at PRDIV-III was prevented when the wild-type PRDIV site was replaced with the canonical CRE site at which the more optimal heterodimer-DNA contact interface in the 3' half-site is predicted to preclude the DNA conformation required for IRF3 binding (77). This effect, however, can also be attributed to changes in sequence rather than the structure of the binding site as IRF3 was shown to make specific base interactions with the 3' PRDIV half-site.

In order to address the issue of cooperativity between ATF2-Jun and IRF3 at PRDIV, Dragan *et al* used isothermal titration calorimetry to measure the effect of ATF2-Jun on the binding of IRF3 to PRDIV (26). ATF2 and Jun did not noticeably affect the

association constant of a phosphomimetic IRF3 dimer to PRDIV-III (26). From this, the authors concluded that IRF3 and ATF2-Jun do not cooperate at PRDIV-III. Differences between the phosphomimetic IRF3 dimer and the minimal IRF3 DNA-binding domains may contribute to this lack of cooperativity as the phosphomimetic IRF3 dimer was shown to bind more distal to the ATF2-Jun heterodimer compared to the binding of the minimal DNA binding domains of IRF3 (26, 32). However, post-translational modifications of IRF3 or heterodimerization with IRF7 could potentially influence interactions between PRDIII and the DNA-binding domain of IRF3. Further experiments are needed to more clearly understand if and how the binding of IRF3 and ATF2-Jun cooperate at the interferon-β enhancer.

III.C. Interactions with HMGI

Past studies have produced discordant results concerning interactions among ATF2-Jun and HMGI at the interferon-β enhancer. Early gel-shift analyses have shown that HMGI and ATF2 bind cooperatively to the PRDIV recognition element, which is mediated by specific protein-protein interactions between HMGI and ATF2 as a naturally occurring splice variant of ATF2 failed to interact with HMGI (28). In contrast, using a series of HMGI protein fragments, Yie *et al.* demonstrated that optimal enhancement of ATF2-Jun binding to PRDIV correlated with the ability of HMGI to bind via intramolecular cooperative interactions to the enhancer and not with its ability of HMGI to interact with ATF2-Jun (106). In studies describing the role of HMGI in the assembly of interferon-β enhanceosome in cells, Munshi *et al.* demonstrated that the recruitment of the full complement of proteins to the enhancer correlated with lysine 71-acetylation of HMGI by PCAF, whereas the disassembly of the complex from the enhancer correlated

with lysine 65-acetylation by CBP. Furthermore, lysine 71-acetylation of HMGI facilitated GST-pull-down of the enhancer proteins by HMGI and protected the enhanceosome from disruption *in vitro* by inhibiting CBP-induced acetylation at K65 (71). However, studies of the interferon-β enhancer region *in vitro* analyses do not mention HMGI either as a component of the complex or as a means responsible for the cooperation of the other components (26, 76, 77).

In order to address the role of HMGI in cooperativity among ATF2-Jun and IRF3 at PRDIV, Dragan *et al.* used isothermal titration calorimetry to measure the effect of HMGI on stabilization of ATF2-Jun-IRF3 complex formation at PRDIV (26). HMGI did not affect the association constant of ATF2-Jun and a phosphomimetic IRF3 dimer to PRDIV-III (26). Likewise, IRF3 did not affect the association constant of ATF2-Jun and HMGI to PRDIV-III (26). From this, the authors concluded that IRF3 and HMGI compete for interactions with the DNA. However, due the indirect nature of these experiments, it is not possible to determine whether competition between HMGI and ATF2-Jun for DNA (in the former experiment) or between IRF3 and ATF2-Jun for DNA (in the later experiment) rather than between IRF3 and HMGI for DNA was occurring. Furthermore, even if such competition does occur, post-translational modifications of HMGI may influence its interactions with ATF2, Jun, and IRF3 at the interferon-β enhancer as suggested by Munshi and colleagues (71). Therefore, the molecular details underlying ATF2, Jun, IRF3, and HMGI interactions at the interferon-β enhancer remains an outstanding problem.

IV. STATEMENT OF THE PROBLEM

My thesis work is predicated on the assumption that understanding the structural basis for the formation of different configurations of the single transcription factor complex will provide a valuable model system for determining the role of nucleoprotein architecture in gene transcription. ATF2-Jun-IRF3 represents a transcription factor complex for which alternative structural configurations have been proposed at the same DNA sequence (26). The atomic resolution structure of minimal DNA-binding domains of ATF2, Jun, and IRF3 bound to the interferon-β enhancer element was previously completed to identify the amino acid residues at the interaction interface of ATF2-Jun heterodimers and IRF3 (77). However, efforts towards characterization of the roles of these and other residues in ATF2-Jun-IRF3 complex formation have proved difficult. Thus, the interactions governing the configuration(s) of this complex remain unknown.

This thesis presents both structural and functional characterization of ATF2-Jun-IRF3 complexes at the interferon-β enhancer. To that end, the techniques of gel-based fluorescence resonance energy transfer (gelFRET), quantitative gel-shift, and quantitative real-time PCR analyses were utilized to describe how symmetry-related amino acid residues in ATF2 and Jun influence interactions with IRF3, the orientation of DNA-binding by ATF2-Jun, and interferon-β gene transcription. Co-expression of IRF3 together with ATF2-Jun heterodimer variants which bind to DNA in opposite orientations *in vitro* had distinct effects on the efficiency of endogenous interferon-β gene expression in Sendai virus-infected cells and this correlated with different relative efficiencies of bATF2-bJun-iIRF3 complex formation at the interferon-β enhancer element *in vitro*. Consistent with a role for cooperative DNA-binding interactions among ATF2, Jun, and

IRF3 in interferon-β activation, we observed that the DNA-binding domains of ATF2 and Jun mediated the effects of heterodimer orientation on interferon-β transcription, whereas the activation domains mediated the effect of heterodimer orientation at genes not regulated by composite ATF2-Jun-IRF3 sites. Further, this work highlights a role for synergistic effects of iIRF3 and HMGI on the stabilization of alternative bATF2-bJun binding orientations *in vitro*. Collectively, these results indicate that alternative interactions between ATF2-Jun and IRF3 permit opposite orientations of heterodimer binding at the interferon-β enhancer, with distinct effects on the stability of complex formation *in vitro* and on endogenous gene expression *in vivo*.

V. BIBLIOGRAPHY

1. **Agalioti, T., S. Lomvardas, B. Parekh, J. Yie, T. Maniatis, and D. Thanos.** 2000. Ordered recruitment of chromatin modifying and general transcription factors to the IFN-beta promoter. Cell **103:**667-78.
2. **Agelopoulos, M., and D. Thanos.** 2006. Epigenetic determination of a cell-specific gene expression program by ATF-2 and the histone variant macroH2A. Embo J **25:**4843-53.
3. **Agre, P., P. F. Johnson, and S. L. McKnight.** 1989. Cognate DNA binding specificity retained after leucine zipper exchange between GCN4 and C/EBP. Science **246:**922-6.
4. **Amoutzias, G. D., A. S. Veron, J. Weiner, 3rd, M. Robinson-Rechavi, E. Bornberg-Bauer, S. G. Oliver, and D. L. Robertson.** 2007. One billion years of bZIP transcription factor evolution: conservation and change in dimerization and DNA-binding site specificity. Mol Biol Evol **24:**827-35.
5. **Avilion, A. A., S. K. Nicolis, L. H. Pevny, L. Perez, N. Vivian, and R. Lovell-Badge.** 2003. Multipotent cell lineages in early mouse development depend on SOX2 function. Genes Dev **17:**126-40.
6. **Balmelle, N., N. Zamarreno, M. S. Krangel, and C. Hernandez-Munain.** 2004. Developmental activation of the TCR alpha enhancer requires functional collaboration among proteins bound inside and outside the core enhancer. J Immunol **173:**5054-63.
7. **Barthel, R., A. V. Tsytsykova, A. K. Barczak, E. Y. Tsai, C. C. Dascher, M. B. Brenner, and A. E. Goldfeld.** 2003. Regulation of tumor necrosis factor alpha gene expression by mycobacteria involves the assembly of a unique enhanceosome dependent on the coactivator proteins CBP/p300. Mol Cell Biol **23:**526-33.
8. **Berman, H. M., J. Westbrook, Z. Feng, G. Gilliland, T. N. Bhat, H. Weissig, I. N. Shindyalov, and P. E. Bourne.** 2000. The Protein Data Bank. Nucleic Acids Res **28:**235-42.
9. **Bewley, C. A., A. M. Gronenborn, and G. M. Clore.** 1998. Minor groove-binding architectural proteins: structure, function, and DNA recognition. Annu Rev Biophys Biomol Struct **27:**105-31.
10. **Bouallaga, I., S. Massicard, M. Yaniv, and F. Thierry.** 2000. An enhanceosome containing the Jun B/Fra-2 heterodimer and the HMG-I(Y) architectural protein controls HPV 18 transcription. EMBO Rep **1:**422-7.
11. **Bruhat, A., Y. Cherasse, A. C. Maurin, W. Breitwieser, L. Parry, C. Deval, N. Jones, C. Jousse, and P. Fafournoux.** 2007. ATF2 is required for amino acid-regulated transcription by orchestrating specific histone acetylation. Nucleic Acids Res **35:**1312-21.
12. **Bruhn, L., A. Munnerlyn, and R. Grosschedl.** 1997. ALY, a context-dependent coactivator of LEF-1 and AML-1, is required for TCRalpha enhancer function. Genes Dev **11:**640-53.

13. **Carey, M., J. Kolman, D. A. Katz, L. Gradoville, L. Barberis, and G. Miller.** 1992. Transcriptional synergy by the Epstein-Barr virus transactivator ZEBRA. J Virol **66:**4803-13.
14. **Carrillo, R. J., A. I. Dragan, and P. L. Privalov.** 2010. Stability and DNA-binding ability of the bZIP dimers formed by the ATF-2 and c-Jun transcription factors. J Mol Biol **396:**431-40.
15. **Chen, L., J. N. Glover, P. G. Hogan, A. Rao, and S. C. Harrison.** 1998. Structure of the DNA-binding domains from NFAT, Fos and Jun bound specifically to DNA. Nature **392:**42-8.
16. **Chen, L., M. G. Oakley, J. N. Glover, J. Jain, P. B. Dervan, P. G. Hogan, A. Rao, and G. L. Verdine.** 1995. Only one of the two DNA-bound orientations of AP-1 found in solution cooperates with NFATp. Curr Biol **5:**882-9.
17. **Chinenov, Y., and T. K. Kerppola.** 2001. Close encounters of many kinds: Fos-Jun interactions that mediate transcription regulatory specificity. Oncogene **20:**2438-52.
18. **Chytil, M., B. R. Peterson, D. A. Erlanson, and G. L. Verdine.** 1998. The orientation of the AP-1 heterodimer on DNA strongly affects transcriptional potency. Proc Natl Acad Sci U S A **95:**14076-81.
19. **Cleynen, I., and W. J. Van de Ven.** 2008. The HMGA proteins: a myriad of functions (Review). Int J Oncol **32:**289-305.
20. **De Cesare, D., D. Vallone, A. Caracciolo, P. Sassone-Corsi, C. Nerlov, and P. Verde.** 1995. Heterodimerization of c-Jun with ATF-2 and c-Fos is required for positive and negative regulation of the human urokinase enhancer. Oncogene **11:**365-76.
21. **Del Blanco, B., J. L. Roberts, N. Zamarreno, N. Balmelle-Devaux, and C. Hernandez-Munain.** 2009. Flexible stereospecific interactions and composition within nucleoprotein complexes assembled on the TCR alpha gene enhancer. J Immunol **183:**1871-83.
22. **DeLano, W. L.** 2008. The PyMOL Molecular Graphics System, 1.1 ed. DeLano Scientific LLC, San Carlos, CA, USA.
23. **Deppmann, C. D., R. S. Alvania, and E. J. Taparowsky.** 2006. Cross-species annotation of basic leucine zipper factor interactions: Insight into the evolution of closed interaction networks. Mol Biol Evol **23:**1480-92.
24. **Diamond, M., J. Miner, S. Yoshinaga, and K. Yamamoto.** 1990. Transcription factor interactions: Selectors of positive or negative regulation from a single DNA element. Science **249:**1266-1272.
25. **Diebold, R. J., N. Rajaram, D. A. Leonard, and T. K. Kerppola.** 1998. Molecular basis of cooperative DNA bending and oriented heterodimer binding in the NFAT1-Fos-Jun-ARRE2 complex. Proc Natl Acad Sci U S A **95:**7915-20.
26. **Dragan, A. I., R. Carrillo, T. I. Gerasimova, and P. L. Privalov.** 2008. Assembling the human IFN-beta enhanceosome in solution. J Mol Biol **384:**335-48.
27. **Du, W., and T. Maniatis.** 1992. An ATF/CREB binding site is required for virus induction of the human interferon beta gene [corrected]. Proc Natl Acad Sci U S A **89:**2150-4.

28. **Du, W., and T. Maniatis.** 1994. The high mobility group protein HMG I(Y) can stimulate or inhibit DNA binding of distinct transcription factor ATF-2 isoforms. Proc Natl Acad Sci U S A **91:**11318-22.
29. **Eisenbeis, C. F., H. Singh, and U. Storb.** 1993. PU.1 is a component of a multiprotein complex which binds an essential site in the murine immunoglobulin lambda 2-4 enhancer. Mol Cell Biol **13:**6452-61.
30. **Erlanson, D. A., M. Chytil, and G. L. Verdine.** 1996. The leucine zipper domain controls the orientation of AP-1 in the NFAT.AP-1.DNA complex. Chem Biol **3:**981-91.
31. **Escalante, C. R., A. L. Brass, J. M. Pongubala, E. Shatova, L. Shen, H. Singh, and A. K. Aggarwal.** 2002. Crystal structure of PU.1/IRF-4/DNA ternary complex. Mol Cell **10:**1097-105.
32. **Escalante, C. R., E. Nistal-Villan, L. Shen, A. Garcia-Sastre, and A. K. Aggarwal.** 2007. Structure of IRF-3 bound to the PRDIII-I regulatory element of the human interferon-beta enhancer. Mol Cell **26:**703-16.
33. **Falvo, J. V., B. M. Brinkman, A. V. Tsytsykova, E. Y. Tsai, T. P. Yao, A. L. Kung, and A. E. Goldfeld.** 2000. A stimulus-specific role for CREB-binding protein (CBP) in T cell receptor-activated tumor necrosis factor alpha gene expression. Proc Natl Acad Sci U S A **97:**3925-9.
34. **Falvo, J. V., B. S. Parekh, C. H. Lin, E. Fraenkel, and T. Maniatis.** 2000. Assembly of a functional beta interferon enhanceosome is dependent on ATF-2-c-jun heterodimer orientation. Mol Cell Biol **20:**4814-25.
35. **Falvo, J. V., D. Thanos, and T. Maniatis.** 1995. Reversal of intrinsic DNA bends in the IFN beta gene enhancer by transcription factors and the architectural protein HMG I(Y). Cell **83:**1101-11.
36. **Fan, C. M., and T. Maniatis.** 1989. Two different virus-inducible elements are required for human beta-interferon gene regulation. Embo J **8:**101-10.
37. **Giese, K., C. Kingsley, J. R. Kirshner, and R. Grosschedl.** 1995. Assembly and function of a TCR alpha enhancer complex is dependent on LEF-1-induced DNA bending and multiple protein-protein interactions. Genes Dev **9:**995-1008.
38. **Giese, K., J. Pagel, and R. Grosschedl.** 1997. Functional analysis of DNA bending and unwinding by the high mobility group domain of LEF-1. Proc Natl Acad Sci U S A **94:**12845-50.
39. **Glass, C. K.** 1994. Differential recognition of target genes by nuclear receptor monomers, dimers, and heterodimers. Endocr Rev **15:**391-407.
40. **Glover, J. N., and S. C. Harrison.** 1995. Crystal structure of the heterodimeric bZIP transcription factor c-Fos-c-Jun bound to DNA. Nature **373:**257-61.
41. **Goodbourn, S., and T. Maniatis.** 1988. Overlapping positive and negative regulatory domains of the human beta-interferon gene. Proc Natl Acad Sci U S A **85:**1447-51.
42. **Gross, P., A. A. Yee, C. H. Arrowsmith, and R. B. Macgregor, Jr.** 1998. Quantitative hydroxyl radical footprinting reveals cooperative interactions between DNA-binding subdomains of PU.1 and IRF4. Biochemistry **37:**9802-11.
43. **Hai, T., and T. Curran.** 1991. Cross-family dimerization of transcription factors Fos/Jun and ATF/CREB alters DNA binding specificity. Proc Natl Acad Sci U S A **88:**3720-4.

44. **Hall, J. M., D. P. McDonnell, and K. S. Korach.** 2002. Allosteric regulation of estrogen receptor structure, function, and coactivator recruitment by different estrogen response elements. Mol Endocrinol **16:**469-86.
45. **Hassler, M., and T. J. Richmond.** 2001. The B-box dominates SAP-1-SRF interactions in the structure of the ternary complex. Embo J **20:**3018-28.
46. **He, X., C. C. Chen, F. Hong, F. Fang, S. Sinha, H. H. Ng, and S. Zhong.** 2009. A biophysical model for analysis of transcription factor interaction and binding site arrangement from genome-wide binding data. PLoS One **4:**e8155.
47. **Herbig, E., L. Warfield, L. Fish, J. Fishburn, B. A. Knutson, B. Moorefield, D. Pacheco, and S. Hahn.** 2010. Mechanism of Mediator recruitment by tandem Gcn4 activation domains and three Gal11 activator-binding domains. Mol Cell Biol **30:**2376-90.
48. **Hirai, S., and M. Yaniv.** 1989. Jun DNA-binding is modulated by mutations between the leucines or by direct interaction of fos with the TGACTCA sequence. New Biol **1:**181-91.
49. **Honda, K., H. Yanai, H. Negishi, M. Asagiri, M. Sato, T. Mizutani, N. Shimada, Y. Ohba, A. Takaoka, N. Yoshida, and T. Taniguchi.** 2005. IRF-7 is the master regulator of type-I interferon-dependent immune responses. Nature **434:**772-7.
50. **Huang, C. Y., and B. P. Sleckman.** 2007. Developmental stage-specific regulation of TCR-alpha-chain gene assembly by intrinsic features of the TEA promoter. J Immunol **179:**449-54.
51. **Ishihara, S., and R. H. Schwartz.** 2011. Two-Step Binding of Transcription Factors Causes Sequential Chromatin Structural Changes at the Activated IL-2 Promoter. J Immunol.
52. **Jabrane-Ferrat, N., N. Nekrep, G. Tosi, L. Esserman, and B. M. Peterlin.** 2003. MHC class II enhanceosome: how is the class II transactivator recruited to DNA-bound activators? Int Immunol **15:**467-75.
53. **Kamachi, Y., M. Uchikawa, and H. Kondoh.** 2000. Pairing SOX off: with partners in the regulation of embryonic development. Trends Genet **16:**182-7.
54. **Karanam, B., L. Wang, D. Wang, X. Liu, R. Marmorstein, R. Cotter, and P. A. Cole.** 2007. Multiple roles for acetylation in the interaction of p300 HAT with ATF-2. Biochemistry **46:**8207-16.
55. **Kerppola, T. K., and T. Curran.** 1993. Selective DNA bending by a variety of bZIP proteins. Mol Cell Biol **13:**5479-89.
56. **Kim, S., C. T. Denny, and R. Wisdom.** 2006. Cooperative DNA binding with AP-1 proteins is required for transformation by EWS-Ets fusion proteins. Mol Cell Biol **26:**2467-78.
57. **Kim, T. K., T. H. Kim, and T. Maniatis.** 1998. Efficient recruitment of TFIIB and CBP-RNA polymerase II holoenzyme by an interferon-beta enhanceosome in vitro. Proc Natl Acad Sci U S A **95:**12191-6.
58. **Kim, T. K., and T. Maniatis.** 1997. The mechanism of transcriptional synergy of an in vitro assembled interferon-beta enhanceosome. Mol Cell **1:**119-29.
59. **Kingston, R. E., C. A. Bunker, and A. N. Imbalzano.** 1996. Repression and activation by multiprotein complexes that alter chromatin structure. Genes Dev **10:**905-20.

60. **Landschulz, W. H., P. F. Johnson, and S. L. McKnight.** 1988. The leucine zipper: a hypothetical structure common to a new class of DNA binding proteins. Science **240:**1759-64.
61. **Leblanc, J. F., L. Cohen, M. Rodrigues, and J. Hiscott.** 1990. Synergism between distinct enhanson domains in viral induction of the human beta interferon gene. Mol Cell Biol **10:**3987-93.
62. **Lee, S. K., H. J. Kim, S. Y. Na, T. S. Kim, H. S. Choi, S. Y. Im, and J. W. Lee.** 1998. Steroid receptor coactivator-1 coactivates activating protein-1-mediated transactivations through interaction with the c-Jun and c-Fos subunits. J Biol Chem **273:**16651-4.
63. **Lee, S. K., S. Y. Na, S. Y. Jung, J. E. Choi, B. H. Jhun, J. Cheong, P. S. Meltzer, Y. C. Lee, and J. W. Lee.** 2000. Activating protein-1, nuclear factor-kappaB, and serum response factor as novel target molecules of the cancer-amplified transcription coactivator ASC-2. Mol Endocrinol **14:**915-25.
64. **Lively, T. N., H. A. Ferguson, S. K. Galasinski, A. G. Seto, and J. A. Goodrich.** 2001. c-Jun binds the N terminus of human TAF(II)250 to derepress RNA polymerase II transcription in vitro. J Biol Chem **276:**25582-8.
65. **Love, J. J., X. Li, D. A. Case, K. Giese, R. Grosschedl, and P. E. Wright.** 1995. Structural basis for DNA bending by the architectural transcription factor LEF-1. Nature **376:**791-5.
66. **Masternak, K., A. Muhlethaler-Mottet, J. Villard, M. Zufferey, V. Steimle, and W. Reith.** 2000. CIITA is a transcriptional coactivator that is recruited to MHC class II promoters by multiple synergistic interactions with an enhanceosome complex. Genes Dev **14:**1156-66.
67. **May, W. A., S. L. Lessnick, B. S. Braun, M. Klemsz, B. C. Lewis, L. B. Lunsford, R. Hromas, and C. T. Denny.** 1993. The Ewing's sarcoma EWS/FLI-1 fusion gene encodes a more potent transcriptional activator and is a more powerful transforming gene than FLI-1. Mol Cell Biol **13:**7393-8.
68. **Merika, M., A. J. Williams, G. Chen, T. Collins, and D. Thanos.** 1998. Recruitment of CBP/p300 by the IFN beta enhanceosome is required for synergistic activation of transcription. Mol Cell **1:**277-87.
69. **Miotto, B., and K. Struhl.** 2006. Differential gene regulation by selective association of transcriptional coactivators and bZIP DNA-binding domains. Mol Cell Biol **26:**5969-82.
70. **Mo, Y., W. Ho, K. Johnston, and R. Marmorstein.** 2001. Crystal structure of a ternary SAP-1/SRF/c-fos SRE DNA complex. J Mol Biol **314:**495-506.
71. **Munshi, N., T. Agalioti, S. Lomvardas, M. Merika, G. Chen, and D. Thanos.** 2001. Coordination of a transcriptional switch by HMGI(Y) acetylation. Science **293:**1133-6.
72. **Munshi, N., M. Merika, J. Yie, K. Senger, G. Chen, and D. Thanos.** 1998. Acetylation of HMG I(Y) by CBP turns off IFN beta expression by disrupting the enhanceosome. Mol Cell **2:**457-67.
73. **Neuberg, M., M. Schuermann, J. B. Hunter, and R. Muller.** 1989. Two functionally different regions in Fos are required for the sequence-specific DNA interaction of the Fos/Jun protein complex. Nature **338:**589-90.

74. **Oakley, M. G., and P. B. Dervan.** 1990. Structural motif of the GCN4 DNA binding domain characterized by affinity cleaving. Science **248:**847-50.
75. **Oliviero, S., and K. Struhl.** 1991. Synergistic transcriptional enhancement does not depend on the number of acidic activation domains bound to the promoter. Proc Natl Acad Sci U S A **88:**224-8.
76. **Panne, D., T. Maniatis, and S. C. Harrison.** 2007. An atomic model of the interferon-beta enhanceosome. Cell **129:**1111-23.
77. **Panne, D., T. Maniatis, and S. C. Harrison.** 2004. Crystal structure of ATF-2/c-Jun and IRF-3 bound to the interferon-beta enhancer. Embo J **23:**4384-93.
78. **Peterson, B. R., L. J. Sun, and G. L. Verdine.** 1996. A critical arginine residue mediates cooperativity in the contact interface between transcription factors NFAT and AP-1. Proc Natl Acad Sci U S A **93:**13671-6.
79. **Pongubala, J. M., C. Van Beveren, S. Nagulapalli, M. J. Klemsz, S. R. McKercher, R. A. Maki, and M. L. Atchison.** 1993. Effect of PU.1 phosphorylation on interaction with NF-EM5 and transcriptional activation. Science **259:**1622-5.
80. **Ptashne, M., and A. Gann.** 1997. Transcriptional activation by recruitment. Nature **386:**569-77.
81. **Qing, J., Y. Zhang, and R. Derynck.** 2000. Structural and functional characterization of the transforming growth factor-beta -induced Smad3/c-Jun transcriptional cooperativity. J Biol Chem **275:**38802-12.
82. **Rajaram, N., and T. K. Kerppola.** 1997. DNA bending by Fos-Jun and the orientation of heterodimer binding depend on the sequence of the AP-1 site. Embo J **16:**2917-25.
83. **Ramirez-Carrozzi, V., and T. Kerppola.** 2003. Asymmetric recognition of nonconsensus AP-1 sites by Fos-Jun and Jun-Jun influences transcriptional cooperativity with NFAT1. Mol Cell Biol **23:**1737-49.
84. **Ransone, L. J., J. Visvader, P. Wamsley, and I. M. Verma.** 1990. Trans-dominant negative mutants of Fos and Jun. Proc Natl Acad Sci U S A **87:**3806-10.
85. **Rastinejad, F., T. Perlmann, R. M. Evans, and P. B. Sigler.** 1995. Structural determinants of nuclear receptor assembly on DNA direct repeats. Nature **375:**203-11.
86. **Reeves, R.** 2001. Molecular biology of HMGA proteins: hubs of nuclear function. Gene **277:**63-81.
87. **Reeves, R.** 2010. Nuclear functions of the HMG proteins. Biochim Biophys Acta **1799:**3-14.
88. **Reeves, R., and L. Beckerbauer.** 2001. HMGI/Y proteins: flexible regulators of transcription and chromatin structure. Biochim Biophys Acta **1519:**13-29.
89. **Remenyi, A., K. Lins, L. J. Nissen, R. Reinbold, H. R. Scholer, and M. Wilmanns.** 2003. Crystal structure of a POU/HMG/DNA ternary complex suggests differential assembly of Oct4 and Sox2 on two enhancers. Genes Dev **17:**2048-59.
90. **Risse, G., K. Jooss, M. Neuberg, H. J. Bruller, and R. Muller.** 1989. Asymmetrical recognition of the palindromic AP1 binding site (TRE) by Fos protein complexes. Embo J **8:**3825-32.

91. **Sano, Y., F. Tokitou, P. Dai, T. Maekawa, T. Yamamoto, and S. Ishii.** 1998. CBP alleviates the intramolecular inhibition of ATF-2 function. J Biol Chem **273:**29098-105.
92. **Sato, M., N. Hata, M. Asagiri, T. Nakaya, T. Taniguchi, and N. Tanaka.** 1998. Positive feedback regulation of type I IFN genes by the IFN-inducible transcription factor IRF-7. FEBS Lett **441:**106-10.
93. **Schrader, M., S. Nayeri, J. P. Kahlen, K. M. Muller, and C. Carlberg.** 1995. Natural vitamin D3 response elements formed by inverted palindromes: polarity-directed ligand sensitivity of vitamin D3 receptor-retinoid X receptor heterodimer-mediated transactivation. Mol Cell Biol **15:**1154-61.
94. **Schwabe, J. W., L. Chapman, J. T. Finch, and D. Rhodes.** 1993. The crystal structure of the estrogen receptor DNA-binding domain bound to DNA: how receptors discriminate between their response elements. Cell **75:**567-78.
95. **Shannon, M. F., L. S. Coles, J. Attema, and P. Diamond.** 2001. The role of architectural transcription factors in cytokine gene transcription. J Leukoc Biol **69:**21-32.
96. **Staal, A., A. J. van Wijnen, J. C. Birkenhager, H. A. Pols, J. Prahl, H. DeLuca, M. P. Gaub, J. B. Lian, G. S. Stein, J. P. van Leeuwen, and J. L. Stein.** 1996. Distinct conformations of vitamin D receptor/retinoid X receptor-alpha heterodimers are specified by dinucleotide differences in the vitamin D-responsive elements of the osteocalcin and osteopontin genes. Mol Endocrinol **10:**1444-56.
97. **Sun, L. J., B. R. Peterson, and G. L. Verdine.** 1997. Dual role of the nuclear factor of activated T cells insert region in DNA recognition and cooperative contacts to activator protein 1. Proc Natl Acad Sci U S A **94:**4919-24.
98. **Tan, S., and T. J. Richmond.** 1998. Crystal structure of the yeast MATalpha2/MCM1/DNA ternary complex. Nature **391:**660-6.
99. **Tanaka, M.** 1996. Modulation of promoter occupancy by cooperative DNA binding and activation-domain function is a major determinant of transcriptional regulation by activators in vivo. Proc Natl Acad Sci U S A **93:**4311-5.
100. **Thanos, D., and T. Maniatis.** 1995. Virus induction of human IFN beta gene expression requires the assembly of an enhanceosome. Cell **83:**1091-100.
101. **Tsai, E. Y., J. V. Falvo, A. V. Tsytsykova, A. K. Barczak, A. M. Reimold, L. H. Glimcher, M. J. Fenton, D. C. Gordon, I. F. Dunn, and A. E. Goldfeld.** 2000. A lipopolysaccharide-specific enhancer complex involving Ets, Elk-1, Sp1, and CREB binding protein and p300 is recruited to the tumor necrosis factor alpha promoter in vivo. Mol Cell Biol **20:**6084-94.
102. **Tsytsykova, A. V., and A. E. Goldfeld.** 2002. Inducer-specific enhanceosome formation controls tumor necrosis factor alpha gene expression in T lymphocytes. Mol Cell Biol **22:**2620-31.
103. **Williams, D. C., Jr., M. Cai, and G. M. Clore.** 2004. Molecular basis for synergistic transcriptional activation by Oct1 and Sox2 revealed from the solution structure of the 42-kDa Oct1.Sox2.Hoxb1-DNA ternary transcription factor complex. J Biol Chem **279:**1449-57.

104. **Yee, A. A., P. Yin, D. P. Siderovski, T. W. Mak, D. W. Litchfield, and C. H. Arrowsmith.** 1998. Cooperative interaction between the DNA-binding domains of PU.1 and IRF4. J Mol Biol **279:**1075-83.
105. **Yie, J., S. Liang, M. Merika, and D. Thanos.** 1997. Intra- and intermolecular cooperative binding of high-mobility-group protein I(Y) to the beta-interferon promoter. Mol Cell Biol **17:**3649-62.
106. **Yie, J., M. Merika, N. Munshi, G. Chen, and D. Thanos.** 1999. The role of HMG I(Y) in the assembly and function of the IFN-beta enhanceosome. Embo J **18:**3074-89.
107. **Yie, J., K. Senger, and D. Thanos.** 1999. Mechanism by which the IFN-beta enhanceosome activates transcription. Proc Natl Acad Sci U S A **96:**13108-13.

CHAPTER 2: ORIENTATION PREFERENCE OF bATF2-bJUN IN AN INTERFERON-β ENHANCER COMPLEX

I. INTRODUCTION

I.A. Principle of gelFRET

In efforts to understand the structural determinants of oriented DNA-binding by bZIP heterodimers, Diebold and Kerppola developed a novel gel-based fluorescence resonance energy transfer (gelFRET) assay (4, 9). Conventional FRET approaches lend several obstacles in studies of nucleoprotein architecture, including interference from unbound protein and DNA during FRET detection and uncertainty in absolute distance measurements. A specific advantage of gelFRET analysis in the analysis of heterodimer-DNA complexes is that the different mobilities of complexes formed by ATF2-Jun heterodimers, Jun homodimers, and ATF2 homodimers during gel electrophoresis allow separation and analysis of the individual complexes. The structural organization of heterodimer-DNA complexes are investigated through comparison of the relative efficiencies of energy transfer from donor fluorophores linked to different positions on DNA to an acceptor fluorophore linked to a unique position on the heterodimer. This provides a quantitative measure of the orientation preference of heterodimer binding without the need to establish the absolute distances between fluorophores.

I.B. Determination of heterodimer orientation preference

Analysis of DNA-binding orientation of bZIP heterodimer complexes by gelFRET requires comparison of the relative efficiencies of energy transfer from a donor fluorophore linked to either end of a double-stranded DNA oligonucleotide to an acceptor fluorophores linked to one subunit of the heterodimer. Complexes in which the donor and acceptor fluorophores are closer together are predicted to exhibit higher efficiencies of energy transfer than complexes in which the donor and acceptor fluorophores are far apart. If placement of the acceptor fluorophore on the opposing heterodimer subunit enhances energy transfer from one end of the DNA while reducing energy transfer from the other end of the DNA [Fig 2.1A], we interpret the relative efficiencies of energy transfer from opposite ends of the DNA to be related to the preferred orientation of heterodimer binding.

Since the gelFRET assay for heterodimer orientation does not require absolute distance measurements, an acceptor-to-donor emissions ratio is used instead of the more traditional efficiency of energy transfer. The acceptor-to-donor ratio is a function of the efficiency of energy transfer and provides a convenient measure for comparison of energy transfer between fluorophore pairs placed at different positions in a complex. Since we are concerned with comparison of energy transfer from opposite ends of the oligonucleotide, the acceptor-to-donor ratio provides the same information regarding the relative abilities of fluorophores on opposite ends of the oligonucleotide to donate energy to the acceptor. The end preference (EP) is calculated based on the acceptor-to-donor ratios in complexes labeled on the left *versus* the right ends.

For a population of heterodimers containing complexes bound in both orientations, end preference reflects the average between the efficiencies of energy transfer for complexes bound in opposite orientations weighted by the fraction of complexes bound in each orientation. Differences in the end preference values of heterodimers labeled on the same subunit are therefore proportional to differences in the fraction of heterodimers bound in each orientation. For a perfectly symmetric complex, the sum of the end preference values is predicted to equal 1. If the complex is unoriented, heterodimer-DNA complexes are predicted to exhibit similar energy transfer from opposite ends of each oligonucleotide, and thus their end preference values should be equal to 0.5. However, for most complexes, the sum of end preference values is not exactly equal to 1 and, when similar, the end preference values were not always equal to 0.5. These deviations from perfect symmetry do not interfere with determination of the relative orientation preferences of different complexes based on differences in the end preference values of heterodimers labeled on different subunits. However, determination of the fraction of heterodimers bound in each orientation requires additional information.

I.B.i. Calibration with oriented heterodimers

To establish the relationship between the end preference values and the fraction of ATF2-Jun heterodimers bound in each orientation, we have used calibration standards to determine the end preference values of fully oriented ATF2-Jun complexes. Comparison of the end preference values of ATF2-Jun heterodimers with those of fully oriented complexes allows for quantification of the absolute fraction of heterodimers bound in each orientation. We developed a calibration strategy by taking advantage of the

influence of the central asymmetric base pair in the AP-1 site on the orientation of Fos–Jun binding. Fos-Jun heterodimers that bind the AP-1 site in opposite orientations contact the central guanine of the AP-1 site using arginine residues from different subunits (7, 10). Our strategy is based on the use of ATF2–Jun heterodimers in which the analogous arginine in either ATF2 or Jun that can contact the central guanine in the interferon-β ATF/Jun site is replaced in either subunit by alanine. Replacement of the arginine residue that contacts the central asymmetric guanine in different subunits (bATF2XG–bJun vs bATF2–bJunXG) is predicted to shift the orientation of heterodimer binding in opposite directions (Fig 2.1B). To determine the fraction of complexes bound in each orientation (ATF2-Jun and Jun-ATF2), we use these standards to calibrate the relationship between end preference and heterodimer binding orientation. Calibration of the gelFRET assay allows us to estimate the end preference values of fully oriented complexes and thus enables calculation of the fraction of complexes bound in each orientation.

II. RESULTS AND DISCUSSION

II.A. Orientation preference of bATF2-bJun at IFNb

To establish whether ATF2-Jun heterodimers bind the interferon-β enhancer in one or both orientations, heterodimers were formed using truncated ATF2 and Jun encompassing the bZIP dimerization and DNA-binding domains and 14 residues on the amino-terminal sides of the basic regions [bATF2 and bJun, Fig. 2.6B]. Either bATF2 or

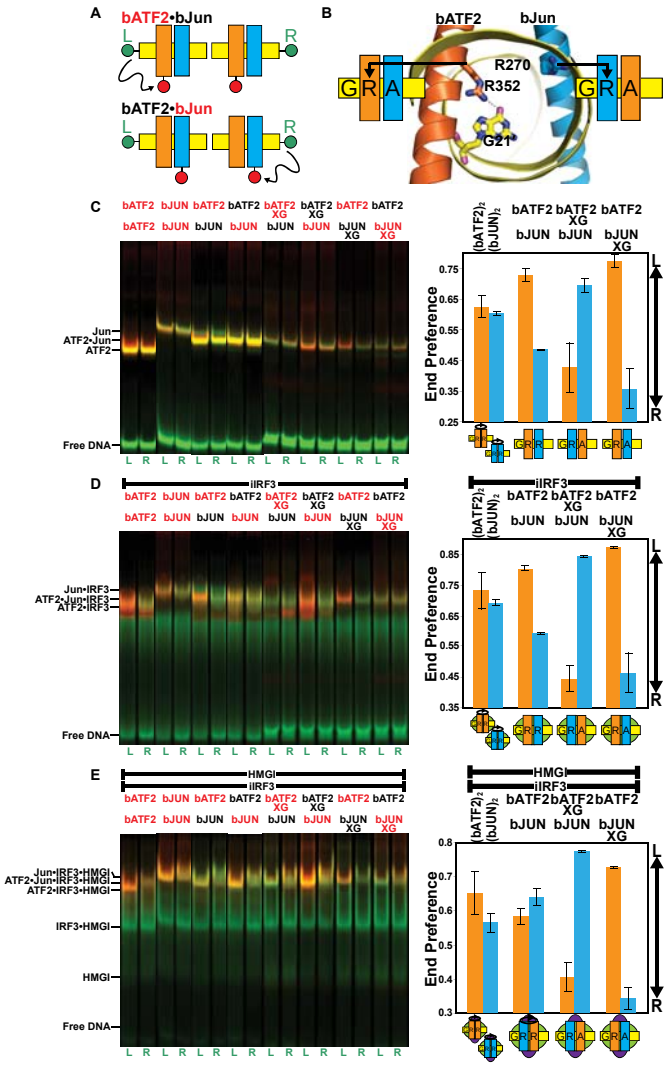

Fig. 2.1. bATF2-bJun heterodimers bind IFNb in both orientations in association with iIRF3 and HMGI. (A) Diagram illustrating the determination of bATF2-bJun heterodimer orientation at IFNb by gelFRET analysis. bATF2(orange)-bJun(cyan) heterodimers labeled with TR (red) on either subunit were bound to IFNb (yellow) labeled with 6-FAM (green) at either the left (L) or the right (R) end. bATF2-bJun heterodimers that bind to IFNb in opposite orientations are predicted to produce different relative efficiencies of energy transfer from donor fluorophores linked to opposite ends of the oligonucleotide. (B) Molecular model depicting symmetry-related arginines in the basic regions of ATF2 (R352) and Jun (R270), only one of which can contact the asymmetric guanine (G21') in IFNb depending on the orientation of heterodimer binding. The model was created using PyMOL Molecular Graphics System (3) and coordinates from the RCSB Protein Data Bank [www.pdb.org (1), PDB ID: 1T2K] in agreement with the published structure (12). The diagrams to the left and right of the structure show the predicted shifts in heterodimer orientation resulting from substitution of the arginine in either subunit by an alanine. (C) GelFRET analysis of the orientation of bATF2-bJun binding at IFNb. The proteins labeled with TR are shown in red type above the lanes. The oligonucleotide ends labeled with 6-FAM are shown below the lanes. The diagrams below the bar graphs indicate the preferred orientations of dimer binding. (D) GelFRET analysis of complexes formed by the same proteins in association with iIRF3 (green oval). (E) GelFRET analysis of complexes formed by the same proteins in association with iIRF3 and HMGI (blue oval). The data shown represent the mean values and standard deviations from at least two separate experiments.

bJun was labeled with Texas red C_5-bromoacetamide (TR) on a cysteine residue at the amino-terminal end [Fig 2.6B]. The heterodimers were incubated with DNA duplexes centered on the ATF2-Jun recognition sequence in the promoter-proximal interferon-beta enhancer element [IFNb, Fig. 2.6A]. IFNb was labeled at the 5' end of either the sense (left end) or the anti-sense (right end) strand with 6-carboxyfluorescein (6-FAM) [Fig. 2.6A]. bATF2-bJun-IFNb complexes were separated by polyacrylamide gel electrophoresis and were analyzed by scanning the gel using a laser that preferentially excited the donor fluorophore. The fluorescence emissions of both donor (green) and acceptor (red) fluorophores were measured at each position of the gel and were superimposed to produce the figure. Complexes formed by bATF2-bJun heterodimers migrated with mobilities distinct from complexes formed by either bATF2 or bJun homodimers [Fig. 2.1C].

We measured the relative efficiencies of energy transfer from the left *versus* right ends of IFNb by comparing the acceptor-to-donor emissions ratios of bATF2-bJun-IFNb complexes labeled on the left *versus* the right end of IFNb. The relative end preferences of complexes labeled on bATF2 (orange bars) *versus* bJun (cyan bars) were used to determine the preferred orientation of heterodimer binding at IFNb. We used labeled bATF2 and bJun homodimers to estimate the end preferences of complexes that had no orientation preference. Homodimers formed by labeled bATF2 or by labeled bJun had similar end preference values. In contrast, heterodimers labeled on bATF2 had a higher (left) end preference than heterodimers labeled on bJun [Fig 2.1C]. This indicates that bATF2-bJun bound IFNb in a preferred orientation in which bATF2 favored the left half-site and bJun favored the right half-site.

II.A.i. Effect of XG-substitutions in bATF2 *versus* bJun

The difference in end preferences between bATF2-bJun heterodimers labeled on bATF2 *versus* bJun indicated that the heterodimer binds to IFNb in a preferred orientation. However, this does not indicate the heterodimer binds in only one orientation. To estimate the degree of orientation preference of bATF2-bJun at IFNb, we compared the end preferences of wild-type heterodimers with those of heterodimers containing amino acid substitutions that are predicted to bias the orientation of heterodimer binding. Previous studies have shown that mutually exclusive interactions between the central asymmetric guanine base in the AP-1 recognition sequence and symmetry-related arginine residues in Fos *versus* Jun mediate opposite orientations of Fos-Jun heterodimer binding (7, 10). The homologous arginine residue in ATF2 (R352) contacts the central asymmetric guanine base (G21') in the crystal structure of DNA-binding domains of ATF2, Jun, and IRF3 bound to the interferon-β enhancer (12). We predicted that alternative interactions between R352 of bATF2 or the homologous arginine in bJun (R270) with the asymmetric guanine base could similarly mediate opposite orientations of bATF2-bJun binding to IFNb.

Substitution of R352 in bATF2 by an alanine (bATF2XG) reversed the relative end preferences of heterodimers labeled on bATF2 *versus* bJun compared to the wild type proteins. Conversely, substitution of the homologous arginine (R270) in bJun by an alanine (bJunXG) increased the difference between the end preferences of heterodimers labeled on bATF2 *versus* those labeled on bJun compared to the wild type proteins. These results are consistent with reversal of the orientation of bATF2-bJun binding by the former substitution and enhancement of the orientation preference by the latter

substitution [Fig 2.1C]. The effects of these amino acid substitutions were reversed by inversion of the asymmetric central base pair, and these substitutions had no detectable effect on end preferences at a binding site containing a symmetrical central dinucleotide (data not shown). Amino acid substitutions at either R352 of bATF2 or R270 in bJun can therefore control the orientation of bATF2-bJun heterodimer binding at IFNb by altering contacts with the asymmetric central guanine.

To determine the proportion of bATF2-bJun heterodimers that bound IFNb in each orientation, we compared the end preferences of wild type bATF2-bJun heterodimers and those of heterodimers containing either the R352A or R270A substitutions. The larger differences in the end preferences of bATF2XG-bJun and bATF2-bJunXG heterodimers labeled on different subunits compared to those of wild-type heterodimers indicate that although wild type bATF2-bJun heterodimers bind IFNb in a preferred orientation, they do not bind IFNb in a fixed orientation. We estimate that no more than 70% of bATF2-bJun heterodimers bind IFNb in the orientation where Jun favors the right half-site.

II.B. Analysis of bATF2-bJun-iIRF3-IFNB complexes

Two IRF3 molecules can bind to sites overlapping and downstream of the ATF2-Jun recognition sequence in IFNb [Fig. 2.1A]. We examined the effect of truncated IRF3 encompassing the minimal DNA binding domain (iIRF3: residues 1 to 111) on the orientation preference of bATF2-bJun binding at IFNb. iIRF3 alone did not form a stable complex at IFNb, but its binding was stabilized by association with bATF2-bJun [Fig. 2.2, compare lanes 2 and 4]. iIRF3 binding was also stabilized by association with bATF2

and bJun homodimers as well as with bATF2XG-bJun and bATF2-bJunXG heterodimers [Fig. 2.1D]. iIRF3 binding can therefore be stabilized by multiple configurations of bATF2 and bJun heterodimers and homodimers.

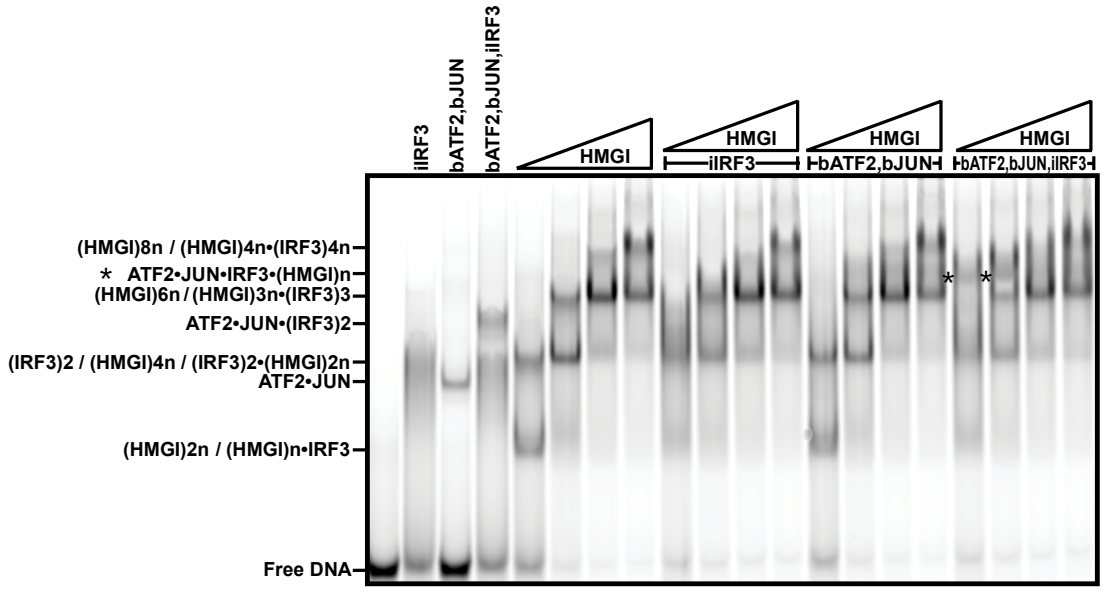

Fig. 2.2. HMGI co-binds with bATF2-bJun-iIRF3 complexes at IFNb. (The proteins indicated above the lanes were incubated with IFNb, and the complexes were separated by gel electrophoresis. Formation of multi-subunit complexes was inferred based on comparison of the banding patterns in lanes with multiple proteins *versus* lanes containing the individual protein or pair-wise combinations of proteins.

iIRF3 binding increased the efficiencies of energy transfer from the left compared to the right end of IFNb for all complexes, resulting in higher absolute end preference values for all heterodimers and homodimers [compare Fig. 2.1C and 2.1D]. However, iIRF3 binding did not change the relative end preferences of heterodimers labeled on bATF2 *versus* bJun compared with those of bATF2 and bJun homodimers. The changes in the absolute, but not in the relative end preference values of these complexes upon iIRF3 binding were likely caused by changes in the structures of these complexes that

altered the relative efficiencies of energy transfer from opposite ends of the oligonucleotide, but did not change heterodimer orientation. Taken together, the absence of a change in bATF2-bJun orientation preference upon iIRF3 binding and the stabilization of iIRF3 binding by bATF2 homodimers, bJun homodimers, and bATF2-bJun heterodimers bound in opposite orientations suggest that iIRF3 can interact equally with bATF2 and with bJun at IFNb.

II.C. Analysis of bATF2-bJun-iIRF3-HMGI complexes

The structural nature and specificity of HMGI interactions with ATF2-Jun-IRF3 and the interferon-β enhancer remain unclear. Studies have suggested that one HMGI molecules bind to at least two sets of AT-rich sequences that flank PRDIV (14). However, attempts to co-crystalize HMGI with ATF2, Jun, and IRF3 at an interferon-β enhancer elements have failed (12). Furthermore, studies by Dragan *et al.* have suggested that HMGI and IRF3 compete for binding to the interferon-β enhancer in the presence of ATF2-Jun heterodimers (5).

II.C.i. Gel-shift analysis of HMGI complexes

We investigated the effects of HMGI binding on the mobility of bATF2-bJun-iIRF3 complexes at IFNb. HMGI alone formed at least four complexes with different electrophoretic mobilities at IFNb [Fig. 2.2, 2.3]. The addition of HMGI to bATF2-bJun produced a complex with mobility distinct from either HMGI or bATF2-bJun alone [Fig. 2.2], indicating the formation of a bATF2-bJun-HMGI complex at IFNb. The addition of

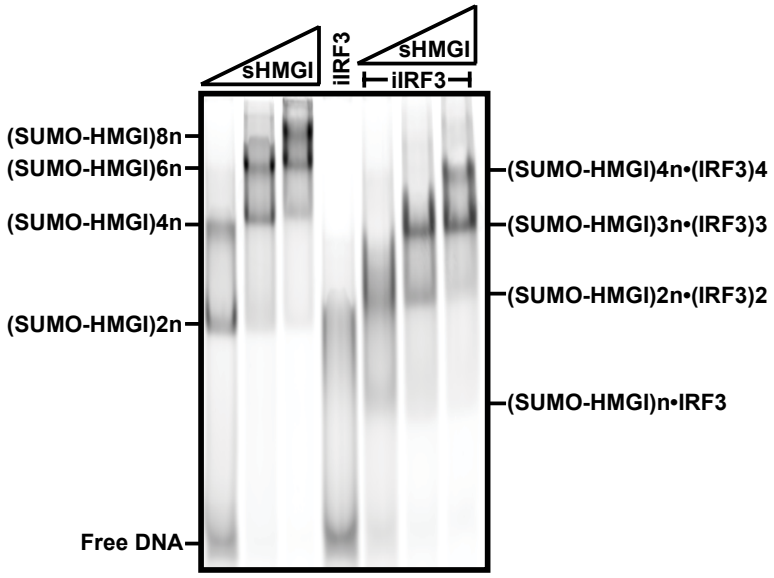

Fig. 2.3. Formation of HMGI-IRF3 heterodimers at IFNb. The proteins indicated above the lanes were incubated with IFNb, and the complexes were separated by gel electrophoresis. To determine whether HMGI and iIRF3 form a complex at IFNb, the banding pattern for SUMO-HMGI fusion protein (sHMGI) together with iIRF3 was compared to the banding pattern for each protein alone. The addition of HMGI to lanes containing iIRF3 eliminated the smearing seen in lanes containing iIRF3 alone yet resulted in bands whose mobilities were indistinguishable from lanes containing HMGI alone.

HMGI to iIRF3 produced the same mobility complexes observed for HMGI alone while eliminating the smearing observed in the presence of iIRF3 alone, indicating that HMGI either competitively inhibits the binding of iIRF3 or that iIRF3 is contained in the bands observed [Fig. 2.2].

To distinguish between complexes containing either HMGI alone or HMGI and iIRF3 together, the bands formed by IFNb were compared in the presence of SUMO-tagged HMGI (SUMO-HMGI), iIRF3, or SUMO-HMGI and iIRF3 together. SUMO-HMGI and iIRF3 in combination formed complexes that were not observed in the presence of either protein alone [Fig. 2.3], indicating that SUMO-HMGI and iIRF3 formed a complex at IFNb. Gradual increases in HMGI concentration to either bATF2-bJun or bATF2-bJun and iIRF3 together produced a complex with mobility

corresponding to HMGI alone at the expense of either bATF2-bJun-HMGI or bATF2-bJun-iIRF3-HMGI complexes, suggesting that HMGI and bATF2-bJun can compete for binding to IFNb [Fig. 2.2].

II.C.ii. Effect of HMGI on heterodimer orientation

To determine the orientation preference of bATF2-bJun in the presence of HMGI and iIRF3, the relative end preference values for bATF2-bJun-iIRF3-HMGI complexes labeled on bATF2 *versus* bJun were compared to the relative end preference values of complexes containing bATF2 homodimers, bJun homodimers, bATF2XG-bJun heterodimers, or bATF2-bJunXG heterodimers bound to IFNb. Similar to the analysis of homodimers alone and homodimers in the presence of iIRF3, bATF2 and bJun homodimers in combination with iIRF3 and HMGI had end preference values that were not significantly different from each other [Fig. 2.1E]. Also, even in the presence of HMGI, bATF2XG-bJun and bATF2-bJunXG had strong, opposite orientation preferences [Fig. 2.1E].

In contrast, HMGI binding caused a shift in the relative end preferences of wild-type bATF2-bJun heterodimers in association with iIRF3 [Fig. 2.1E]. Whereas bATF2 favored binding to the left half-site and bJun to the right half-site alone and in the presence of iIRF3, the difference in the end preference values of bATF2-bJun heterodimers labeled on different subunits was markedly reduced upon HMGI binding to complexes containing iIRF3 at IFNb [compare Fig. 2.1D and 2.1E]. In contrast, HMGI binding had little effect on the relative end preference values of bATF2XG-bJun and bATF2-bJunXG heterodimers [compare Fig. 2.1D and 2.1E]. Thus XG amino acid substitutions inhibit the effect of HMGI on heterodimer orientation preference, indicating

that the effects of HMGI on the orientation preference of wild-type heterodimers are mediated through interactions between bATF2-bJun and DNA.

II.D. Comparison of different fluorophores and oligonucleotides

Labeling of the protein and DNA with fluorescent probes could alter their functional properties by inducing alternative conformations or steric hindrance. We investigated potential effects of the fluorophore used to label bATF2 and bJun on gelFRET analysis of the orientation of bATF2-bJun binding in complexes with iIRF3 and HMGI [Fig. 2.4]. There was no detectable difference in the effects observed when bATF2-bJun heterodimers labeled with Alexa568 (AX) [Fig. 2.4] compared to heterodimers labeled with Texas red C_5-bromoacetamide (TR). Thus, the fluorescent label did not influence the fraction of heterodimers bound in each orientation. Similarly, DNA oligonucleotides 47 bp in length (IFN47) resulted in equivalent orientation preferences obtained after calibration of the end preference values [Fig. 2.4]. Thus, the fluorescent labels did not influence the orientation of bATF2-b-Jun heterodimer binding.

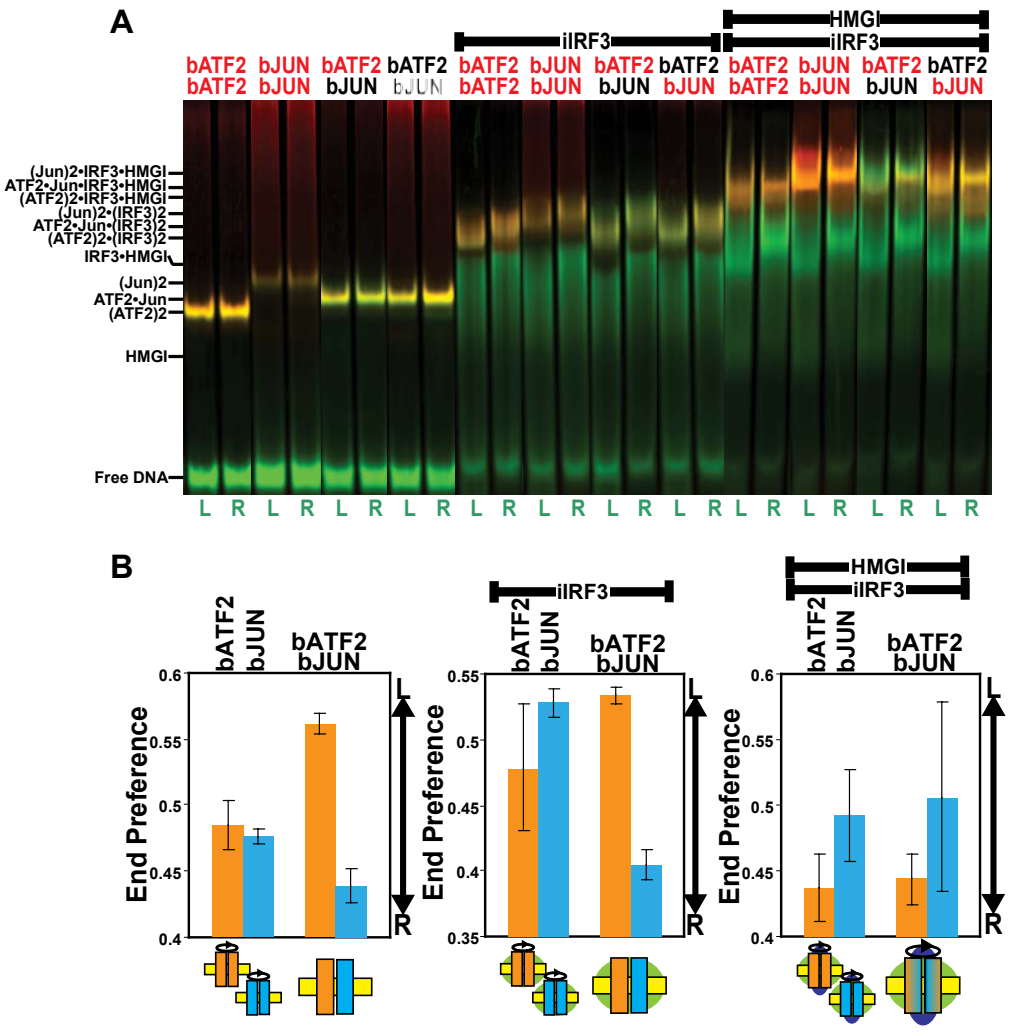

Fig. 2.4. The effects iIRF3 and HMGI on bATF2-bJun orientation preference are comparable in complexes that are conjugated to a different acceptor label and that include a larger oligonucleotide. (A) Gel separated of Alexa568 (AX)-labeled $(bATF2)_2$, $(bJun)_2$, and bATF2-bJun complexes bound to a 47-bp oligonucleotide (IFN47). (B) Relative end preferences of complexes labeled on different subunits.

II.E. Effects of regions outside of bATF2 and bJun

To test potential effects of regions missing in bATF2 and bJun, we measured the effects of iIRF3 and HMGI on the end preferences of heterodimers formed by full-length ATF2 with labeled bJun and labeled bATF2 with full-length Jun. iIRF3 binding to IFNb had little effect on the relative end preferences of these heterodimers, consistent with the lack of an effect of iIRF3 on the orientation of bATF2-bJun heterodimers [Fig. 2.5]. Moreover, the relative end preferences of heterodimers formed by full-length ATF2 with labeled bJun and labeled bATF2 with full-length Jun in association with iIRF3 were reduced upon HMGI binding to IFNb [Fig 2.5]. Thus, iIRF3 as well as HMGI had similar effects on the orientations of bATF2-bJun heterodimers and on heterodimers formed by the full-length protein with bATF2 and with bJun. bATF2 and bJun are therefore valid models for studies of interactions with iIRF3 and HMGI.

III. SUMMARY AND CONCLUSIONS

Previous studies regarding the mechanism of cooperative DNA-binding by ATF2-Jun and IRF3 at the interferon-β enhancer element have produced discordant results (6, 12). We believe that our assay more accurately reveals the true nature of this regulatory complex than past methods because the photo-crosslinking method assay was designed in the absence of a detailed structural understanding of the complex, whereas bATF2, bJun, and IFNb labels used in my analysis were placed at safe distances from the heterodimer-IRF3 interaction surfaces that have been revealed by x-ray crystallography (12).

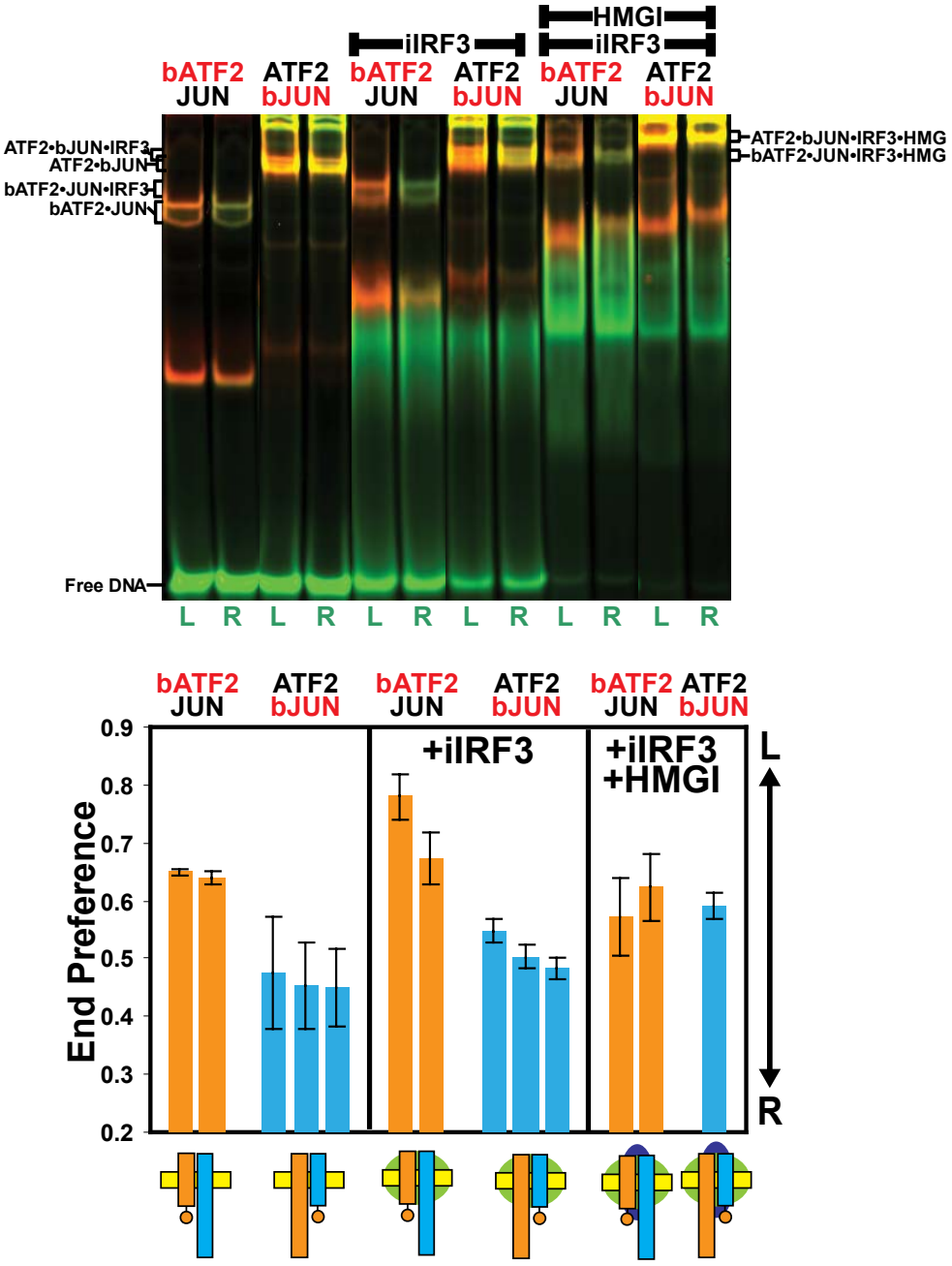

Fig. 2.5. Domains outside of either bATF2 or bJun do not qualitatively influence the relative end preferences of bATF2-bJun, bATF2-bJun-iIRF3, or bATF2-bJun-iIRF3-HMGI complexes at IFNb. The end preferences of heterodimers containing one labeled truncated subunit and one full-length subunit (ATF2-bJunTR *versus* ATF2TR-Jun) were determined at the IFN40 site alone, with bound iIRF3, or with bound iIRF3 and HMGI. Similar to complexes containing two truncated subunits, the end preference value for Jun-labeled subunits was significantly higher than the end preference value for ATF2-labeled complexes in either the absence or presence of iIRF3. Also similar to complexes containing two truncated subunits, the end preference value for Jun-labeled subunits was more similar to the end preference value for ATF2-labeled complexes in the presence of HMGI. Together, this indicated that domains not included in bATF2 or bJun do not interact with iIRF3 or iIRF3 and HMGI together.

Furthermore, although the crystal structure can accurately reflect specific protein-protein and protein-DNA contacts that occur, it can at the same time, impose artificial order restrictions on intrinsic disorder within the complex such as an opposite binding orientation that occurs in a minority of complexes. Similar interpretations have been made for incongruous results for x-ray crystallographic and solution studies of the DNA-binding orientation preference of TATA-binding protein (2).

My orientation preference results are supported by recent microcalorimetry analysis that indicate 70% of ATF2-Jun-DNA complexes have a heterodimer orientation in which Jun is bound to the right half-site and that this orientation preference does not change with the addition of IRF3 (5, 8). My study, however, contradicts their data that indicates IRF3 and ATF2-Jun bind independently. We clearly show that specific amino acid mutations in ATF2, Jun, and IRF3 can functionally interact in the context of heterodimer binding orientation preference and IRF3 binding. Although these interactions do not significantly affect the amount of ATF2-Jun binding, they do significantly affect IRF3 binding. It appears that cooperative binding with IRF3 in some way inhibits the interaction of ATF2-Jun with its binding site such that the effect of favorable interactions with ATF2-Jun on ATF2-Jun binding is cancelled out. This observation is supported by the x-ray crystal structure where the binding of the 5' IRF3 molecule appears to bend the DNA away from the heterodimer subunit that binds the right half-site.

Recent publications do not mention HMGI as a component of the enhanceosome or as a means responsible for the cooperation of its components (5, 11, 12). Exclusion of HMGI from considerations of enhanceosome assembly was perhaps a consequence of

failure to co-crystallize HMGI and other components of the complex previously thought to interact with HMGI (12). Furthermore, in a recent study, similar fluorescence anisotropy binding isotherms for IRF3 titrated against either the interferon-β enhancer element or ATF2-Jun-HMGI-DNA complexes have indicated that HMGI does not contribute to cooperative DNA-binding by ATF2-Jun and IRF3 on the interferon-β enhancer element (5). Furthermore, since the difference between the two binding isotherms was so small, they concluded that IRF3 displaces HMGI entirely from the DNA (5). Thus, the role of HMGI in the assembly of the enhanceosome remains an outstanding problem. We have shown that although HMGI only contributes modestly to ATF2-Jun-IRF3-DNA complex formation and that IRF3 may displace the 3' HMGI molecule, at least one HMGI molecule indeed co-binds with ATF2-Jun and IRF3 on DNA where it decreases the energy barrier between two opposite ATF2-Jun binding orientations at the IFNβ enhancer. This reveals the limitations of solution studies which may not be as sensitive to specific multi-component complexes that have multiple potential stoicheometries and interactions.

IV. MATERIALS AND METHODS

IV.A. Design of fluorescently-labeled complexes

For the analysis of the orientation preference of ATF2-Jun heterodimers within *in vitro* assembled interferon-β enhancer complexes, it was necessary to construct longer ATF2 and Jun proteins than the bZIP protein fragments traditionally used for gelFRET in order to examine the effects of these additional residues on cooperative interactions with

other proteins. It was also necessary to utilize longer oligonucleotides that included sequences from the interferon-β enhancer which contained binding sites for other proteins. These minimal adjustments allowed detection of the effect of cooperative interactions with other proteins on the orientation of ATF2-Jun binding while, at the same time, allowing FRET to occur between donor fluorophores places at either end of the oligonucleotide to the N-terminal residue of either ATF2 or Jun.

IV.A.i. Donor and acceptor fluorophores

Fluorescein derivatives are the most common organic dyes used for labeling proteins and nucleic acids. Although fluorescein derivatives bleach relatively easily, this is not a concern for gelFRET experiments, since the fluorophores are exposed to the excitation beam for a very short time (approximately 1 ms). The more stable carboxyfluorescein (FAM) is a convenient green fluorophore for oligonucleotide labeling. Fluorescein is a good donor fluorophore due to its high quantum yield and excitation maximum (494 nm), which allows optimal excitation by the 488-nm argon-ion laser. Fluorescein has an emission spectrum (maximum: 525) that overlaps with the excitation spectrum of the long-wavelength dye Texas Red (maximum: 582). Texas Red conjugates have a fluorescence emission spectrum (maximum: 600) that makes them good long-wavelength acceptor dyes for FRET analysis with fluorescein donors. Texas Red conjugates have a higher quantum yield and provide a higher signal over background than conjugates of other long-wavelength red fluorescent dyes, such as rhodamines. In addition, the maleimide and bromoacetamide derivative of Texas Red enables thiol-specific labeling of proteins. Hence fluorescein and Texas Red is a useful donor–acceptor pair for gelFRET analysis of nucleoprotein complexes.

The R_0 distances for most commonly used donor–acceptor pairs are in the range 20–60 A°, and are therefore comparable to the distances between sites on multisubunit complexes and the diameters of many biomolecules. Changes in the distance between the fluorophores have a larger effect on FRET when the distance separating the fluorophores is near the R_0 value for the donor–acceptor pair used. If the donor–acceptor distance narrows to about half the R_0 value, the FRET efficiency is increased to nearly quantitative energy transfer; conversely, if the donor–acceptor distance increases by half the R_0 value, the FRET efficiency is reduced to a nearly undetectable level. Given that the efficiency of FRET depends on the distance between the fluorophores, structural transitions in nucleoprotein architecture can be detected by measuring changes in the efficiency of energy transfer which are due to changes in the proximity of the two fluorophores.

IV.A.ii. Preparation of IFNb oligonucleotides

We use DNA oligonucleotides that are designed to place the donor fluorophores at symmetric positions on opposite sides of the PRDIV recognition element [IFNb, Fig 2.6A]. A 5 base-pair symmetry extension (indicated by line) was appended to the 5’ end of the sense strand and the 3’ end of the anti-sense strand in order to ensure that the local environments of the donor fluorophores on opposite ends of the oligonucleotide are equivalent. Oligonucleotide synthesis and conjugation of the 5’ phosphates to 6-carboxyfluorescein was performed by Integrated DNA Technologies, Inc. (Coralville, IA) Duplexes were prepared by annealing 5’-labeled oligonucleotides to unlabeled strands (4 mg/ml duplex) in the presence of 10 mM KCl by heating to 95°C for a few minutes in a

Fig. 2.6. Design of donor- and acceptor-labeled bATF2-bJun-IFNb complexes. (A) Diagram illustrating recognition sequences in the interferon-β enhancer oligonucleotide (IFNb). The IFNb oligonucleotide contained base pairs -109 to -75 of the human interferon-β element with an additional 5 base pairs symmetrical to the downstream end added to the upstream end (indicated by line). The core ATF2, Jun, and IRF3 recognition sequences are indicated by brackets. The approximate sequences that are contacted by HMGI (indicated by brackets) have been determined based on DNase I protection analysis (13, 14). The 5'-phosphates labeled with 6-FAM in left- and right-end labeled duplexes are indicated by arrows. (B) Diagram illustrating bATF2 (amino acid residues 322-397 of human ATF2) and bJun (amino acid residues 240-315 of human Jun) protein fragments. bATF2 residues 353-397 and bJun residues 271-315 are not shown. Amino acid residues in bATF2 and bJun that were included in the crystal structure (Panne *et al.* 2004) are depicted as alpha-helices whereas residues not included in the crystal structure are depicted as coils. The amino-terminal cysteine residues used for labeling with TR are indicated by red font. Arginine residues in bATF2 and bJun that contact the central guanine bases of AP-1 and CRE sites are highlighted in yellow.

water bath and then slowly reducing the temperature to 25°C. The duplexes were separated from single strands by 5% PAGE in 25 mM Tris, 195mM glycine gel buffer run for 2 h at room temperature. The labeled duplex bands were visualized using an UV transilluminator and excised. Subsequently, the annealed duplexes were recovered by overnight incubation in TE buffer at 37°C. Approximately 60% of the annealed DNA was recovered under these conditions. The annealed duplexes were stored in the dark at -20°C. The concentrations of the duplexes were determined spectrophotometrically at 260 nm.

IV.A.iii. Preparation of bATF2, bJun, iIRF3, and HMGI proteins

Since the X-ray crystal structure of ATF2-Jun-IRF3 at the interferon-β enhancer element was available, sites for fluorophore coupling could be introduced at positions that are predicted not to alter biological functions such as DNA binding and interactions with IRF3. The amino acid residues on the amino-terminal sides of the basic regions of ATF2 and Jun project down out of the major groove. These residues are shifted by approximately 30 Å between the two orientations of ATF2-Jun heterodimer binding and are not involved in any direct contact with DNA or the DNA-binding domain of IRF3 (12). Therefore, opposite orientations of heterodimer binding were predicted to cause a large change in distance between a fluorophore attached on the amino-terminal side of the basic region of ATF2 or Jun and a fluorophore attached to the end of the IFNb oligonucleotide.

Proteins encompassing amino acid residues 322-397 of ATF2 [Fig. 2.6B, bATF2], 240-315 of Jun [Fig. 2.6B, bJun], 1-111 of IRF3 (iIRF3), 1-107 of HMGI (full-length) were expressed as His-SUMO fusions in *Rosetta2* competent cells (Novagen) induced with 1 mM IPTG for 3 h at 37°C. Proteins were purified from cell lysates by nickel chelate affinity chromatography in the presence of 6M guanine-hydrochloride (10). The guanine-extracted proteins were renatured at 4°C by dialyses using 8-kDa molecular mass cutoff membranes in 1) 25 mM succinate pH 4, 10% glycerol, 5 mM β-mercaptoethanol, and 1 M guanidine hydrochloride for at least 2 h, 2) 25 mM succinate pH 4, 10% glycerol, 1 mM DTT, and 0.1 M guanidine hydrochloride at least 1 h, 3) 25 mM succinate pH 4, 10% glycerol, 1mM DTT at least 3 h, and 4) 25 mM succinate pH 4, 10% glycerol, 1mM DTT overnight. The His-SUMO tag was removed by incubation

with His-tagged ULP1 protease in a reaction buffer containing 0.5M tris-HCl pH 8, 2% NP-40, 10 mM DTT, and 1.5 M NaCl for at least 24 hours at 4°C. The cleaved proteins were then purified from His-SUMO and His-ULP1 by nickel chelate affinity chromatography using an equilibration/elution buffer containing high salt (25 mM tris-HCl pH 8, 5% glycerol, 1mM DTT, 10 mM imidazole pH 8, and 1M NaCl) in order to prevent retention of the cleaved proteins on the column. 3-kDa molecular mass cutoff Microcon columns were used for salt removal and protein concentration according to the manufacturer's protocol (Millipore, Inc.). The proteins were eluted with a buffer containing of 25 mM succinate pH 4, 10% glycerol, and 1 mM DTT.

bATF2 and bJun proteins used for labeling were treated with 25 mM β-mercaptoethanol for 10 minutes at room temperature and dialyzed at 4°C in buffer containing 0.2M $NaPO_4$ pH 8, 6M guanidine-hydrochloride, 0.5M EDTA, and 200 μM DTT overnight. Following dialysis, the buffer was exchanged for a buffer containing 6M guanidine-hydrochloride, 50 mM tris-HCl, and 700 μM TCEP (adjusted to pH 7.4) using size exclusion chromatography. During labeling, Texas red's thiol-reactive bromoacetamide functional group alkylates the thiols present on the protein's cysteine residues to generate chemically stable thioethers. Therefore, I treated the protein with β-mercaptoethanol and dialyzed in the initial buffer to ensure optimal reduction of thiol-groups, and then substituted DTT with TCEP and reduced the pH from 8 to 7.4 in the second buffer in order to eliminate competition with the label for the protein's thiol group and prevent amine labeling, respectively, while still maintaining a reduced state.

The proteins were labeled on unique cysteine residues appended to the amino-terminal ends [Fig. 2.6] with a 20-fold molar excess of Texas red C_5 bromoacetamide

(Molecular Probes, Eugene, OR) added dropwise while lightly vortexing the protein in an amber-colored tube. Labeling reactions were carried out for at least 3 h at room temperature and overnight at 4°C. Excess dye was removed using size exclusion chromatography. Removal of the remaining dye was accomplished by performing extensive dialyses in the dark over several days in 25 mM succinate pH 4, 10% glycerol, and 3 M guanidine hydrochloride. Renaturation was performed in the dark at 4°C by dialyses in 1) 25 mM succinate pH 4, 10% glycerol, and 1 M guanidine hydrochloride for at least 2 h, 2) 25 mM succinate pH 4, 10% glycerol, and 0.1 M guanidine hydrochloride at least 1 h, 3) 25 mM succinate pH 4 and 10% glycerol at least 3 h, and 4) 25 mM succinate pH 4, 10% glycerol overnight. The proteins were analyzed by SDS-PAGE and concentrations were measured using Bradford reagent (Bio-Rad, Hercules, CA).

IV.B. Heterodimer-DNA complex formation and separation by PAGE

Complexes are formed by incubation of heterodimers containing one subunit labeled with a TR acceptor with oligonucleotides (500 nM) labeled with a FAM donor on either end. A 2:1 molar ratio of Jun to ATF2 is used to minimize the formation of ATF2 homodimer complexes. To obtain more than 50% binding of the labeled oligonucleotides after gel electrophoresis, the proteins were used at 500 nM dimer. The protein concentration and the amount of complex formed did not influence the end preference values. The heterodimers and IFNb oligonucleotides were incubated for 10 min at room temperature in a binding buffer containing of 20 mM Hepes, pH 7.6, 100 mM KCl, 5% glycerol, 1 mM EDTA, 5 mM DTT, 0.5 mg/ml bovine serum albumin, 0.1% (w/w) Nonidet P-40, and 0.1 mg/ml poly(dI-dC). The ATF2–Jun heterodimer complexes were

separated from ATF2 homodimer complexes and free DNA by native 8% PAGE in a gel buffer containing 25 mM Tris, 195 mM glycine for 2 h in the dark at 4C and 300 V. The gels were prepared between low-fluorescence glass plates (C.B.S. Scientific Co.) to minimize background when scanning. The total background including the contribution from thin polyacrylamide gels was generally very low, accounting for approximately 2% of the signal.

IV.C. Detection of fluorescence emissions

The gelFRET assay requires the use of a fluorescence imaging instrument that allows measurement of the donor and acceptor emissions at each position of the gel. A 488-nm laser beam is directed to each position across the gel by a galvanometer-controlled mirror. When the laser beam hits a spot containing a fluorophore, the fluorophore emits light with a characteristic spectrum. In complexes where the donor and acceptor fluorophores are in close proximity, a portion of the excitation energy from the donor fluorophore is transferred to the acceptor fluorophore. The emitted light from both donor and acceptor fluorophores is collected by a fiberoptic bundle and is passed through emission filters. Subsequently, a photomultiplier tube detects the light that passes through the filters and differences in signal intensity are used to produce a digital image.

To separate the donor and acceptor fluorescence emissions, the gel is scanned twice times using different emission filters (donor emission filter and acceptor emission filter) and the data are collected in a pixel-by-pixel alignment for each scan. Thus, both donor and acceptor fluorescence emissions can be determined for each nucleoprotein complex resolved by gel electrophoresis.

V. BIBLIOGRAPHY

1. **Berman, H. M., J. Westbrook, Z. Feng, G. Gilliland, T. N. Bhat, H. Weissig, I. N. Shindyalov, and P. E. Bourne.** 2000. The Protein Data Bank. Nucleic Acids Res **28:**235-42.
2. **Cox, J. M., M. M. Hayward, J. F. Sanchez, L. D. Gegnas, S. van der Zee, J. H. Dennis, P. B. Sigler, and A. Schepartz.** 1997. Bidirectional binding of the TATA box binding protein to the TATA box. Proc Natl Acad Sci U S A **94:**13475-80.
3. **DeLano, W. L.** 2008. The PyMOL Molecular Graphics System, 1.1 ed. DeLano Scientific LLC, San Carlos, CA, USA.
4. **Diebold, R. J., N. Rajaram, D. A. Leonard, and T. K. Kerppola.** 1998. Molecular basis of cooperative DNA bending and oriented heterodimer binding in the NFAT1-Fos-Jun-ARRE2 complex. Proc Natl Acad Sci U S A **95:**7915-20.
5. **Dragan, A. I., R. Carrillo, T. I. Gerasimova, and P. L. Privalov.** 2008. Assembling the human IFN-beta enhanceosome in solution. J Mol Biol **384:**335-48.
6. **Falvo, J. V., B. S. Parekh, C. H. Lin, E. Fraenkel, and T. Maniatis.** 2000. Assembly of a functional beta interferon enhanceosome is dependent on ATF-2-c-jun heterodimer orientation. Mol Cell Biol **20:**4814-25.
7. **Glover, J. N., and S. C. Harrison.** 1995. Crystal structure of the heterodimeric bZIP transcription factor c-Fos-c-Jun bound to DNA. Nature **373:**257-61.
8. **Lagrange, T., T. K. Kim, G. Orphanides, Y. W. Ebright, R. H. Ebright, and D. Reinberg.** 1996. High-resolution mapping of nucleoprotein complexes by site-specific protein-DNA photocrosslinking: organization of the human TBP-TFIIA-TFIIB-DNA quaternary complex. Proc Natl Acad Sci U S A **93:**10620-5.
9. **Leonard, D. A., and T. K. Kerppola.** 1998. DNA bending determines Fos-Jun heterodimer orientation. Nat Struct Biol **5:**877-81.
10. **Leonard, D. A., N. Rajaram, and T. K. Kerppola.** 1997. Structural basis of DNA bending and oriented heterodimer binding by the basic leucine zipper domains of Fos and Jun. Proc Natl Acad Sci U S A **94:**4913-8.
11. **Panne, D., T. Maniatis, and S. C. Harrison.** 2007. An atomic model of the interferon-beta enhanceosome. Cell **129:**1111-23.
12. **Panne, D., T. Maniatis, and S. C. Harrison.** 2004. Crystal structure of ATF-2/c-Jun and IRF-3 bound to the interferon-beta enhancer. Embo J **23:**4384-93.
13. **Thanos, D., and T. Maniatis.** 1995. Virus induction of human IFN beta gene expression requires the assembly of an enhanceosome. Cell **83:**1091-100.
14. **Yie, J., S. Liang, M. Merika, and D. Thanos.** 1997. Intra- and intermolecular cooperative binding of high-mobility-group protein I(Y) to the beta-interferon promoter. Mol Cell Biol **17:**3649-62.

CHAPTER 3: STRUCTURAL MECHANISM OF COOPERATIVE DNA-BINDING BY iIRF3 AND NON-ORIENTED bATF2-bJUN HETERODIMERS AT THE INTERFERON-β ENHANCER

I. INTRODUCTION

I.A. Atomic modeling of bATF2-bJun-iIRF3 complexes

The simplest model to account for the observations that both orientations of bATF2-bJun heterodimers as well as bATF2 and bJun homodimers cooperated with iIRF3 at IFNb is that iIRF3 can contact structurally related amino acid residues in both bATF2 and in bJun. Therefore, we examined the crystal structure for potential symmetrical heterodimer interactions with iIRF3. Additionally, since regions in the N-terminal domains of ATF2 and Jun that would fall proximal iIRF3 were missing from the crystal structure, we extended the N-terminal ends of the basic-region alpha helices of Jun and ATF2 to include 14 additional residues.

I.A.i. Potential amino acid interactions in the left half-site

R345 in ATF2 contacts D45 in IRF3 in the ATF2-Jun-IRF3-IFNb crystal structure where ATF2 binds to the left half-site [Fig 3.1, upper left panel] (6). R263 in Jun is located at a symmetry-related position related to R345 in ATF2 by a 180° rotation about the dimer axis [Fig 3.1, lower left panel]. R263 in Jun could therefore contact D45

in iIRF3 when the heterodimer binds in the opposite orientation. This model predicts that substitution of R345 in bATF2 *versus* R263 in Jun should have opposite effects on the orientation of bATF2-bJun binding at IFNb in association with iIRF3.

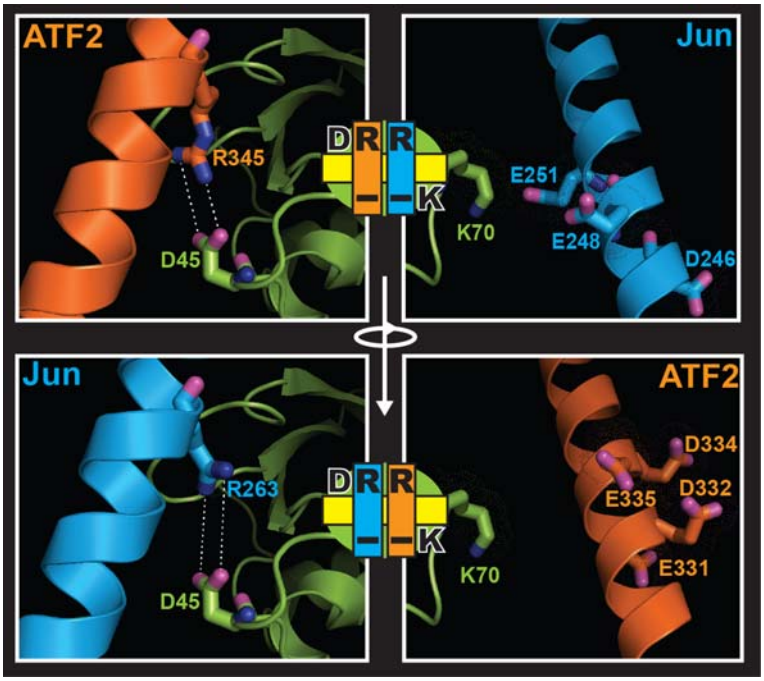

Fig. 3.1. Molecular models for interaction interfaces in iIRF3 and the bATF2-bJun heterodimer. The model contains fourteen additional α-helical amino acid residues on the amino-terminal sides of the basic-regions of ATF2 and Jun compared to the fragments used for crystalization. The upper left panel shows the contact between D45 of IRF3 and R345 in ATF2. The bottom left panel shows the symmetry-related R263 residue in bJun, which could contact D45 when the heterodimer binds in the opposite orientation. The upper right panel shows potential electrostatic interactions between K70 of IRF3 and negatively charged residues adjacent to the basic region in Jun. The lower right panel depicts the symmetry-related negatively charged residues in bATF2, which could interact with K70 when the heterodimer binds in the opposite orientation. The figure was created using the PyMOL Molecular Graphics System (3) and coordinates from the RCSB Protein Data Bank [www.pdb.org (1), PDB ID: 1T2K] in agreement with the published structure (6).

II.A.ii. Potential amino acid interactions in the right half-site

To identify additional interactions between bATF2-bJun and iIRF3 that could affect heterodimer orientation, we examined the roles of amino acid residues on the amino-terminal sides of the bZIP domains of ATF2 and Jun. Both bATF2 and bJun contain a cluster of negatively charged residues adjacent to their basic regions (E331,

D332, D334, E335 in bATF2 and D246, E248, E251 in bJun). Modeling of the residues adjacent to the basic regions by extension of the basic region α-helices in ATF2 and Jun showed that these residues in Jun are in close proximity to K70 of IRF3 [Fig. 3.1, upper right panel] and that these residues in ATF2 are in a similar position relative to K70 of IRF3 when the heterodimer binds to DNA in the opposite orientation [Fig. 3.1, lower right panel].

II. RESULTS AND DISCUSSION

II.A. GelFRET analysis of XD substitutions in bATF2 and bJun

To test the roles of potential interactions between iIRF3 and either bATF2 or bJun in the orientation of heterodimer binding at IFNb, we examined the effects of R345A substitution in bATF2 (bATF2XD) and R263A substitution in bJun (bJunXD) on the orientation of heterodimer binding in the presence and absence of iIRF3. The substitutions in bATF2XD and bJunXD had small effects on the orientation of heterodimer binding in the absence of iIRF3 [Fig. 3.2A]. In complexes formed with iIRF3, the R345A substitution in bATF2 reversed the orientation of bATF2XD-bJun binding compared with wild-type heterodimers [Fig. 3.2B]. Conversely, the R263A substitution in bJun enhanced the opposite orientation preference of bATF2-bJunXD compared with wild type heterodimers in complexes formed with iIRF3 [Fig. 3.2B].

Thus, whereas iIRF3 had a minimal effect on the orientation preference of wild-type bATF2-bJun binding at IFNb, iIRF3 caused opposite shifts in the orientation preferences of bATF2XD-bJun and bATF2-bJunXD binding at IFNb [compare the end

preference values of each heterodimer between Fig. 3.2A and 3.2B]. In each case, the shift in the heterodimer orientation preference caused by iIRF3 binding reflected a decrease in binding by the mutated (XD) subunit to the left IFNb half-site proximal to D45 of iIRF3 and a corresponding increase in binding by the wild type subunit to the left half-site. These results are consistent with contacts between the wild type R263 of bJun or R345 of bATF2 with D45 of iIRF3 at the left IFNb half-site. Simultaneous substitution of both amino acid residues in bATF2 and bJun (bATF2XD-bJunXD)

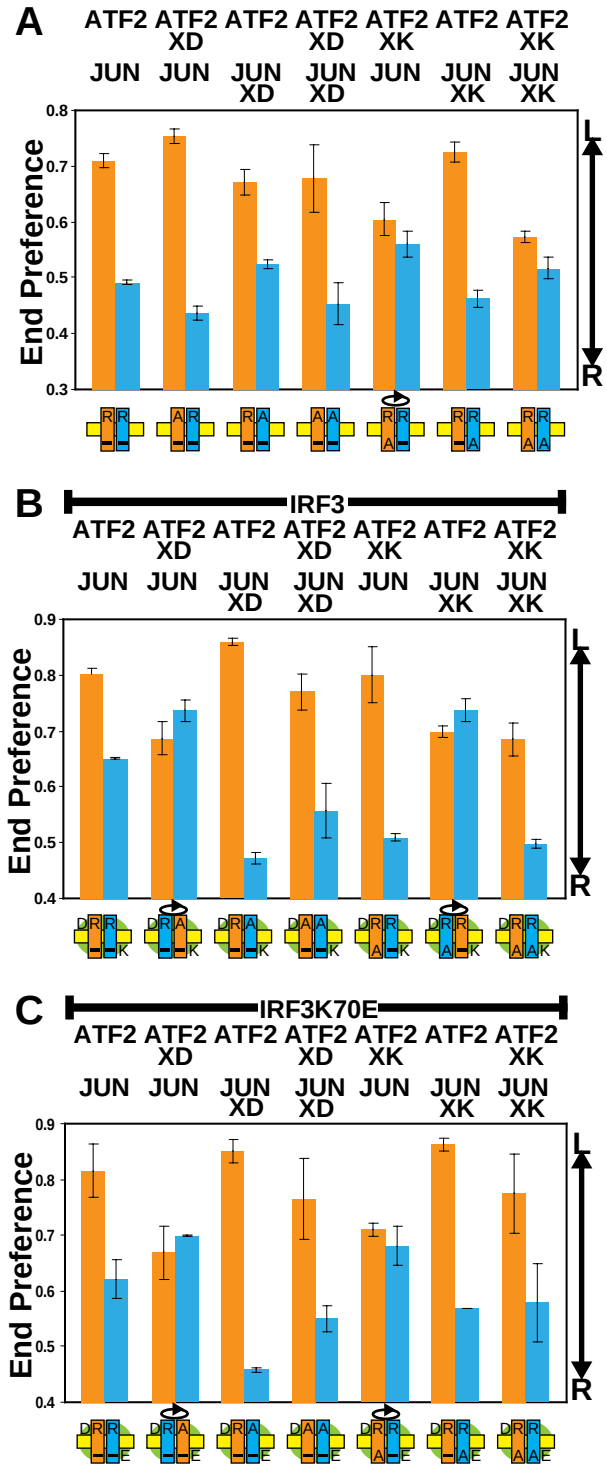

Fig. 3.2. Substitution of symmetry-related amino acid residues in bATF2 *versus* bJun shifts the orientation of heterodimer binding in opposite directions in complexes formed with iIRF3 at IFNb. (A) GelFRET analysis of the effects of symmetry-related amino acid substitutions in bATF2 and bJun on the orientation of heterodimer binding at IFNb. The orientations of heterodimer binding were analyzed for complexes formed with (B) iIRF3, (C) iIRF3K70E. The diagrams below the bars reflect the preferred orientation of heterodimer binding using the symbols described in Fig. 2.1. The data shown represent the mean values and standard deviations from at least two independent experiments.

eliminated the effect of iIRF3 on the orientation of heterodimer binding [compare Fig. 3.2A and 3.2B]. These observations indicate that R345 in ATF2 and R263 in Jun have opposing effects on the orientation of bATF2-bJun binding at IFNb in association with iIRF3.

We attempted to determine the effects of D45A and D45R substitutions in iIRF3 on the orientation of heterodimer binding. Both D45A and D45R substitutions reduced the intrinsic affinity of iIRF3 with IFNb (data not shown). The reduced levels of bATF2-bJun-iIRF3-IFNb complexes formed by these iIRF3 mutants prevented determination of the effects of these mutations in IRF3 on the orientation of bATF2-bJun binding at IFNb.

II.B. GelFRET analysis of XK substitutions in bATF2 and bJun

The amino acid substitutions in bATF2XD and bJunXD that could alter contacts with D45 in IRF3 had smaller effects on heterodimer orientation preference than the amino acid substitutions in bATF2XG and bJunXG that could alter contacts with the central asymmetric guanine. To identify additional interactions between bATF2-bJun and iIRF3 that could affect heterodimer orientation, we examined the roles of amino acid residues on the amino-terminal sides of the bZIP domains of ATF2 and Jun. Both bATF2 and bJun contain a cluster of negatively charged residues adjacent to their basic regions (E331, D332, D334, E335 in bATF2 and D246, E248, E251 in bJun). Modeling of the residues adjacent to the basic regions by extension of the basic region α-helices in ATF2 and Jun suggested that these residues were in the vicinity of K70 of iIRF3 in the heterodimer subunit bound to the right half-site. We examined the effects of substituting

these residues by alanines either in bATF2 (bATF2XK) or in bJun (bJunXK) on heterodimer orientation in the presence and absence of iIRF3.

In the absence of iIRF3, replacement of the negatively charged residues adjacent to the basic region of bATF2 resulted in a lower orientation preference of bATF2XK-bJun heterodimers compared with that of wild type heterodimers at IFNb [Fig. 3.2A]. The corresponding substitutions in bJun had little effect on the orientation of bATF2-bJunXK heterodimer binding. In complexes containing iIRF3, these substitutions in bATF2 increased the orientation preference of bATF2XK-bJun heterodimer binding compared with that of wild type heterodimers at IFNb [Fig. 3.2B]. Conversely, in complexes containing iIRF3, these substitutions in bJun eliminated the orientation preference of bATF2-bJunXK binding at IFNb. Thus, iIRF3 caused opposite shifts in the orientation preferences of bATF2XK-bJun and bATF2-bJunXK binding at IFNb [compare the end preferences of each complex between Fig. 3.2A and Fig 3.2B].

In each case, the shift in the orientation of heterodimer binding reflected a decrease in binding by the mutated (XK) subunit to the right half-site proximal to K70 of iIRF3 and a corresponding increase in binding by the wild type subunit of each heterodimer to the right half-site in which the remaining negatively charged residues could interact with K70 of iIRF3. As expected, simultaneous substitution of both clusters of negatively charged residues in bATF2XK-bJunXK reduced the effect of iIRF3 binding on heterodimer orientation compared to heterodimers in which residues in only one subunit were substituted. These results indicate that residues E331, D332, D334, or E335 in bATF2 and residues D246, E248, or E251 in bJun had opposing effects on the orientation of bATF2-bJun binding at IFNb in association with iIRF3.

K70 in iIRF3 was predicted to interact with the negatively charged residues in either bJun or bATF2, depending on the orientation of heterodimer binding. We tested if replacement of K70 in iIRF3 with glutamate (iIRF3K70E) altered the effects of the negatively charged amino acid residues adjacent to the basic regions in bJun and bATF2 on heterodimer orientation. In complexes formed with iIRF3K70E, the bATF2XK-bJun and bATF2-bJunXK heterodimers had orientation preferences at IFNb that were indistinguishable from their orientation preferences in the absence of iIRF3 [compare the end preferences of each complex between Fig. 2D and Fig. 2B]. Thus, the K70E substitution in iIRF3 eliminated the effects of iIRF3 on the orientation preferences of bATF2XK-bJun and bATF2-bJunXK heterodimers at IFNb. The K70E substitution also eliminated the effects of iIRF3 on the orientations of heterodimers containing individual alanine substitutions at either E331, D332, D334, or E335 in bATF2 or residues D246, E248, or E251 in bJun (data not shown). In contrast, iIRF3K70E caused the same shifts in the orientations of bATF2XD-bJun and bATF2-bJunXD binding at IFNb as those that were caused by wild type iIRF3. These results suggest that the negatively charged residues adjacent to the basic regions of bATF2 and bJun affected heterodimer orientation through mutually exclusive interactions with K70 of iIRF3 at the right half-site of IFNb.

II.C. Quantitative gel-shift analysis of heterodimer-iIRF3 interactions

We investigated if the amino acid residues in bATF2, bJun and iIRF3 whose interactions affected the orientation of heterodimer binding also affected the affinity of complex formation at IFNb. We compared affinities of wild type iIRF3, iIRF3(D45A),

and iIRF3(K70A) association with wild type bATF2-bJun heterodimer at IFNb [Fig. 3.3A]. We also compared the affinities of wild type iIRF3, iIRF3(D45A) and iIRF3(K70A) association with heterodimers containing symmetrical amino acid substitutions in the basic region [Fig. 3.3B, bATFXD-bJunXD] and adjacent to the basic region [Fig. 3.3C, bATF2XK-bJunXK] at IFNb. The K70A substitution in iIRF3 slightly reduced association with wild type bATF2-bJun, severely reduced association with bATF2XD-bJunXD, and slightly enhanced association with bATF2XK-bJunXK at IFNb. In contrast, the D45A substitution in iIRF3 severely reduced association with wild-type bATF2-bJun, moderately reduced association with bATF2XD-bJunXD, and most severely reduced association with bATF2XK-bJunXK at IFNb.

Simultaneous substitution of D45A and K70A in iIRF3 eliminated detectable association with bATF2-bJun at IFNb (data not shown). Likewise, simultaneous substitution of the amino acid residues in bATF2 and bJun predicted to interact with iIRF3 (bATF2XDXK-bJunXDXK) eliminated detectable iIRF3 association with the heterodimer at IFNb (data not shown). These results indicate that interactions between K70 in iIRF3 and the symmetry-related negatively charged residues adjacent to the basic regions of bATF2 (E331, D332, D334, and E335) and bJun (D246, E248, E251) stabilize iIRF3 binding at IFNb and interactions between D45 in iIRF3 and the symmetry-related arginines in the basic regions of bATF2 (R345) and bJun (R263) are the primary determinates of the recruitment of iIRF3 to IFNb by bATF2-bJun.

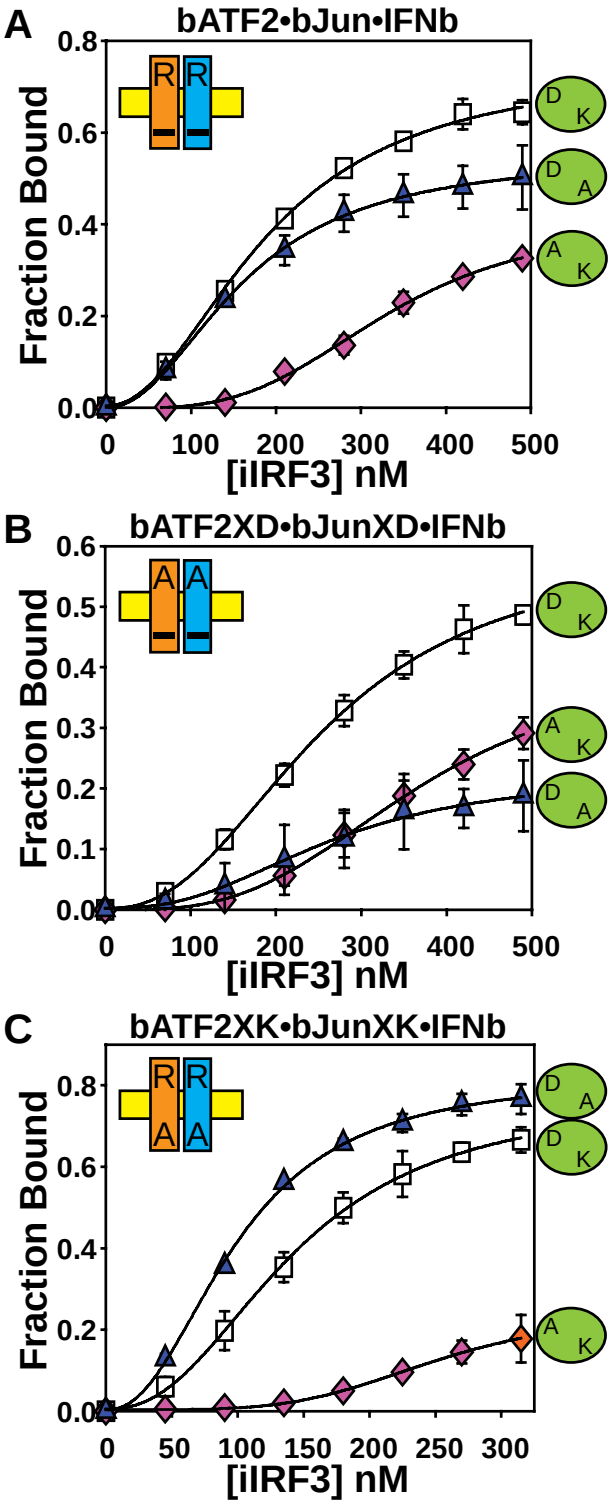

Fig. 3.3. Symmetrical amino acid substitutions in bATF2 and bJun influence the relative affinities of different iIRF3 variants at IFNb. The indicated concentrations of iIRF3, iIRF3D45A, and iIRF3K70A were incubated with IFNb [25 nM] and either (A) bATF2 [35 nM] and bJun [70 nM], (B) bJunXD[35nM] and bATF2XD [70 nM], or (C) bJunXK [35 nM] and bATF2XK [70 nM]. The complexes were separated by gel electrophoresis and the fraction of the heterodimer-IFNb complexes bound by the wild type or mutant iIRF3 was plotted as a function of iIRF3 concentration. The data was fit with sigmoidal logistic curves using SigmaPlot.

II.D. Effect of HMGI on interactions in the complex

HMGI binding reduced the orientation preference of bATF2-bJun association with iIRF3 at IFNb [Fig 2.1E]. We investigated whether HMGI binding affected heterodimer orientation by altering bATF2-bJun interactions with iIRF3, or through independent mechanisms. Substitution of R345 of bATF2 (bATF2XD) or R263 of bJun (bJunXD) had opposite effects on heterodimer orientation both in complexes containing HMGI and iIRF3 and those containing iIRF3 alone [compare Fig. 3.4A and 3.2B]. HMGI therefore did not alter the effects of these symmetry-related amino acid substitutions on heterodimer orientation.

In contrast, substitution of the negatively charged residues adjacent to the basic region of bATF2 (bATF2XK) or bJun (bJunXK) had a large effect on heterodimer orientation in complexes containing iIRF3 alone, but almost no effect in complexes containing iIRF3 together with HMGI [compare Fig. 3.2B and 3.4A]. Therefore, amino acid substitutions in bATF2 and bJun that altered heterodimer interactions with D45 of iIRF3 had equivalent effects on heterodimer orientation in the presence or absence of HMGI, whereas the amino acid substitutions that altered heterodimer interactions with K70 of iIRF3 had distinct effects in the presence of HMGI.

We compared the effects of the K70E substitution in IRF3 on heterodimer orientation in the presence and absence of HMGI to determine if HMGI altered bATF2-bJun interactions with K70 of iIRF3. The K70E substitution had opposite effects on the orientations of bATF2XK-bJun and bATF2-bJunXK heterodimers both in complexes containing HMGI and in those lacking HMGI. Likewise, the K70E substitution had no detectable effects on the orientations of bATF2-bJun, bATF2XD-bJun, bATF2-bJunXD,

bATF2XD-bATF2XD, or bATF2XK-bATF2XK heterodimers either in complexes containing HMGI or in those lacking HMGI (compare Fig. 3.2B with 3.2C and 3.4A with 3.4B). Thus, HMGI did not alter the effects of interactions with K70 in iIRF3 on heterodimer orientation. The distinct effects of amino acid residues in bATF2 and bJun that can contact K70 of iIRF3 on heterodimer orientation in the presence *versus* the absence of HMGI were therefore independent of K70 of iIRF3.

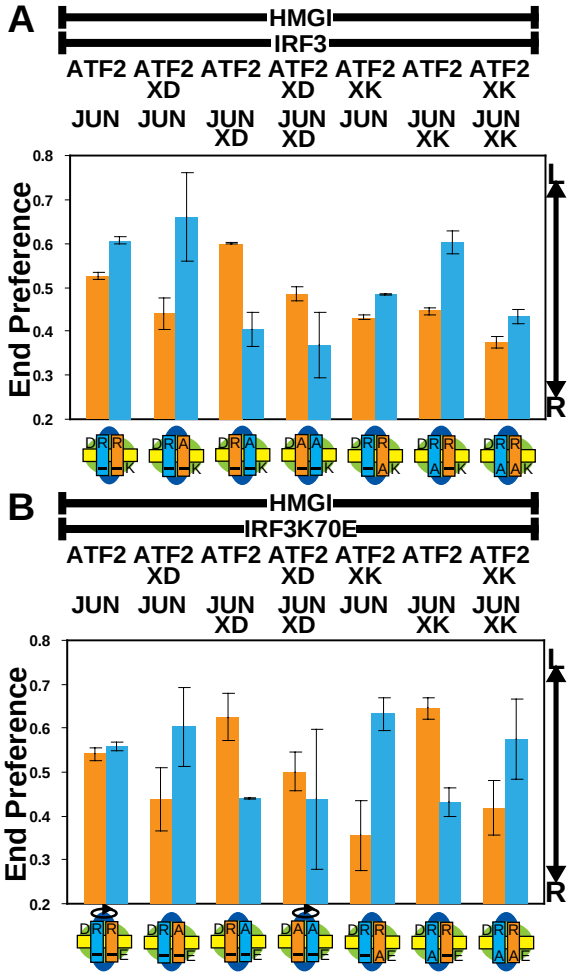

Fig. 3.4. K70E substitution in iIRF3 preferentially influences the orientation preference of bATF2XK-bJun and bATF2-bJunXK heterodimers in complexes containing HMGI. Effects of symmetry-related amino acid substitutions in bATF2 and bJun on the orientation of heterodimer binding at IFNb in complexes formed with (A) iIRF3 and HMGI and (B) iIRF3K70E and HMGI were analyzed by gelFRET. The diagrams below the bars reflect the preferred orientation of heterodimer binding using the symbols described in Fig. 2.1. The data shown represent the mean values and standard deviations from at least two independent experiments.

III. SUMMARY AND CONCLUSIONS

Our results demonstrate that ATF2-Jun-IRF3-HMGI complexes bind cooperatively to the interferon-b enhancer in different configurations. These results establish that the structural organization of multi-protein transcription regulatory complexes can be more variable than predicted by previous studies. Previous studies using different experimental approaches have produced results consistent with opposite orientations of ATF2-Jun association with IRF3 proteins at IFNb (5, 6). It has also been reported that ATF2 and Jun do not bind cooperatively with IRF3 to the interferon-b enhancer (4). The contrasting conclusions from different studies of the orientation of ATF2-Jun heterodimer binding in association with IRF3 at the interferon-β enhancer are consistent with our observation that bATF2-bJun can bind the interferon-β enhancer in both orientations in association with IRF3.

This unexpected flexibility of ATF2-Jun association with IRF3 is due to the presence of charged residues at symmetry-related positions in ATF2 and in Jun that can contact IRF3. Electrostatic interactions between these residues mediate both the opposite orientations of bATF2-bJun binding as well as the stabilization of IRF3 binding at the interferon-b enhancer. The redundancy of the interacting residues in ATF2 and Jun is also consistent with the previous observation that substitution of these residues in ATF2 does not eliminate cooperative DNA binding with IRF3 (6). Consequently, cooperative DNA binding by ATF2 and Jun with IRF3 and HMGI does not require or fix a unique orientation of heterodimer binding.

IV. MATERIALS AND METHODS

IV.A. Generation of alanine-substituted proteins

In order to determine the role of specific amino acid residues in bATF2, bJun, and iIRF3 in cooperative DNA-binding interactions between bATF2-bJun and iIRF3, alanine codon substitutions in bATF2, bJun, and iIRF3 expression vectors were introduced using QuikChange II site-directed mutagenesis kit (Strategene Inc., La Jolla, CA). bATF2XK contained alanine substitutions at amino acid residues E331, D332, D334, and E335, bATF2XD contained an alanine substitution at amino acid residue R345, bJunXK contained alanine substitutions at amino acid residues D246, E248, and E251, and bJunXD contained an alanine substitution at amino acid residue R263 [Fig 3.5]. SUMO-fusion proteins containing the alanine substitutions were expressed and purified in parallel with wild-type proteins (see Chapter 2 Materials and Methods).

Fig. 3.5. Design of alanine substituted bATF2 and bJun proteins. Diagram illustrating locations of charged amino acid residues in bATF2 and bJun (shown in green font) substituted by alanine. Amino acid residues in bATF2 and bJun that were included in the crystal structure (6) are depicted as alpha-helices whereas residues not included in the crystal structure are depicted as coils. The amino-terminal cysteine residues used for labeling with TR are indicated by red font.

IV.B. Quantitative gel-shift analysis of cooperative DNA-binding

Gel mobility shift assays are routinely used to visualize protein-nucleic acid interactions. Quantitative applications of this method enable determination of the thermodynamic properties of protein-nucleic acid complexes. Assay designs can include titration, competition, and stoichiometry experiments. For the analyses of the role of specific amino acid contacts between bATF2-bJun and iIRF3 in cooperative DNA-binding, I have utilized titration experiments in order to determine relative affinities of wild-type *versus* alanine-substituted iIRF3 for heterodimer-DNA complexes containing different alanine substitutions.

IV.B.i. Oligonucleotide labeling

5'-6-FAM-labeled sense and anti-sense IFNb oligonucleotide containing the sequences shown in figure 2.6 was synthesized by Integrated DNA Technologies, Inc. (Coralville, IA). Double-labeled IFNb duplexes were prepared by annealing 5'-labeled IFNb sense strands to 5'-labeled IFNb anti-sense strands (4 mg/ml duplex) in the presence of 10 nM KCl by heating to 95°C for a few minutes in a water bath and then slowly reducing the temperature to 25°C. The duplexes were separated by single strands by 5% PAGE in 25 nM Tris, 195 mM glycine gel buffer run for 2 h at room temperature. The labeled duplex bands were visualized using an UV transilluminator and excised. Subsequently, the annealed duplexes were recovered by overnight incubation in TE buffer at 37°C. The concentrations of the duplexes were determined spectrophotometrically at 260 nm.

IV.B.ii. Titrations with iIRF3 and separation by PAGE

This gel mobility shift assay relies on the property that nucleic acids will migrate through a gel matrix towards an anode upon application of an electric field. The migration through the gel is governed by four primary properties: the molecular weight, charge, and three-dimensional shape of the nucleic acid as well as the physical properties of the gel substrate. Interaction with a protein that modulates the nucleic acid conformation or substantially increases the molecular weight can lead to differential mobility in the gel. The choice of the gel matrix can amplify or dampen this effect depending upon the size and shape of the protein-DNA complex. By this approach, the formation of bATF2-bJun-iIRF3-IFNb complexes can be monitored by comparing the mobility of bATF2-bJun-IFNb complexes in the presence and absence of iIRF3. Differential mobilities if bATF2-bJun-IFNb complexes in the presence *versus* absence of iIRF3 is indicative of an interaction between iIRF3 and bATF2-bJun-IFNb complexes.

This type of experiment is often performed with a single concentration of protein and is sufficient to corroborate binding observed in a separate method. However, a single concentration is not suitable to compare the binding properties of different nucleic acid-binding complexes. This is because the fraction of bound nucleic acid is sensitive to changes in protein concentration for only a narrow range surrounding the equilibrium dissociation constant. For experiments that utilize only one protein concentration, this insensitivity can lead to serious misinterpretations of relative binding affinities.

The concentrations of bATF2, bJun, iIRF3, and IFNb used in the assay must be limiting (sub-saturating) in order to ensure affinity-dependent (rather than concentration-dependent) binding of iIRF3. Under ideal conditions, the total molar concentration of all

of the components should be 10- to 100- fold less than the dissociation constant of the binding protein. Conversely, weak interactions are difficult to measure because significant dissociation of the protein-DNA complex can occur during the time that is takes to load and run the gel. Dissociation can lead to smearing of the bound species and difficulty in quantification, and equilibrium dissociation constants greater than 1-3 μM typically cannot be accurately determined. Previous fluorescence anisotropy analyses of the binding of IRF3 to different length interferon-β enhancer elements in the absence or presence of ATF2-Jun heterodimers have produced binding constants in the low micromolar range (2, 4). Therefore, I predicted that the affinity of iIRF3 binding to bATF2-bJun-IFNb complexes could be feasible using gel-shift fluorescence measurements which, in my hands, can yield precise measurements using ~100 nM total concentration of components. Rather than calculate actual dissociate constant values, I have analyzed different titration experiments in the same gel in order to estimate relative binding affinities.

The protein concentration stocks should be prepared by serial dilution in order to minimize variation and pipette error that can skew results. The final concentration series used for the measurement should be chosen to maximize the number of data points within the binding transition. bATF2-bJun-DNA complexes formed from 93.75nM bJun, 46.875nM bATF2 and 25nM IFNb probe (labeled with FAM on both ends) was titrated with up to 490nM of iIRF3.

IV.B.iii. Quantification of fraction of complexes bound

The fraction of bound heterodimer-IFNb complexes was estimated by dividing the background-corrected intensity of the bATF2-bJun-iIRF3-IFNb (bound) band by the sum of background-corrected intensities of the bATF2-bJun-IFNb (unbound) and bATF2-bJun-iIRF3-IFNb bands.

V. BIBLIOGRAPHY

1. **Berman, H. M., J. Westbrook, Z. Feng, G. Gilliland, T. N. Bhat, H. Weissig, I. N. Shindyalov, and P. E. Bourne.** 2000. The Protein Data Bank. Nucleic Acids Res **28:**235-42.
2. **Carrillo, R. J., A. I. Dragan, and P. L. Privalov.** 2010. Stability and DNA-binding ability of the bZIP dimers formed by the ATF-2 and c-Jun transcription factors. J Mol Biol **396:**431-40.
3. **DeLano, W. L.** 2008. The PyMOL Molecular Graphics System, 1.1 ed. DeLano Scientific LLC, San Carlos, CA, USA.
4. **Dragan, A. I., R. Carrillo, T. I. Gerasimova, and P. L. Privalov.** 2008. Assembling the human IFN-beta enhanceosome in solution. J Mol Biol **384:**335-48.
5. **Falvo, J. V., B. S. Parekh, C. H. Lin, E. Fraenkel, and T. Maniatis.** 2000. Assembly of a functional beta interferon enhanceosome is dependent on ATF-2-c-jun heterodimer orientation. Mol Cell Biol **20:**4814-25.
6. **Panne, D., T. Maniatis, and S. C. Harrison.** 2004. Crystal structure of ATF-2/c-Jun and IRF-3 bound to the interferon-beta enhancer. Embo J **23:**4384-93.

CHAPTER 4: FUNCTIONAL EFFECTS OF ORIENTED HETERODIMER BINDING *IN VITRO* AND *IN VIVO*

I. INTRODUCTION

I.A. Control of the orientation of heterodimer binding

Previous investigations of the functional role of bZIP heterodimer orientation in *in vivo* have required manipulations of the DNA recognition element, thus precluding analysis of the effects of heterodimer binding orientation at endogenous genomic loci (2, 18). By utilizing ATF2 and Jun substitutions which force asymmetric heterodimer interactions with either the DNA (XG substitutions) or with IRF3 (XD and XK substitutions) we have developed parallel strategies for manipulating heterodimer orientation at IFNb oligonucleotides *in vitro* and at the endogenous interferon-β enhancer element *in vivo*, thus allowing more biologically relevant insights into the role of alternative bZIP heterodimer binding orientations in transcriptional regulation.

We investigated whether the amino acid substitutions in bATF2 and bJun that individually affected heterodimer orientation in association with iIRF3 affected the orientation of heterodimer binding in concert. Simultaneous substitution of the arginine in the basic region of one subunit (XD) and the negatively charged residues adjacent to the basic region in the other subunit (XK) was predicted to eliminate interactions with both K70 and D45 in iIRF3 when the heterodimer bound in one orientation but not to affect these interactions when the heterodimer bound in the opposite orientation. In

complexes lacking iIRF3, bATF2XD-bJunXK heterodimers bound IFNb with a stronger orientation preference than wild type bATF2-bJun [Fig. 4.1, left panel]. The orientation of bATF2XD-bJunXK at IFNb was reversed by iIRF3 binding. The resulting complex

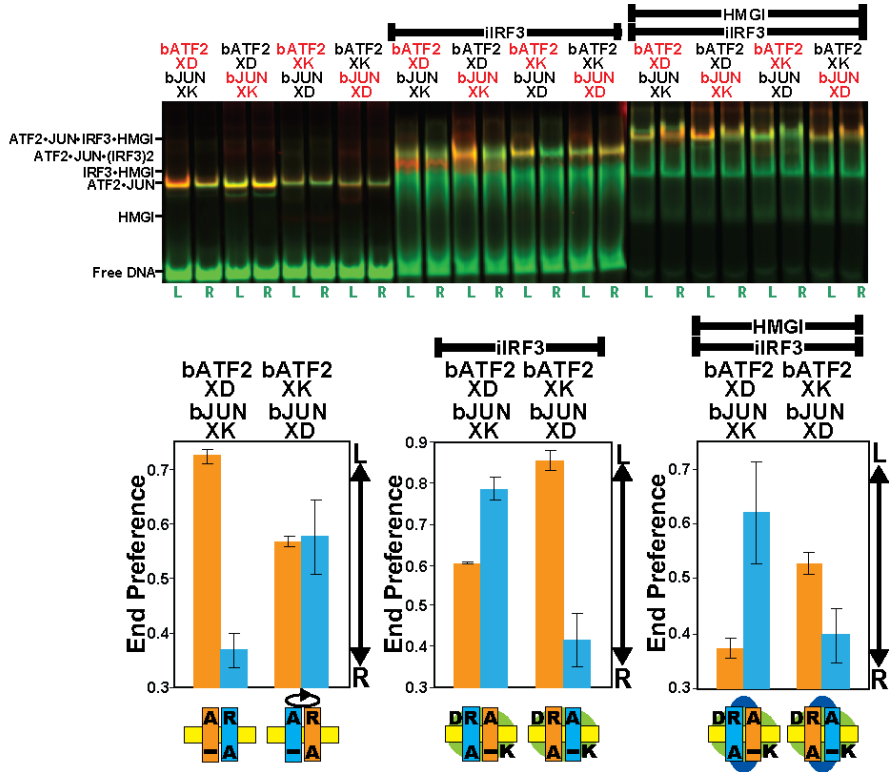

Fig. 4.1. Combinations of amino acid substitutions in bATF2 and bJun have concerted effects on the orientation of heterodimer binding in association with iIRF3 and HMGI. Effects of combinations of asymmetric amino acid substitutions in bATF2 and bJun on the orientation of heterodimer binding alone (left panel), in association with iIRF3 (middle panel), and in association with iIRF3 and HMGI (right panel). The orientations of heterodimer binding at IFNb in complexes formed by the proteins indicated above the lanes were analyzed as described in Fig. 2.1. The diagrams below the bars reflect the preferred orientations of heterodimer binding using the symbols described in Fig. 2.1. The end preference values represent the mean values and standard deviations from at least two independent experiments.

had a stronger orientation preference than those of complexes formed by heterodimers containing either of the individual substitutions (bATF2XD-bJun or bATF2-bJunXK).

Conversely, iIRF3 binding caused the opposite shift in the orientation of bATF2XK-bJunXD at IFNb [Fig. 4.1, middle panel]. The resulting complex had a stronger orientation preference than those of complexes former by heterodimers

containing either of the individual substitutions (bATF2XK-bJun or bATF2-bJunXD). These combinations of amino acid substitutions also had opposite effects on the orientations of bATF2-bJun heterodimer binding in complexes containing iIRF3 and HMGI [Fig. 4.1, right panel]. The effects of combined XD and XK substitutions on heterodimer orientation preference in the presence of either iIRF3 or HMGI and iIRF3 were comparable to the effects of XG substitutions in the same complexes. Thus, simultaneous contacts by the arginine in the basic region of the subunit bound to the left half-site and by the negatively charged residues adjacent to the basic region of the subunit bound to the right half-site with D45 and K70 of iIRF3, respectively, are the primary determinants of heterodimer orientation preference in the presence of iIRF3.

I.B. Regulation of interferon-β expression in cells

The first response of an organism to intruding pathogens is an inflammatory reaction that includes secretion of cytokines and chemokines. During viral infections, some of the most prominent cytokines produces are the interferons. Interferons have numerous regulatory functions that affect both innate and adaptive immunity (13). Interferons are classified as type I (interferon-α and interferon–β) and type II (interferon-γ) based on the receptor complex that they activate. In epithelial and fibroblast cells, interferon-β is expressed and secreted within hours following virus infection and triggers the expression of interferon-α in an autocrine fashion (10, 19). Therefore, the regulation of interferon-β expression is a crucial step in the induction of the type I interferon response.

I.B.i. Model for Sendai virus-induced activation of interferon-β

Because the induction of interferon-β is so critical for the immune response, the mechanism underlying its control has been the subject of detailed study. Interferon-β, like the interferon-α proteins, is regulated primarily at the transcriptional level (9). The enhancer region of the interferon-β gene contains at least four regulatory DNA sequences named positive regulatory domain I, II, III, and IV (4, 7, 8). The PRDI and PRDIII elements are activated by members of the IRF family, whereas the PRDII and PRDIV are activated by NF-κB and ATF2-Jun heterodimers.

Studies of the transcriptional regulation of interferon-β have been mainly carried out using Sendai virus-infected fibroblast and epithelial cells (6, 14, 15, 21, 23, 25). In this context, interferon-β transcription is first activated by signals that induce the activation and localization of IRF3, NF-kB, and ATF2-Jun to the interferon-β enhancer. IRF3 is expressed constitutively in a variety of cells and localized in the cytoplasm as an inactive monomer (22). Virus-mediated phosphorylation of IRF3 induces IRF3 activation, homodimerization, and translocation to the nucleus (22). In the nucleus, IRF3 is believed to form a complex with the co-activator CBP (20). This activated form of IRF3 is also known to directly induce chemokine genes such as RANTES during viral infection (11).

II. RESULTS AND DISCUSSION

II.A. Effects of orientation on complex formation

To investigate potential functional consequences of the orientation of heterodimer binding on complex assembly *in vitro*, we measured the effects of the amino acid substitutions in bATF2 and bJun that alter the orientation of heterodimer binding on the affinities of complex formation at IFNb in the presence of iIRF3 and HMGI. I compared the fraction of bATF2-bJun-IFNb complexes bound by iIRF3 and HMGI separately and in combination when bATF2 and bJun contained substitutions that favored opposite orientations of heterodimer binding (bJun-bATF2XG *versus* bJunXG-bATF2, and bATF2XD-bJunXK *versus* bATF2XK-bJunXD). bATF2-bJun and iIRF3 formed more complexes when bATF2 occupied the left and bJun occupied the right IFNb half-site (Fig. 4.2Ai, iii). Similarly, bATF2-bJun and HMGI formed more complexes when bATF2 occupied the left and bJun occupied the right IFNb half-site (Fig 4.2Bi, iii). In the presence of HMGI, the concentration of iIRF3 that produced half-maximal binding was reduced 2-4-fold and there was no detectable difference in iIRF3 binding with bATF2-bJun variants that favored opposite orientations of heterodimer binding (Fig. 4.2Aii). In the presence of iIRF3, the concentrations of HMGI that produced half-maximal binding was slightly reduced fold and there was also no detectable difference in HMGI binding with bATF2-bJun variants that favored opposite orientations of heterodimer binding (Fig 4.2Bii). Thus, iIRF3 and HMGI cooperatively reduce the effect of heterodimer binding orientation on the stability of complex formation at IFNb, consistent with their cooperative reduction of bATF2-bJun orientation preference at IFNb.

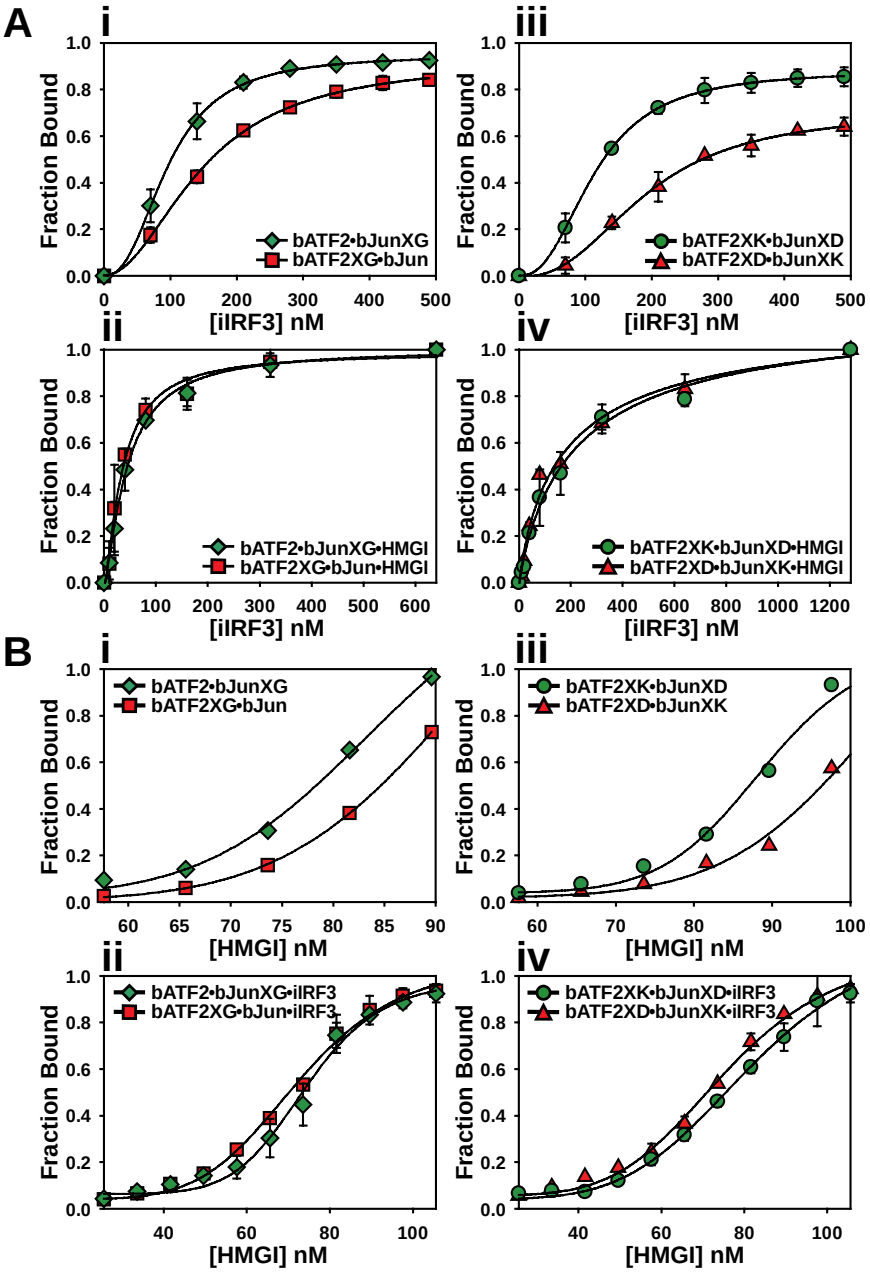

Fig. 4.2. iIRF3 and HMGI cooperatively reduce the effect of bATF2-bJun orientation on the stability of complex formation at IFNb. (A) bATF2 [35 nM] and bJun [70 nM] variants which form heterodimers that bind IFNb [25 nM] with opposite orientation preferences were titrated with iIRF3 in the absence (i, iii) or presence (ii, iv) of HMGI [112nM]. XG-substituted heterodimers were analyzed in (i, ii), and XD-XK-substituted heterodimers were analyzed in (iii, iv) (as indicated on the abscissa). (B) bATF2 [35 nM] and bJun [70 nM] variants which form heterodimers that bind IFNb [25 nM] with opposite orientation preferences were titrated with HMGI in the absence (i, iii) or presence (ii, iv) of iIRF3 [70nM]. XG-substituted heterodimers were analyzed in (i, ii), and XD-XK- substituted heterodimers were analyzed in (iii, iv) (as indicated on the abscissa). The complexes were separated by gel electrophoresis and the fraction of complexes bound by either iIRF3 (A) or HMGI (B) was plotted as a function of iIRF3 or HMGI concentration, respectively. The data shown in B(i, iii) qualitatively represents at least four separate experiments. All other data represents the mean values and standard deviations from at least two separate experiments.

II.B. Analysis of endogenous interferon-β gene transcription

To investigate the role of the orientation of ATF2-Jun heterodimer binding in transcription regulation, we examined endogenous interferon-β gene transcription in cells that expressed full length ATF2 and Jun that contained the amino acid substitutions that altered the orientation of bATF2-bJun binding *in vitro*. Interferon-β transcript levels were measured in HeLa cells transfected with plasmids encoding full-length ATF2 and Jun together with or without IRF3 following Sendai virus infection. We examined the effects of amino acid substitutions predicted to alter the intrinsic heterodimer orientation preference (ATF2XG-Jun and ATF2-JunXG) as well as the effects of substitutions predicted to alter the orientation of heterodimer binding in association with IRF3 (ATF2XK-JunXD and ATF2XD-JunXK) on the level of interferon-β transcripts.

In the absence of exogenous IRF3, amino acid substitutions in ATF2 and Jun had no significant effect on the level of interferon-β transcripts (Fig. 4.3, left panel). In contrast, co-expression of exogenous IRF3 with heterodimers in which Jun was predicted to favor binding to the right half-site (ATF2XK-JunXD and ATF2-JunXG) produced a higher level of interferon-b transcripts than co-expression of IRF3 with heterodimers in which Jun was predicted to favor binding the left half-site (ATF2XD-JunXK and ATF2XG-Jun) (Fig 4.3, left panel). Taken together, the effects of amino acid substitutions that affect the orientation of heterodimer binding *in vitro* on interferon-β transcription in cells were consistent with a role for heterodimer orientation in the control of interferon-b transcription.

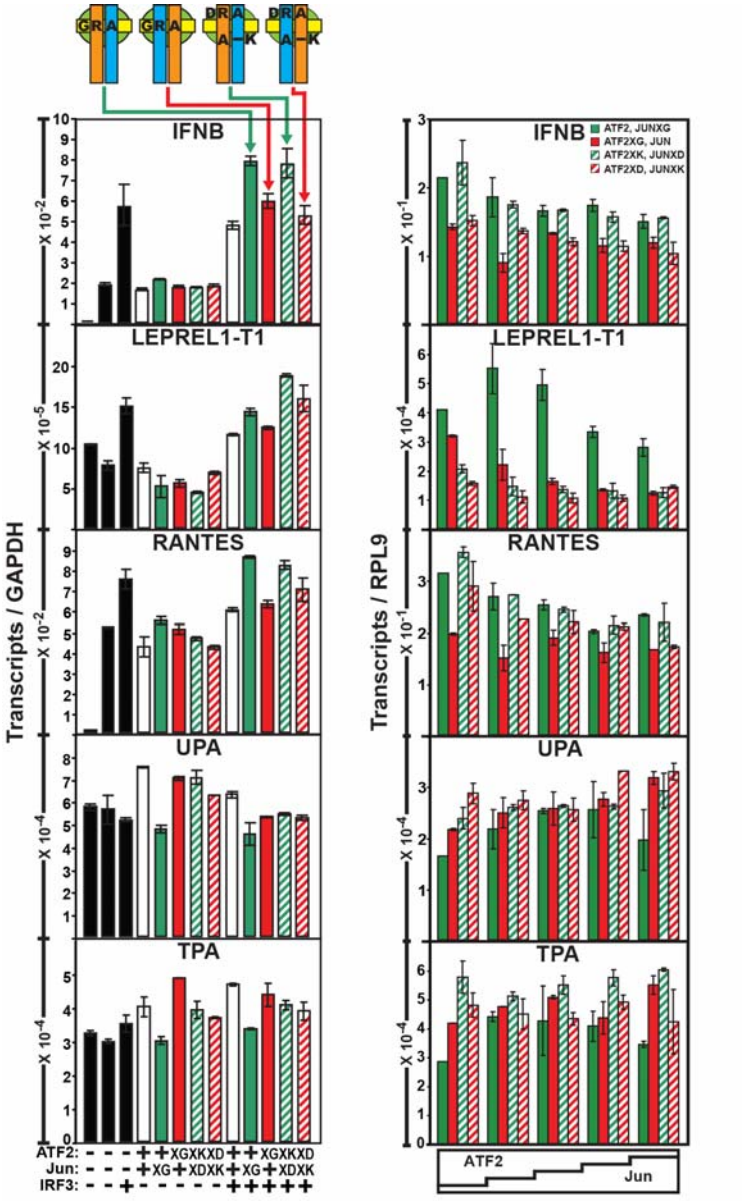

Fig. 4.3. ATF2-Jun heterodimers that bind IFNb in opposite orientations in vitro have distinct effects on transcription of different endogenous genes. (A) The levels of gene transcripts were measured in cells that expressed the proteins indicated below the bar graphs. Transiently transfected HeLa cells were infected with Sendai virus and the transcript levels were measured 6 hours after infection. Transcript levels were measured in the same cells and were normalized to the level of GAPDH transcripts. The orientations of bATF2-bJun heterodimer binding at IFNb in association with iIRF3 are indicated by the diagrams above the bar graphs. The levels of transcripts in cells that expressed heterodimers containing amino acid substitutions that favor Jun binding to the right *versus* the left half-site are shown by green and red bars, respectively. The levels of interferon-b transcripts in cells that expressed wild-type ATF2-Jun are shown by white bars, and those in cells that expressed IRF3 alone, or no exogenous proteins are shown by black bars. (B) The levels of gene transcripts were measured in cells transfected with different ratios of plasmids encoding the proteins indicated by the legend in the upper right. The plasmid ratios for all combinations of ATF2 and Jun variants were 5:1, 3:1, 1:1, 1:3 and 1:5, respectively from the left to the right. Transcript levels were measured in the same cells and were normalized to the level of RPL9 transcripts. All data show the mean and standard deviation of replicate qPCR reactions and are representative of at least two independent transfection experiments.

II.C. Effects of ATF2-Jun substitutions on other genes

We investigated if the amino acid substitutions that affected ATF2-Jun heterodimer orientation at IFNb and interferon-β transcription also affected transcription of other genes. We searched the human genome for sequences similar to the composite ATF2-Jun-IRF3-HMGI recognition sequence in the interferon-β enhancer. We identified four sequences that contained 18 of the 19 base-pairs in the composite ATF2-Jun-IRF3 recognition sequence in the interferon-β enhancer. We focused on the LEPREL1-T1 transcript (ENST00000437063), which is transcribed 100,225 base pairs downstream of an ATF2-Jun-IRF3 recognition sequence. Because of the strict conservation of the recognition sequence, we predicted that the amino acid substitutions that affected the orientation of bATF2-bJun binding at IFNb *in vitro* would have the same effects on the orientation of ATF2-Jun binding at the site upstream of the LEPREL1-T1 transcript.

We measured the levels of LEPREL1-T1 transcripts in cells that expressed the ATF2 and Jun variants alone and in combination with IRF3. Cells that expressed IRF3 together with the combinations of ATF2 and Jun variants that were predicted to favor Jun binding to the right half-site (ATF2-JunXG and ATF2XD-JunXK) produced a higher level of LEPREL1-T1 transcripts than cells that expressed IRF3 together with the combinations of ATF2 and Jun variants predicted to favor Jun binding to the left half-site (ATF2XG-Jun and ATF2XK-JunXD) [Fig. 4.3., left panel]. In the absence of IRF3 co-expression, the amino acid substitutions in ATF2 and Jun produced smaller and opposite differences in the level of LEPREL1-T1 transcripts [Fig. 4.3., left panel]. LEPREL1-T1 transcription was not induced by Sendai virus infection, indicating that the effects of the amino acid substitutions in ATF2 and Jun on transcription were not caused by differences

in signaling related to virus infection. The parallel effects of mutations in ATF2 and Jun on the levels of interferon-β and LEPREL1-T1 transcripts are consistent with similar effects of the orientation of heterodimer binding on transcription of these genes.

We investigated if the amino acid substitutions in ATF2 and Jun also affected transcription of other genes that contained ATF2-Jun and IRF3 recognition sequences. The RANTES chemokine gene contains ATF2-Jun and IRF3 recognition sequences that are separated by a longer distance than those in the interferon-β enhancer. Cells that co-expressed IRF3 with different ATF2 and Jun variants produced different levels of RANTES transcripts [Fig. 4.3, left panel]. The amino acid substitutions in ATF2 and Jun had similar effects on the level of RANTES transcripts as they had on the levels of interferon-β and LEPREL1-T1 transcripts. These amino acid substitutions also had similar, albeit smaller, effects on the level of RANTES transcripts when ATF2 and Jun were expressed in the absence of IRF3 [Fig. 4.3, left panel].

We also investigated the effects of the amino acid substitutions in ATF2 and Jun on transcription of genes that contained ATF2-Jun recognition sequences, but no known IRF3 recognition sequences. IRF3 expression alone or in combination with the ATF2 and Jun variants had little effect on the levels of UPA or TPA transcripts, consistent with the absence of known IRF3 recognition sequences in these genes. The amino acid substitutions in ATF2 and Jun that altered the intrinsic orientation preference of heterodimer binding at IFNb (ATF2-JunXG *versus* ATF2XG-Jun) affected the levels of UPA and TPA transcripts both in the absence and in the presence of IRF3 (Fig. 4.3, left panel). These ATF2 and Jun variants had opposite effects on the levels of UPA and TPA transcripts compared to their effects on the levels of interferon-β, LEPREL1-T1 and

RANTES transcripts in the presence of IRF3. The amino acid substitutions in ATF2 and Jun that altered the orientation of heterodimer binding at IFNb mainly in the presence of IRF3 (ATF2XD-JunXK and ATF2XK-JunXD) had small effects on the levels of UPA and TPA transcripts in the absence and presence of IRF3. Taken together, the results of these experiments demonstrate that the amino acid substitutions in ATF2 and Jun that affected the orientation of heterodimer binding at IFNb *in vitro* had distinct effects on transcription of different endogenous genes.

II.D. Effects of ATF2-Jun substitutions under different conditions

We investigated if the amounts of the ectopic ATF2 and Jun variants expressed in cells affected the levels of the endogenous transcripts. The levels of endogenous ATF2 and Jun proteins were undetectable compared with ectopic ATF2 and Jun variants (Fig. 4.4), yet ectopic ATF2 and Jun expression generally did not significantly increase the levels of endogenous gene transcripts. The relative amounts of different ATF2 and Jun protein variants varied between different experiments [Fig 4.4] and the levels of endogenous transcripts did not correlate with the differences in the amounts of the ATF2 and Jun variants expressed. The amounts of ATF2 and Jun in HeLa cells were therefore not limiting for transcription of the endogenous genes examined, which is consistent with a past report (1). It is therefore likely that the differences in the levels of the endogeous transcripts observed in cells that expressed different combinations of ATF2 and Jun variants were caused by displacement of endogenous ATF2 and Jun by the ectopically expressed ATF2 and Jun variants.

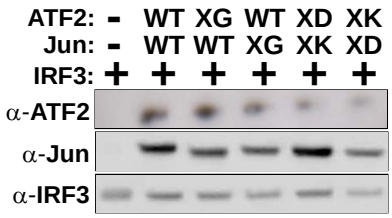

Fig. 4.4. Protein expression of different ATF2 and Jun variants did not influence the expression of IRF3. (A) Western analyses of ATF2 expression levels in HeLa cells transfected with IRF3 together with different combinations of ATF2 and Jun variants. (B) Western analyses of Jun expression in same samples. (C) Western analyses of IRF3 expression in the same samples. Lane 1: IRF3; lane 2: ATF2, Jun, and IRF3; lane 3: ATF2XG, Jun, IRF3; lane 4: ATF2, JunXG, IRF3; lane 5: ATF2XD, JunXK, IRF3; lane 6: ATF2XK, JunXD, IRF3. 1.5 μg of each plasmid was transfected for all samples. Lane 1 contained 3 μg of pcDNA.

We investigated if the relative amounts of the ectopic ATF2 and Jun variants expressed in cells affected the levels of the endogenous transcripts. We varied the relative amounts of ectopic ATF2 to Jun variants in cells by transfecting different ratios of plasmids encoding the ATF2 *versus* Jun variants. The levels of ectopic ATF2 and Jun transcripts varied 10 to 5-fold, respectively among in cells transfected with different concentrations of the plasmids [Fig. 4.5, left panel]. By comparison, the relative levels of transcripts encoding ATF2 or Jun variants that favored opposite orientations of heterodimer binding (ATF2 vs. ATF2XG, Jun vs. JunXG, ATF2XD vs. ATF2XK, JunXD vs. JunXK) varied less than 15% on average when equivalent amounts of plasmids encoding these variants were transfected and did not correlate with the relative levels of IFN-b transcripts [Fig. 4.5, right panel]. The amino acid substitutions in ATF2 and Jun had consistent effects on the level of interferon-β transcripts when different ratios of the plasmids encoding the ATF2 and Jun variants were transfected into cells [Fig. 4.3, right panel].

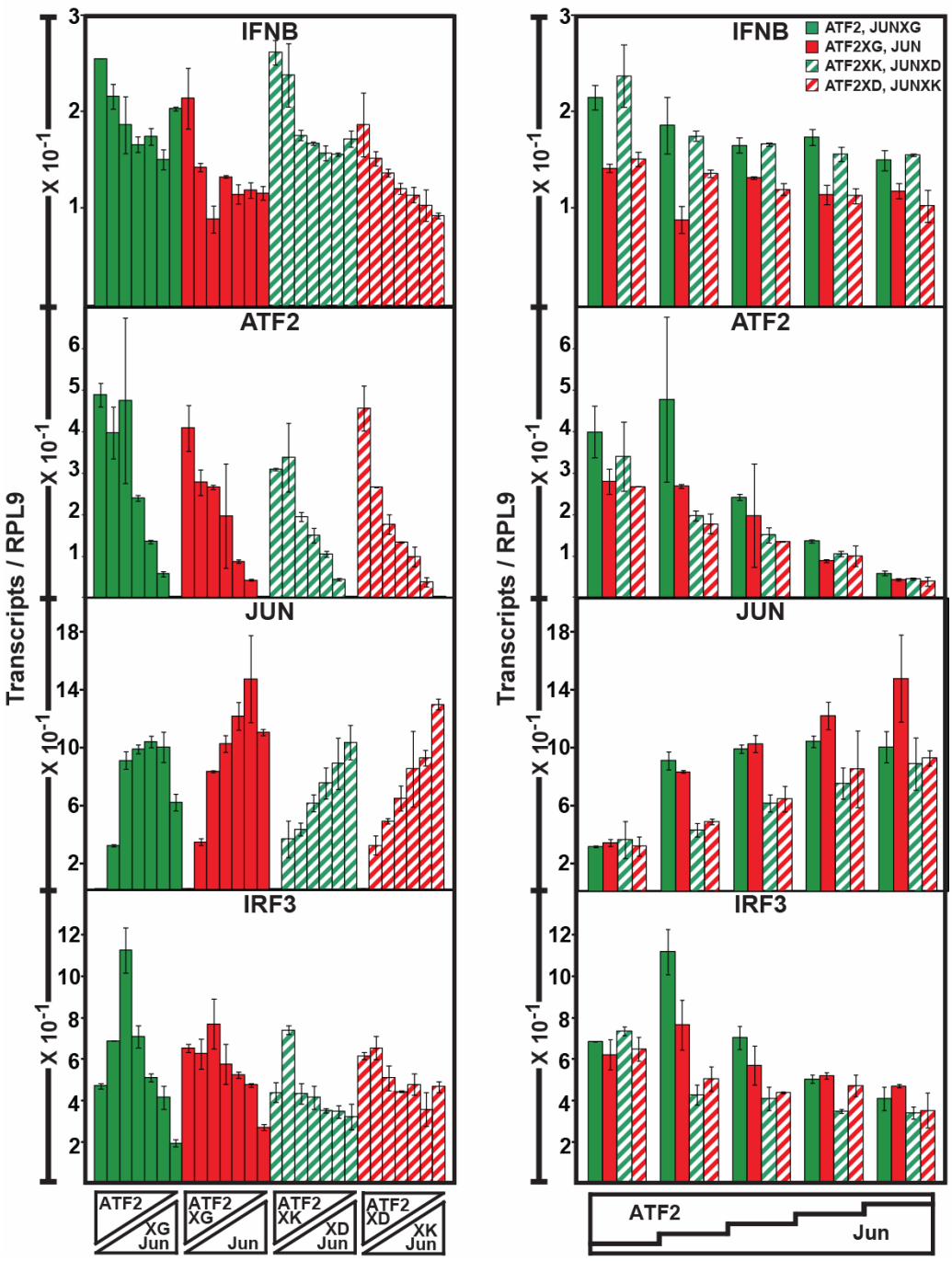

Fig. 4.5. Different ratios of transfected ATF2-to-Jun plasmid produce different amounts of IFN-b and ectopic ATF2, Jun, and IRF3 transcripts. (A) qRT-PCR detection of (i) IFN-b and plasmid-derived (ii) ATF2, (iii) Jun, and (iv) IRF3 transcripts in cells co-transfected with 1.5 μg of IRF3 together with either 0, 0.5, 1, 1.5, 2, 2.5, or 3 μg and Jun and either 3, 2.5, 2, 1.5, 1, 0.5, or 0 μg of ATF2, respectively. (B) For the same experiment, the levels of (i) IFN-b, (ii) ATF2, (iii) Jun, and (iv) IRF3 transcripts were compared between samples transfected with the same ratio of ATF2 to Jun plasmid (from left to right 5:1, 3:1, 1:1, 1:3, 1:5) but differed in their amino acid substitutions as indicated the upper right figure legend. All samples were digested with DNase I, and the addition of cDNA from reactions lacking reverse transcriptase did not result in qRT-PCR amplification (data not shown), indicating that this analysis did not detect plasmid DNA.

Despite consistency in relative levels of interferon-β transcripts in cells transfected with the same ratio of ATF2 to Jun plasmid, the absolute levels of interferon-β transcripts varied between cells transfected with different ratios of the plasmids [Fig 4.5, left panel]. Specifically, transcription of genes regulated by IRF3 (interferon-β, RANTES, LEPREL-T1) was reduced in cells transfected with higher ratios of plasmids encoding Jun relative to ATF2 variants [Figs 4.3, right panel]. In contrast, transcription of genes that were not regulated by IRF3 (TPA, UPA) was not reduced under these conditions. This selective reduction in transcription of genes regulated by IRF3 correlated with a reduction in the level of IRF3 expression in cells transfected with higher ratios of plasmids encoding Jun relative to ATF2 variants [Fig. 4.5, left panel]. This reduction is likely due to the higher absolute level of ectopic Jun expression compared to ectopic ATF2 expression [Fig 4.6, right panel]. Nonetheless, the reduction in transcription of genes regulated by IRF3 in cells transfected with higher ratios of plasmids encoding Jun relative to ATF2 variants did not alter, and is likely to be unrelated to, the effects of the amino acid substitutions in ATF2 and Jun on endogenous gene transcription.

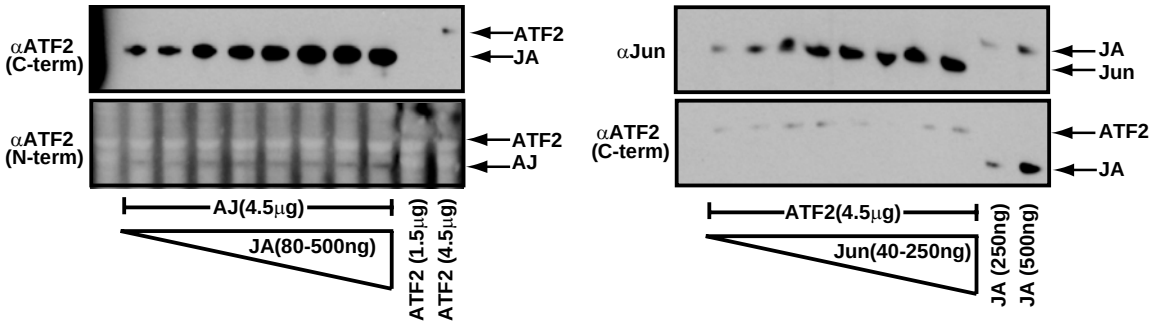

Fig. 4.6. Comparison of the relative expression levels of JUN-atf2 *versus* ATF2-jun and Jun *versus* ATF2 ectopic proteins. (A) Western analyses of cells transfected with 4.5 μg of ATF2-jun (AJ) chimera-encoding plasmid and (from left to right) 80 ng, 140 ng, 200 ng, 260 ng, 320 ng, 380 ng, 440 ng, or 500 ng of JUN-atf2 (JA) chimera-encoding plasmid. The left-most lane is untransfected cells. The two right-most lanes are cells expressing protein from (from left to right) 1.5 μg and 4.5 μg of ATF2-encoding plasmid, which is recognized by both ATF2 antibodies. (B) Western analyses of cells transfected with 4.5 μg of ATF2-encoding plasmid and (from left to right) 40 ng, 70 ng, 100 ng, 130 ng, 160 ng, 190 ng, 220 ng, or 250ng of Jun-encoding plasmid. The left-most lane is untransfected cells. The two right-most lanes are cells expressing protein from (from left to right) 250 ng and 500 ng of JUN-atf2 chimera-encoding plasmid, which is recognized by ATF2 and Jun antibodies. The expression level of JUN-atf2 chimeric protein in cells transfected with 250 ng plasmid is approximately two-fold higher than ATF2 expression in cells transfected with 4.5 μg of ATF2 and is approximately equivalent to Jun expression in cells transfected with 40 ng of Jun. Therefore, expression of ectopic Jun is approximately 56-fold greater than ectopic ATF2 (2250 / 40 = 56.25).

II.E. Regions of ATF2-Jun that mediate effects on transcription

We investigated if the amino acid substitutions in ATF2 and Jun that determined the intrinsic orientation of heterodimer binding at IFNb affected transcription of different genes through similar or distinct mechanisms. To this end, we compared the regions of ATF2 and Jun that determined the effects of XG heterodimer substitutions at different genes by using chimeric proteins in which the amino- and carboxyl-terminal regions of ATF2 and Jun were exchanged [JUN-atf2, ATF2-jun Fig. 4.7]. JUN-atf2 proteins were expressed at levels that were about 100-fold higher than those of the ATF2-jun variants when equal amounts of the plasmids were transfected into cells [Fig. 4.6, left panel].

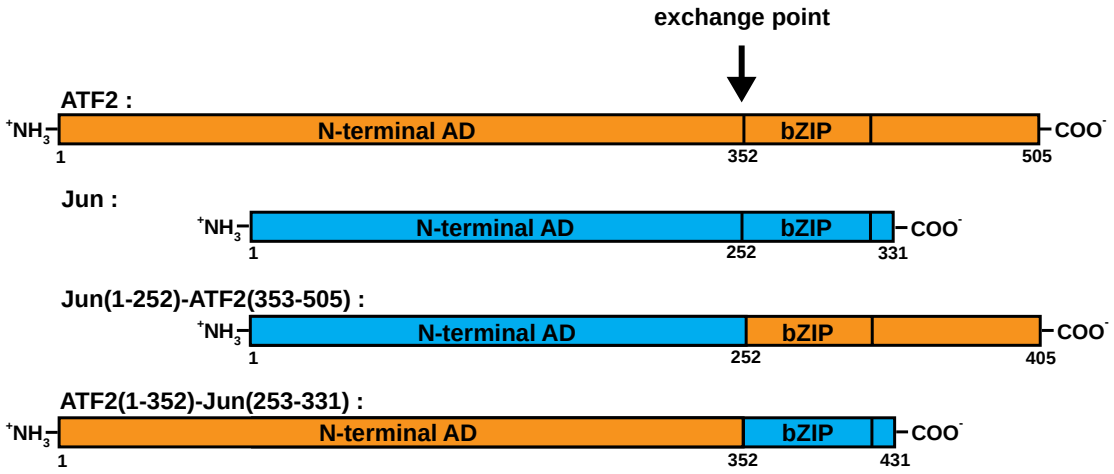

Fig. 4.7. Maps of ATF2, Jun, JUN-atf2, and ATF2-jun proteins. Full-length ATF2 (orange) and Jun (teal) proteins are shown divided into amino- and carboxy-terminal domains. The start of the carboxy-terminal domain coincided with the start of bZIP domain. The amino- and carboxy-terminal domains of ATF2 and Jun were swapped to produce JUN-atf2 and ATF2-jun chimeric proteins, as indicated in the bottom two maps. The relative sizes of the amino- and carboxy-terminal domains of ATF2 and Jun are drawn to proportion.

We compensated for this difference between the efficiencies of ectopic JUN-atf2 *versus* ATF2-jun and for ectopic Jun *versus* ATF2 [Fig. 4.6, right panel] expression by transfecting higher ratios of the plasmids encoding ATF2-jun or ATF2 variants relative to plasmids encoding JUN-atf2 or Jun variants, respectively. Under these conditions, the amino acid substitutions in ATF2 and Jun had consistent effects on the levels of IFN-b, LEPREL1-T1, RANTES, TPA, and UPA transcripts. The consistent effects of the amino acid substitutions in ATF2 and Jun on endogenous gene transcription under the wide range of conditions examined suggest that the same protein complexes were assembled at the endogenous regulatory elements regardless of the relative amounts of the ATF2 and Jun variants expressed in the cells.

At the interferon-β and LEPREL1-T1 genes, the amino acid substitutions that affected heterodimer orientation had the same effects on the activities of the chimeric

proteins that contained the same bZIP and carboxyl-terminal regions as they had on non-chimeric ATF2 and Jun [Fig. 4.8]. Cells in which the chimeric protein containing the bZIP and carboxyl-terminal regions of Jun was predicted to bind to the right IFNb half-site (Jun:ATF2-ATF2:JunXG) produced higher levels of interferon-β and LEPREL1-T1 transcripts than cells in which the chimeric protein containing the bZIP and carboxyl-terminal regions of ATF2 was predicted to bind to the right IFNb half-site (Jun:ATF2XG-ATF2:Jun) [Fig. 4.8]. These results indicate that the bZIP and carboxyl-terminal regions of ATF2 and Jun determined the effects of the orientation of heterodimer binding on transcription of the interferon-β and LEPREL1-T1 genes.

At the RANTES, TPA and UPA genes, the amino acid substitutions that affected intrinsic heterodimer orientation had the opposite relative effects on the activities of the chimeric proteins that contained the carboxy-terminal regions of ATF2 and Jun as they had on non-chimeric ATF2 and Jun [Fig. 4.8]. Cells in which the chimeric protein containing the carboxy-terminal region of Jun was predicted to bind to the right half-site at IFNb (JUN-atf2-ATF2-junXG) produced lower levels of RANTES, TPA and UPA transcripts than cells in which the chimeric protein containing carboxy-terminal region of ATF2 was predicted to bind to the right half-site at IFNb (JUN-atf2XG-ATF2-jun) [Fig. 4.8]. Taken together, these results indicate that different regions of ATF2 and Jun determined the effects of the orientation of heterodimer binding on transcription of different genes.

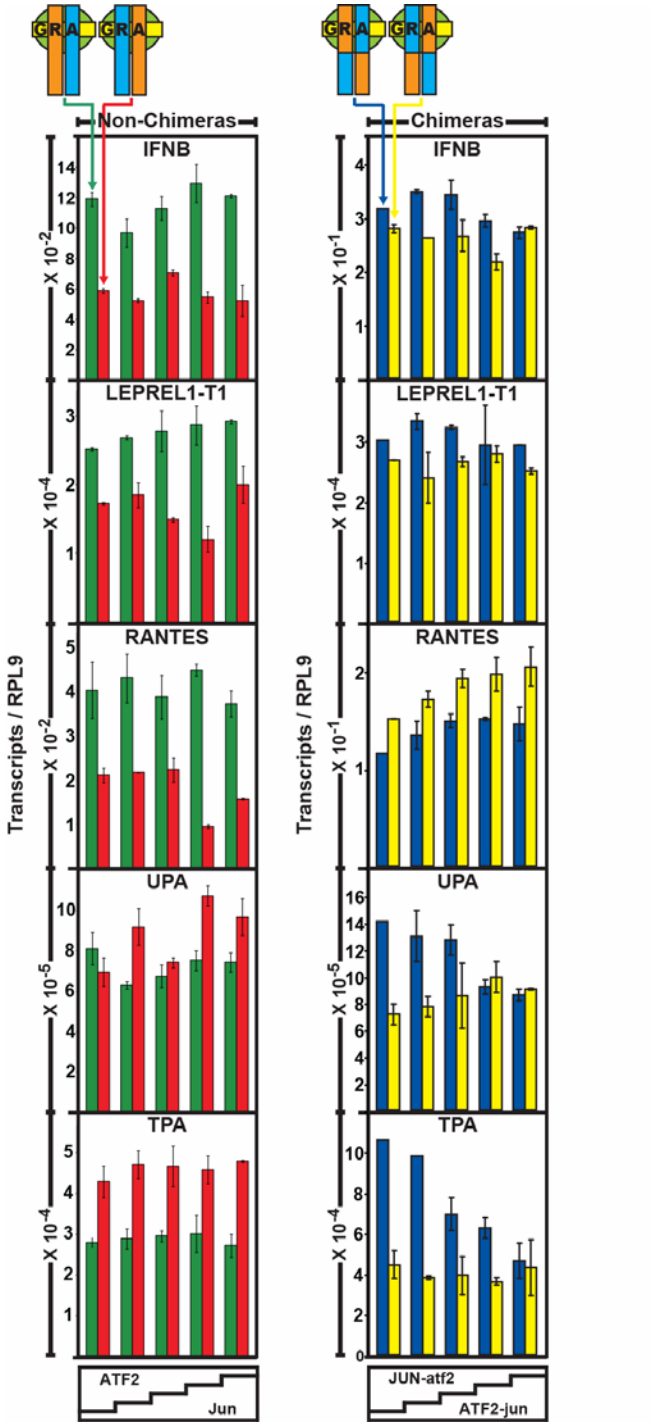

Fig. 4.8. Effects of XG substitutions in non-chimeric *versus* chimeric ATF2 and Jun proteins on transcription of endogenous genes using different plasmid ratios. (A) Levels of IFN-b, LEPREL1-T1, RANTES, UPA and TPA transcripts were measured in cells transfected with different ratios (from left to right: 120:1, 60:1, 30:1, 14:1, or 9:1) of either ATF2 to JunXG (green) or ATF2XG-to-Jun (red). B) Levels of IFN-b, LEPREL1-T1, RANTES, UPA, and TPA transcripts were measured in cells transfected with different ratios (from left to right: 1:18, 1:30, 1:45, 1:90, 1:180) of either JUN-atf2 to ATF2-junXG (blue) or JUN-atf2XG to ATF2-jun (yellow). The data show the mean from two qPCR reactions and are representative of at least two independent transfection experiments.

III. SUMMARY AND CONCLUSIONS

The interferon-β enhancer is one of the few transcription regulatory complexes for which both the atomic-resolution structure as well as the functional synergy among the transcription factors have been analyzed (3, 5, 6, 12, 15-17, 22, 24). These data have been interpreted to show that cooperative binding by a unique configuration of regulatory proteins mediates synergistic activation of interferon-β reporter genes.

The discovery that ATF2-Jun heterodimers can bind the interferon-β enhancer in both orientations in association with iIRF3 and HMGI raised the question whether the orientation of heterodimer binding affects transcriptional activity. Our results demonstrate that two different combinations of amino acid substitutions in ATF2 and Jun produced opposite orientations of heterodimer binding produced corresponding changes in transcription of the endogenous interferon-β gene. These results suggest that opposite orientations of ATF2-Jun heterodimer binding at the interferon-β enhancer resulted in different levels of interferon-β transcription. Moreover, these data indicate that the same interactions with DNA and with iIRF3 mediate ATF2-Jun association with the interferon-β enhancer in vitro and in cells.

The effects of the amino acid substitutions that reverse the orientation of ATF2-Jun heterodimer binding on transcriptional activity could be mediated by several different mechanisms. The amino acid substitutions had consistent effects on transcriptional activity when different relative amounts of ATF2 and Jun were expressed. It is therefore unlikely that the effects were due to changes in the relative amounts of different ATF2 or Jun dimers in the cells. Heterodimers in which Jun favored the right half-site had a significantly greater affinity for IFNb compared with heterodimers in which ATF2

favored the right half-site in the presence of either iIRF3 or HMGI , which is consistent with the intrinsic orientation preference of ATF2-Jun heterodimers at IFNb in the absence or presence of iIRF3. Therefore, it is possible the effects of substitutions in ATF2 and Jun are mediated by differences in the stability of ATF2-Jun-iIRF3 complex formation at IFNb. Consistent with this, regions of ATF2 and Jun which mediated the effects of amino acid substitutions on the expression of interferon-β contained the DNA-binding domains of ATF2 and Jun. Consistent with the idea that the formation of ATF2-Jun-IRF3 complexes is a limiting factor in the transcription of interferon-b, monoallelic IFN-β expression occurs in HeLa cells six hours after infection (1). Therefore, ectopic ATF2-Jun-IRF3 complexes have the potential activate five to six other interferon-β loci that would otherwise be silent.

Amino acid substitutions in ATF2 and Jun that affected heterodimer orientation had distinct effects on transcription of several endogenous genes. Among the genes investigated, the amino acid substitutions in ATF2 and Jun had qualitatively similar effects at genes that contained composite ATF2-Jun as well as IRF3 recognition sequences, but different relative effects at genes that did not contain composite sites. These results suggest that the effects of heterodimer orientation on transcriptional activity depend on the sequences of the enhancer and/or promoter regions. The qualitatively similar effects of the amino acid substitutions on transcription of the interferon-b and LEPREL1-T1 genes are consistent with the interpretation that the local sequences encompassing the enhancer regions are more important than the distance from the promoter region or the nature of the core promoter in determining the effect of the orientation of ATF2-Jun binding on transcriptional activity.

The amino acid substitutions in ATF2 and Jun that alter contacts to the asymmetric central based pair (ATF2XG and JunXG) were predicted to influence the orientation of heterodimer binding at all of the genes investigated. The effects of these substitutions on transcription of different genes indicate that ATF2-Jun heterodimer orientation is likely to affect transcription of many endogenous genes, and that the orientation that produces optimal activation differs among these genes.

The amino acid substitutions in ATF2 and Jun that affected contacts with IRF3 (ATF2XD, ATF2XK, JunXD, JunXK) were predicted to alter heterodimer orientation specifically at genes containing composite ATF2-Jun-IRF3 recognition sequences. Unexpectedly, these substitutions had opposite effects on transcription of several genes that are not known to contain IRF3 recognition sequences and that were not affected by IRF3 expression. The mechanisms whereby these substitutions affected transcription of these endogenous genes remain unknown, and could reflect the effects of these substitutions on interactions with the DNA or orientation-dependent contacts with other interaction partners. Consistent with the former interpretation, we found that XD and XK substitutions had opposite effects on the orientation preferences of ATF2-Jun heterodimers in the absence of IRF3 *in vitro*.

The amino- and carboxyl-terminal regions of ATF2 and Jun had distinct effects on the heterodimer orientation that produced the higher level of transcription at different genes. At the interferon-β and LEPREL1-T1 genes, the carboxyl-terminal regions of ATF2 and Jun had a dominant effect on the orientation of heterodimer binding that produced a higher level of transcription. This result is consistent with roles of orientation-dependent interactions between the bZIP domains or carboxyl-terminal

regions of ATF2 and/or Jun with IRF3 in transcription activation. Consistent with this, these interactions affected the affinity IRF3 binding to the IFNb in the absence of HMGI *in vitro*. Conversely, the amino-terminal regions of ATF2 and Jun had a dominant effect on the orientation-dependence of transcription activation at the RANTES, UPA and TPA genes. Thus, there appear to exist multiple molecular mechanisms that mediate the effect of the orientation of ATF2-Jun heterodimer binding on transcription of different genes.

IV. MATERIALS AND METHODS

IV.A. Generation of ATF2-Jun orientation isomers

Past analyses of the functional effects of heterodimer orientation in transcription have utilized alterations in DNA sequences to control the orientation of heterodimer binding (2, 18) . A downside of this strategy is that it necessitates the use of reporter plasmids rather than assaying the effects on chromatinized templates. Another disadvantage of this strategy is that the changes in the DNA sequence that influence the preferred orientation of heterodimer binding could also influence the binding affinity of the heterodimer as well as proteins that bind to overlapping sequences. Therefore, using my understanding of heterodimer-DNA contacts required for bATF2-bJun binding to IFNb as well as amino acid contacts required for cooperative DNA-binding interactions between bATF2-bJun and iIRF3, I have designed mutationally-trapped orientation isomers of bATF2-bJun heterodimers. These orientation isomers allow manipulation of the preferred orientation of heterodimer binding in independent ways at endogenous genomic loci.

Heterodimers in which bJun preferred the right PRDIV half-site contained alanine substitutions at either R270 in Jun (ATF2-JunXG) or alanine substitutions at E331, D332, D334, E335 in ATF2 and R263 in Jun (ATF2XK-JunXD). Heterodimers in which ATF2 preferred the right PRDIV half-site contained alanine substitutions at either R352 in ATF2 (ATF2XG-Jun) or alanine substitutions at D246, E248, E251 in Jun and R345A in bATF2 (ATF2XD-JunXK).

IV.B. Over-expression of exogenous protein in HeLa cells

Full-length ATF2, Jun, and IRF3 human open reading frames were cloned into pcDNA3.1+ (Invitrogen) eukaryotic expression plasmids. All plasmids were purified in parallel using EndoFree plasmid maxi kit (Qiagen, Valencia, CA) to avoid potential toxic side-effects on cells following transfection with high amounts of plasmid. HeLa cells were seeded at a concentration of ~200,000 cells per well in a 6-well plate. 18 hours after plating, cells were transfected with untagged plasmids purified using Endo-Free plasmid purification kit (Stratagene) using FuGENE6(μl) (Roche, Nutley, NJ) :DNA(μg) ratio of 1.5 : 1.

IV.C. Measurement of endogenous gene expression

15-18 hours after transfection cells were washed twice with PBS and infected with 200 hemagluttanin units of Sendai virus per ml. Six hours after infection, cells were harvested and total mRNA was isolated and treated with RNase-free DNAase using RNeasy RNA purification kit (Strategene) following the manufacturer's protocol. 1μg of total RNA was used to synthesize cDNA using Transcriptor first strand synthesis kit

(Roche). Amplification primers for interferon-β, LEPREL1-T1, RANTES, UPA, and TPA gene transcriptions were designed at https://www.roche-applied-science.com/sis/rtpcr/upl/index.jsp?id=UP030000 and synthesized by Integrated DNA Technologies, Inc. (Coralville, IA) and added to cDNA samples. The amount of amplified product was quantified using the LightCycler480 system (Roche, Nutley, NJ).

V. BIBLIOGRAPHY

1. **Apostolou, E., and D. Thanos.** 2008. Virus Infection Induces NF-kappaB-dependent interchromosomal associations mediating monoallelic IFN-beta gene expression. Cell **134:**85-96.
2. **Chytil, M., B. R. Peterson, D. A. Erlanson, and G. L. Verdine.** 1998. The orientation of the AP-1 heterodimer on DNA strongly affects transcriptional potency. Proc Natl Acad Sci U S A **95:**14076-81.
3. **Dragan, A. I., R. Carrillo, T. I. Gerasimova, and P. L. Privalov.** 2008. Assembling the human IFN-beta enhanceosome in solution. J Mol Biol **384:**335-48.
4. **Du, W., and T. Maniatis.** 1992. An ATF/CREB binding site is required for virus induction of the human interferon beta gene [corrected]. Proc Natl Acad Sci U S A **89:**2150-4.
5. **Escalante, C. R., E. Nistal-Villan, L. Shen, A. Garcia-Sastre, and A. K. Aggarwal.** 2007. Structure of IRF-3 bound to the PRDIII-I regulatory element of the human interferon-beta enhancer. Mol Cell **26:**703-16.
6. **Falvo, J. V., B. S. Parekh, C. H. Lin, E. Fraenkel, and T. Maniatis.** 2000. Assembly of a functional beta interferon enhanceosome is dependent on ATF-2-c-jun heterodimer orientation. Mol Cell Biol **20:**4814-25.
7. **Fan, C. M., and T. Maniatis.** 1989. Two different virus-inducible elements are required for human beta-interferon gene regulation. Embo J **8:**101-10.
8. **Goodbourn, S., and T. Maniatis.** 1988. Overlapping positive and negative regulatory domains of the human beta-interferon gene. Proc Natl Acad Sci U S A **85:**1447-51.
9. **Goodbourn, S., K. Zinn, and T. Maniatis.** 1985. Human beta-interferon gene expression is regulated by an inducible enhancer element. Cell **41:**509-20.
10. **Honda, K., H. Yanai, A. Takaoka, and T. Taniguchi.** 2005. Regulation of the type I IFN induction: a current view. Int Immunol **17:**1367-78.
11. **Imaizumi, T., F. Sato, H. Tanaka, T. Matsumiya, H. Yoshida, T. Yashiro-Aizawa, K. Tsuruga, R. Hayakari, H. Kijima, and K. Satoh.** 2011. Basic-helix-loop-helix transcription factor DEC2 constitutes negative feedback loop in IFN-beta-mediated inflammatory responses in human mesangial cells. Immunol Lett **136:**37-43.
12. **Kim, T. K., and T. Maniatis.** 1997. The mechanism of transcriptional synergy of an in vitro assembled interferon-beta enhanceosome. Mol Cell **1:**119-29.
13. **Malmgaard, L.** 2004. Induction and regulation of IFNs during viral infections. J Interferon Cytokine Res **24:**439-54.
14. **Merika, M., A. J. Williams, G. Chen, T. Collins, and D. Thanos.** 1998. Recruitment of CBP/p300 by the IFN beta enhanceosome is required for synergistic activation of transcription. Mol Cell **1:**277-87.
15. **Munshi, N., T. Agalioti, S. Lomvardas, M. Merika, G. Chen, and D. Thanos.** 2001. Coordination of a transcriptional switch by HMGI(Y) acetylation. Science **293:**1133-6.

16. **Panne, D., T. Maniatis, and S. C. Harrison.** 2007. An atomic model of the interferon-beta enhanceosome. Cell **129:**1111-23.
17. **Panne, D., T. Maniatis, and S. C. Harrison.** 2004. Crystal structure of ATF-2/c-Jun and IRF-3 bound to the interferon-beta enhancer. Embo J **23:**4384-93.
18. **Ramirez-Carrozzi, V., and T. Kerppola.** 2003. Asymmetric recognition of nonconsensus AP-1 sites by Fos-Jun and Jun-Jun influences transcriptional cooperativity with NFAT1. Mol Cell Biol **23:**1737-49.
19. **Sato, M., N. Hata, M. Asagiri, T. Nakaya, T. Taniguchi, and N. Tanaka.** 1998. Positive feedback regulation of type I IFN genes by the IFN-inducible transcription factor IRF-7. FEBS Lett **441:**106-10.
20. **Suhara, W., M. Yoneyama, I. Kitabayashi, and T. Fujita.** 2002. Direct involvement of CREB-binding protein/p300 in sequence-specific DNA binding of virus-activated interferon regulatory factor-3 holocomplex. J Biol Chem **277:**22304-13.
21. **Thanos, D., and T. Maniatis.** 1995. Virus induction of human IFN beta gene expression requires the assembly of an enhanceosome. Cell **83:**1091-100.
22. **Wathelet, M. G., C. H. Lin, B. S. Parekh, L. V. Ronco, P. M. Howley, and T. Maniatis.** 1998. Virus infection induces the assembly of coordinately activated transcription factors on the IFN-beta enhancer in vivo. Mol Cell **1:**507-18.
23. **Whittemore, L. A., and T. Maniatis.** 1990. Postinduction repression of the beta-interferon gene is mediated through two positive regulatory domains. Proc Natl Acad Sci U S A **87:**7799-803.
24. **Yie, J., K. Senger, and D. Thanos.** 1999. Mechanism by which the IFN-beta enhanceosome activates transcription. Proc Natl Acad Sci U S A **96:**13108-13.
25. **Zinn, K., and T. Maniatis.** 1986. Detection of factors that interact with the human beta-interferon regulatory region in vivo by DNAase I footprinting. Cell **45:**611-8.

CHAPTER 5: SUMMARY, IMPACT, AND OUTLOOK

I. SUMMARY

Transcription initiation is controlled by multi-protein transcription factor complexes assembled at regulatory elements and at the site of transcription initiation. Two types of models have been proposed to explain how multiple proteins function in concert to regulate transcription. According to "jigsaw puzzle" type models, the transcription factors must assemble in a specific configuration to function. According to "independent agents" type models, the configuration of the transcription factors is not essential for function.

The difference between these two types of models reflects different assumptions concerning the influence of steric constraints on the multivalent interactions among proteins and nucleic acids that regulate transcription. Interactions among proteins that bind to closely juxtaposed sequences (composite regulatory elements) are generally thought to require a specific arrangement of the transcription factors at regulatory elements. Conversely, interactions between proteins that bind to distal enhancers and proteins that bind to the core promoter, are predicted not to require a specific arrangement of the proteins on the DNA.

The interferon-β enhancer has been investigated as a model for synergistic transcription activation by proteins that bind to closely juxtaposed sequences (7, 9, 14, 15, 19, 37, 41, 44, 45). The structural nature of complexes at the interferon-β enhancer has

been investigated using several different experimental approaches. Photo-crosslinking experiments indicate that the orientation of ATF2-Jun heterodimers binding is fixed upon IRF3 binding such that ATF2 contacts the half-site proximal to IRF3 (9). In contrast, the X-ray crystal structure of the minimal DNA binding domains of ATF2, Jun and IRF3 shows the opposite orientation of ATF2-Jun heterodimer binding in which Jun contacts the half-site proximal to IRF3 (23). The results from each of these studies were interpreted to indicate that ATF2-Jun heterodimers interact with IRF3 in a fixed, albeit opposite, orientation.

We investigated the effects of interactions with IRF3 and HMGI on the orientation of ATF2-Jun heterodimer binding at the interferon-β enhancer and the effects of heterodimer orientation on the cooperativity of complex formation *in vitro* and on endogenous interferon-β gene transcription in cells. IRF3 and HMGI bound cooperatively with both orientations of ATF2-Jun heterodimers at the interferon-β enhancer. Cooperative DNA binding by both ATF2-Jun heterodimer orientations with IRF3 was mediated at least in part by interactions between charged residues in IRF3 and symmetry-related residues in both subunits of the heterodimer.

Mutations in ATF2 and Jun that caused opposite orientations of heterodimer binding *in vitro* also resulted in distinct levels of endogenous interferon-β gene transcription. Different regions of ATF2 and Jun determined the effects of heterodimer orientation on transcription of different endogenous genes. The orientation of heterodimer binding therefore has gene-specific effects on transcription that are mediated by distinct mechanisms.

I.A. Cooperative DNA-binding by ATF2-Jun and IRF3

I have applied gelFRET analysis (25) to the examination of the orientation of binding by ATF2-Jun heterodimers at the interferon-β enhancer. This revealed a previously unobserved conformational heterogeneity within ATF2-Jun-IRF3-DNA complexes, where iIRF3 interacts equivalently with both bATF2-bJun binding orientations. Although bATF2-bJun has a significant preference for the orientation in which bJun binds to the right IFNb half-site, bATF2-bJun can also bind to IFNb in the opposite orientation. The relative preferences for these two orientations are precisely conserved in the presence of the DNA-binding domain of iIRF3, indicating that iIRF3 can interact equivalently with either orientation of bATF2-bJun binding at IFNb. Moreover, in the presence of iIRF3 together with HMGI, bATF2-bJun binds to IFNb with no orientation preference [Fig 5.1]. This can be indicative of either asymmetric interactions between bATF2-bJun and HMGI or asymmetric interactions between bATF2-bJun and iIRF3 in the presence of HMGI.

The previous model of cooperativity between ATF2-Jun and IRF3 derived from x-ray crystallographic analysis evokes indirect, DNA-mediated interactions between ATF2-Jun and IRF3 in which complementary protein-induced changes in the DNA structure promotes more favorable DNA-binding (23). Our model of cooperativity between bATF2-bJun and iIRF3 includes a heterodimer-iIRF3 contact previously observed in the crystal structure as well as additional heterodimer-iIRF3 interactions that involve regions of bATF2 and bJun not included in the crystal structure. Due to the redundant nature of the heterodimer-iIRF3 interactions, previous methods for the analyses of the role of residues in individual subunits on cooperative interactions between

bATF2-bJun and iIRF3 were not possible.

By analyzing the reciprocal effects of mutations in bATF2 *versus* bJun on DNA-binding in the presence of iIRF3, I was able to detect competing alternative interactions between iIRF3 and conserved amino acid charges in bATF2 and bJun. Moreover, the relative effects of mutations in bATF2 *versus* bJun on heterodimer orientation preference were qualitatively similar in the presence of HMGI, indicating that HMGI does not influence the nature of the interaction between bATF2-bJun and iIRF3. Therefore, depending on the charged state of ATF2 and Jun, the heterodimer can adopt different binding orientation preferences in higher order interferon-β enhancer complexes containing IRF3 and HMGI.

Substitutions in bATF2-bJun that forced interactions between either bATF2 and iIRF3 in the left half-site or bJun and iIRF3 in the right half-site were slightly more potent than substitutions that forced interactions between iIRF3 and the opposite orientation of heterodimer binding. Cooperative DNA-bending interactions between ATF2-Jun and IRF3 have previously been hypothesized to promote the orientation where ATF2 binds to the left half-site and Jun binds to the right half-site. Therefore, it is possible that indirect interactions of this nature may add an asymmetric component to the interactions between bATF2-bJun and iIRF3. Alternatively, the intrinsic orientation preference of heterodimers for the orientation where bJun binds to the right half-site, may also contribute to the incomplete re-orientation of heterodimers that are deficient in direct interactions with iIRF3. Whatever the underlying cause of orientation dependent stability of the complex, this is an important aspect of the bATF2-bJun-iIRF3 complex formation at the interferon-β enhancer. The interplay between asymmetric interactions and amino

acid interactions between the heterodimer and iIRF3 that allow the heterodimer to bind in either orientation could potentially permit the modulation of the stability of the complexes at the same enhancer site through charge modifications in ATF2 and Jun.

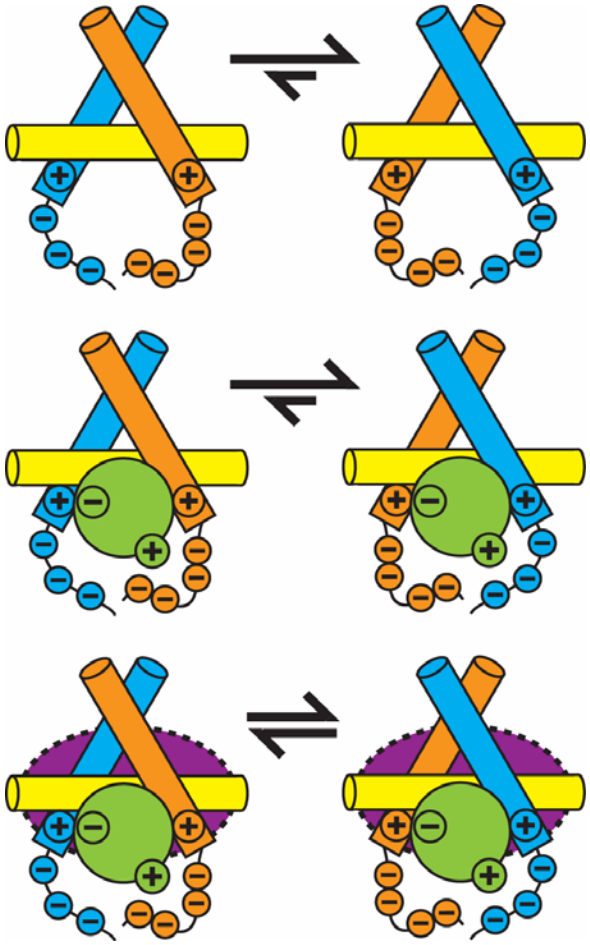

Figure 5.1 Model for the role of charged amino acid residues in the configuration of IFNb complexes containing bATF2-bJun, iIRF3, and HMGI. *Upper diagram:* bATF2-bJun heterodimers have an intrinsic orientation preference at IFNb (yellow) where bJun (cyan) favors the right IFNb half-site and bATF2 (orange) favors the left IFNb half-site. *Middle diagram:* Negatively charged amino acid residues N-terminal to the bZIP basic region (indicated by negative signs) and an arginine (indicated by plus sign) in the bZIP basic region are conserved in bATF2 and bJun. This allows equivalent interactions with D45 (indicated by negative sign) and K70 (indicated by plus sign) of iIRF3 (light green circle) regardless of the orientation of DNA-binding by bATF2-bJun. *Lower diagram:* Interactions between bATF2-bJun and iIRF3 are preserved in the presence of an unknown number of HMGI molecules (dotted purple circle). Indirect or direct interactions between HMGI and bATF2-bJun eliminate the orientation preference of bATF2-bJun binding at IFNb.

I.B. Role of ATF2-Jun orientation in interferon-β transcription

The functional significance of the structural organization of transcription regulatory complexes has been investigated mainly using artificial reporter genes (5, 9, 10, 15, 24, 37, 39). Chimeric proteins that contain the DNA binding domain of one protein fused to a regulatory region from another protein can regulate reporter gene transcription. This fact has been interpreted to indicate that the architecture of the transcription complex is not important for transcription regulation; however, artificial reporter genes are unlikely to adopt the same chromatin structure and transcription factor configuration as endogenous genes.

The role of heterodimeric transcription factor orientation in native gene transcription has not been determined. In order to elucidate the functional role(s) of ATF2-Jun orientation at the endogenous interferon-β gene, I have used my structural understanding of ATF2-Jun-IRF3-DNA complexes to design mutationally-trapped ATF2-Jun orientation isomers in which specific alanine substitutions permit favorable interactions between ATF2-Jun and IRF3 only when ATF2-Jun is bound to DNA in either one or the other orientation. Using these oriented complexes, I first wanted to know whether the orientation of heterodimer binding influences the stability of enhancer complexes *in vitro*.

GelFRET analysis showed that wild-type ATF2-Jun heterodimers bound to the interferon-β enhancer element have a significant preference for the orientation in which Jun binds to the right DNA half-site. Therefore, amino acid substituted heterodimers which differ in the direction that the heterodimer is forced to interact with the DNA should also differentially affect the formation of heterodimer-DNA complexes. To test

this, I compared the effect of increasing concentrations of iIRF3 on the formation of complexes containing oppositely oriented bATF2-bJun heterodimers and found that heterodimers in which bJun favors the right IFNb half-site produce significantly more complexes over a range of iIRF3 concentrations.

If asymmetric heterodimer-DNA interactions do in fact differentially affect the stability of DNA binding by oppositely oriented heterodimers, I hypothesized that interactions with HMGI which eliminate bias in the orientation of wild-type ATF2-Jun heterodimers should also eliminate differences in the stability of DNA-binding by oppositely oriented heterodimers. Consistent with this, I found that when titrating oppositely oriented heterodimer-HMGI complexes with increasing amounts of iIRF3 or, conversely, when titrating heterodimer-iIRF3 complexes with increasing amounts of HMGI, equal amounts of complexes are formed. Thus, iIRF3 and HMGI cooperatively reduce the effect of heterodimer orientation of the stability of complex formation at IFNb, consistent with their cooperative reduction in the orientation preference of ATF2-Jun heterodimers.

The discovery that ATF2-Jun heterodimers can bind the interferon-β enhancer in both orientations equally well in association with iIRF3 and HMGI raised the question of whether a particular orientation of heterodimer binding is actually required for functionally active enhancer complexes. To address this question, I measured the virus-induced activation of endogenous interferon-β transcript levels in HeLa cells co-over-expressing full-length IRF3 and full-length ATF2 and Jun that contained the amino acid substitutions predicted to alter heterodimer orientation. In the absence or presence of exogenous IRF3, I saw reproducible differences between cells expressing different

heterodimer variants, where heterodimers that strongly favor the orientation in which Jun binds to the right have higher levels of interferon-β transcripts.

When comparing the *in vitro* binding results to the *in vivo* results, I saw that the heterodimer orientation which produces higher levels of interferon-β transcripts *in vivo* also has a relatively greater stability of DNA binding. Therefore, I hypothesized that the effect of binding orientation on transcription could is mediated by differences in the amount of ATF2-Jun-IRF3 complexes formed in HeLa cells in a manner potentially not even related to differences stereo-specific architecture of the complexes. In order to distinguish between the effects of heterodimer orientation on DNA-binding affinity *versus* trans-activation, I divided ATF2 and Jun into two regions: an amino-terminal region that contained the trans-activation domain and a carboxy-terminal region that contained the DNA-binding domain; and constructed chimeric proteins, abbreviated as AJ or JA, in which the amino- and carboxy-terminal regions of ATF2 and Jun were exchanged.

It was predicted that, for genes regulated by the stability of heterodimer binding to DNA, the C-terminal regions of ATF2 and Jun should be sufficient to mediate the effects of heterodimer orientation on endogenous gene transcript levels regardless of whether the activation domains are switched. On the other hand, for genes that are regulated primarily by stereo-specific interactions between the heterodimer trans-activation domains and other regulatory proteins, exchange of the N-terminal regions of ATF2 and Jun should reverse the effects of heterodimer orientation on gene transcript levels. I found that reversal of the entire N-terminal regions of XG-substituted heterodimers did influence the relative effects of XG substitution in ATF2 *versus* Jun on interferon-β and

LEPREL1-T1 transcript levels over a range of JA and AJ plasmid ratios. In contrast, exchange of the N-terminal regions of ATF2 and Jun reversed the relative effects of XG substitution in ATF2 *versus* Jun on RANTES, TPA, and UPA genes over a range of plasmid ratios.

Taken together, these results indicate that the regions of ATF2 and Jun that contain the trans-activation domain mediate the effect of heterodimer orientation on the efficiency on several endogenous genes including RANTES, TPA, and UPA, consistent with previously reported role of activation domain positioning in mediating the effects of Fos-Jun orientation on reporter gene activation. In contrast, for genes such as interferon-β and LEPREL1-T1, that contain a composite ATF2-Jun-IRF3-HMGI site, regions of ATF2 and Jun which contain the DNA-binding domain primarily determines the effects of heterodimer orientation on gene activation [Fig 5.2].

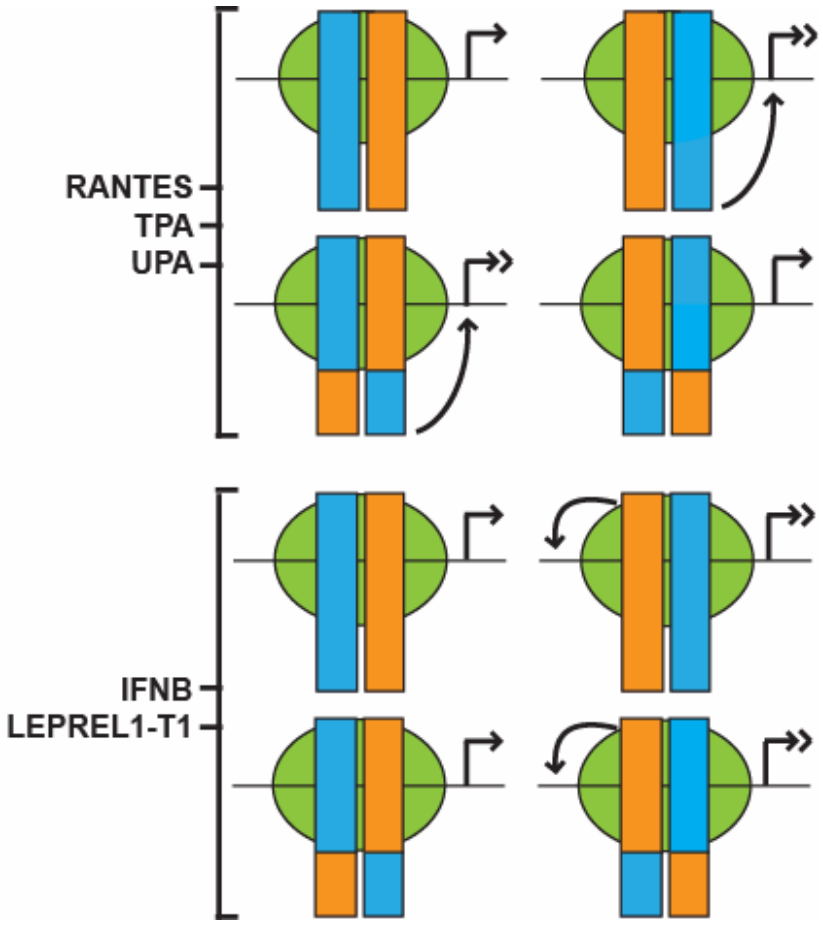

Figure 5.2 Model for role of ATF2-Jun orientation in the transcription of different genes. Cells expressing heterodimers with substitutions that force ATF2 (orange) to the left IFNb half-site and Jun (cyan) to the right IFNb half-site produce more interferon-β (IFNB) as well as LEPREL1-T1 transcripts (indicated by double-headed arrows). Exchange of the N-terminal domains of ATF2 and Jun (bottom domain) does not influence the effects of these substitutions on transcription. The effects of orientation on IFNB and LEPREL1-T1 transcription are therefore mediating by the DNA-binding activity of ATF2-Jun (indicated by curved arrow). In contrast, exchange of the N-terminal domains of ATF2 and Jun reverses the relative effect of heterodimer orientation on expression of RANTES, TPA, and UPA. The effect of orientation on RANTES, TPA, and UPA transcription is therefore mediated by the trans-activation activity of ATF2-Jun (indicated by curved arrow).

II. IMPACT

Cells must generate complex developmental programs and responses to their environments, which are largely encoded by different combinations of transcription factors that have a synergistic or "greater-than-additive" effect on gene expression. This process certifies that no specific transcription factor alone, which has the capacity to recognize hundreds of gene regulatory loci, will erroneously activate the expression of inappropriate genes. Therefore, understanding how groups of transcription factors work together to achieve gene activation is important for understanding the underlying principles of cellular regulation. Many mechanisms for transcriptional synergy have been proposed, but few have been critically tested. With this dissertation research, I have begun to paint a clearer picture of both the structural basis and the functional significance of synergistic interactions within transcription factor complexes.

II.A. Comparison with other ternary complexes

Comparison of cooperative complex formation by Fos-Jun-NFAT and ATF2-Jun-IRF3 reveal distinct mechanisms of cooperativity between these transcription factor complexes. Whereas asymmetric heterodimer-DNA contacts together with asymmetric Fos-Jun and NFAT interactions modulate the stability of Fos-Jun-NFAT complex formation at different nonconcensus DNA sites (24), asymmetric heterodimer-IRF3 contacts in complexes that contain different charge modification together with asymmetric ATF2-Jun-DNA interaction modulate the stability of ATF2-Jun-IRF3 complex formation at the same DNA site.

The structures of many transcription factors vary at different binding sites (6, 16, 21, 24, 28, 31, 33, 36, 38). These differences in structure are thought to contribute to the differences in the effects of these factors on transcription of different genes (1, 6, 11, 21, 32, 34, 38). In the case of nuclear hormone receptors, the spacing and the relative orientations of multiple recognition sequences can influence the transcriptional activity of the complex(1, 6, 11, 21, 32, 34). Our results demonstrate that ATF2-Jun, IRF3 and HMGI can bind to one recognition sequence in different configurations.

This discovery demonstrates that transcription factor complexes consisting of multiple proteins can adopt more than one configuration at a single regulatory element. We also found that the bATF2-bJun-iIRF3-HMGI complex has a half-life shorter than 30 seconds in the presence of an excess of competitor oligonucleotide. Different configurations of this complex are therefore in dynamic exchange, at least *in vitro*. Some of the residues that influence the configurations of the complex can be modified (13, 22). It is therefore possible that the balance between alternative configurations of bATF2-bJun-iIRF3-HMGI binding is regulated by post-translational modifications or by interactions with additional proteins.

II.B. Implications in gene regulatory specificity

This and the previously described gelFRET analyses were utilized in concert to illustrate how subtle charge modifications in ATF2 and Jun can dramatically affect a balance between two alternative interactions between ATF2-Jun and IRF3 at sites of active gene transcription. Post-translational modification of transcription factors occurs frequently (18, 35), and is a potential means by which the cell can control the orientation

preference of heterodimer binding at the interferon-β enhancer. Mass spectrometry has shown acetylation of the basic region of ATF2 at K339 (13). Although this residue is not predicted to directly contact any residue in IRF3, acetylation of K339 in ATF2 could potentially alter either contacts with the DNA in the presence of IRF3 or the conformation of ATF2 and thus the positioning of the R345 side chain, thereby influencing the orientation preference at the enhancer.

In addition to asymmetric charge modifications in ATF2 and Jun, I have shown that the binding of HMGI can also influence the orientation preference of ATF2-Jun heterodimers at the interferon-β enhancer. HMGI has been shown to play a pivotal role in the assembly and disassembly of the interferon-β enhanceosome (22). Acetylation of HMGI on lysine 71 correlates with the recruitment of the full complement of transcription factors to the endogenous enhancer in Sendai-virus-infected HeLa cells, whereas deacetylation of lysine 71 followed by acetylation of lysine 65 precedes the disassembly of this complex (22).

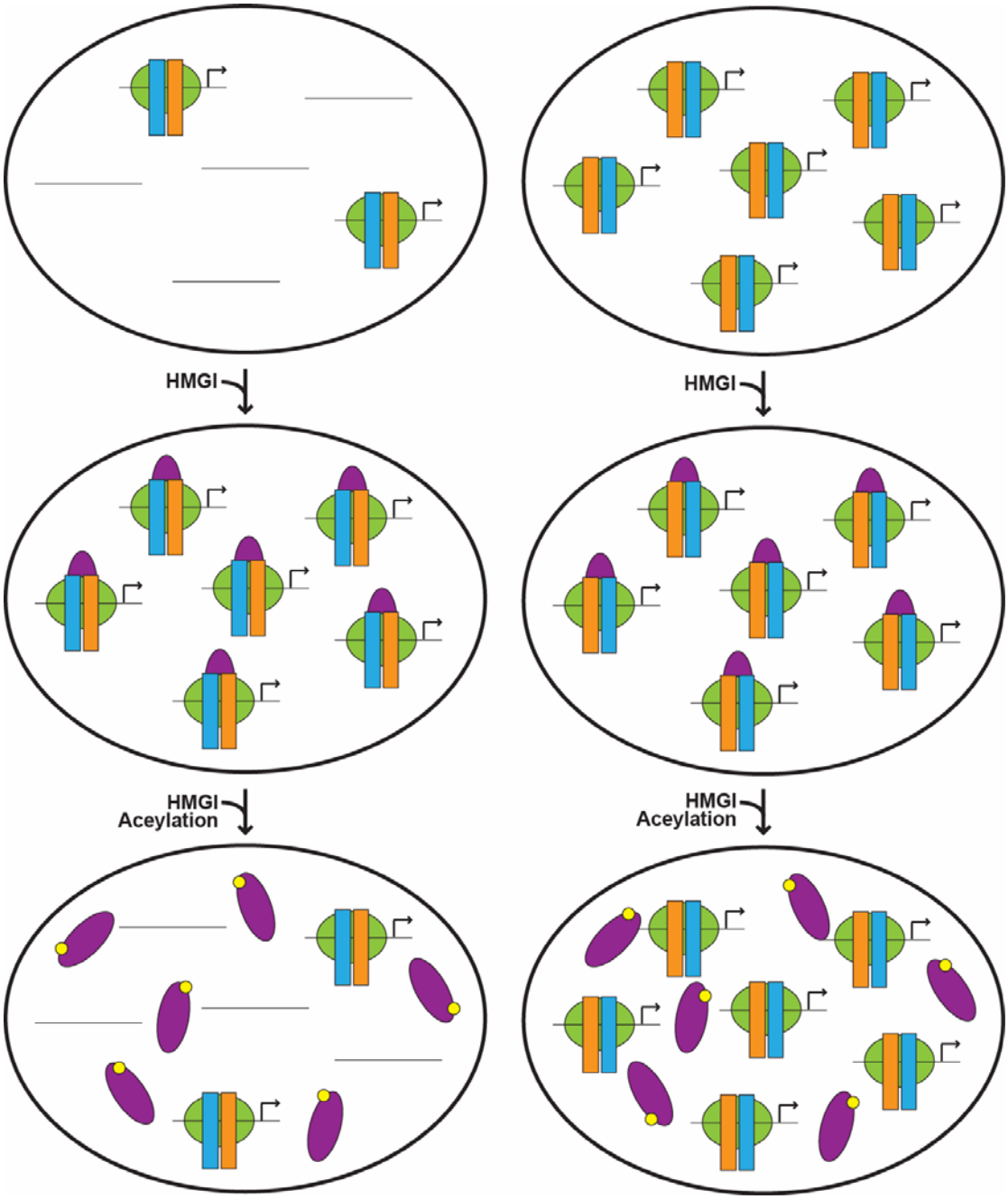

Figure 5.3 Proposed interplay of heterodimer orientation, HMGI, HMGI acetylation the formation of ATF2-Jun-IRF3 complexes at the endogenous interferon-β enhancer. *Upper diagram:* There are at least six alleles of the single human interferon-β gene in HeLa cells that are indicated by horizontal black lines. Cells expressing heterodimers that favor the binding of Jun (cyan) to the left half-site (left diagram) are predicted to form less enhancer complexes than cells expressing heterodimers that favor the binding of Jun to the right half-site (right diagram). *Middle diagram:* Cells expressing oppositely oriented heterodimers are predicted to form similar amounts of enhancer complexes in the presence of HMGI (purple oval). *Bottom diagram:* In the presence of lysine 71-acetylated HMGI, recruitment of HMGI to the composite ATF2-Jun-IRF3 site is predicted to be inhibited, resulting in different amounts of enhancer complexes and, consequently, different levels of interferon-β transcription depending on the orientation of heterodimer binding (compare left *versus* right diagram).

Although the recruitment of acetylated HMGI to the interferon-β enhancer occurs concomitantly with the recruitment of ATF2, Jun, and IRF3, efforts to detect ATF2-Jun-IRF3-HMGI complexes have been elusive. I have found that HMGI binds cooperatively with ATF2-Jun-IRF3 complexes at the interferon-β enhancer. Various modifications of HMGI (K65Q, K65E, K71Q, K71E) had no measurable effect on the orientation preference of bATF2-bJun heterodimers and resulted is less efficient binding to the IFNb oligonucleotide in either the presence or absence of other proteins. Further studies are required to determine the role of HMGI and HMGI modifications on interferon-β activation by ATF2, Jun, and IRF3 *in vivo* [Fig. 5.3].

III. OUTLOOK

Using ATF2-Jun-IRF3 complexes as model system, further investigations into the significance of nucleoprotein structure in gene regulation are possible. In particular, the techniques of single-cell qPCR analysis and single-molecule mRNA visualization allow determination of the role heterodimer orientation preference on steady-state and dynamic properties of gene expression.

III.A. Fine tuning "noisy" gene expression

In many circumstances, measurement of gene expression in a large population of cells does an excellent job in predicting average behavior. At the single-cell level, however, you often see large cell-to-cell variability in gene expression (8, 12, 27). This heterogeneity can be tied to many important biological processes, such as the evolution of genetically identical organisms and the immunological response to viral infection (30).

Therefore, ensemble measurements of gene expression can potentially mask significant physiological differences between different populations of cells that have similar mean mRNA levels but very different variations from the mean. This need for single-cell analyses has led to the development of a number of novel techniques that rely on automated technology to isolate and perform measurements on individual cells, including single-cell protein reporter assays (2, 4, 17, 20, 29, 40, 42, 43). Protein reporter assays tend to add translational noise to the data generated as well as measurement noise due to cellular autofluorescence and other limiations of direct fluorescence assays.

To determine the noise, differential expression from different interferon-β alleles of human cultured cells can be measured used a common readout polymorphism of interferon-β. Different allelic mRNAs differ by a single nucleotide and the amplified single cell PCR product is predicted to preserve their relative levels of expression within each cell. Since factors such as viral load, transcription factor expression levels, signaling components, or polymerase activity should affect both alleles equally in a given cell, differential expression from different alleles in the same cell will represent noise intrinsically tied to the transcription process itself such as that associated with conformational variability in the nucleoprotein architecture at gene loci.

III.A.i. Role of heterodimer orientation in allele-specific transcription

My experimental model of un-oriented ATF2-Jun binding at sites of transcription which clearly favor a particular orientation begs the question: WHY? Single-cell proteomic studies in yeast have revealed that proteins that are essential for responding to environmental or pathogenic stimuli tend to display high levels of cell-to-cell expression

variability. In particular, genes which are responsive to factors such SAGA and SWI/SNF that act on chromatin structure to reversibly convert inactive DNA to active DNA tend to encode proteins whose levels fluctuate considerably. As suggested by Blake *et al.* (3) and Raser *et al*. (26), high noise is likely to be due, at least in part, to the introduction of a slow step into the production of mRNA, making the process more prone to bursts. Therefore, it is my hypothesis that un-oriented ATF2-Jun binding may introduce an obligatory element of randomness to interferon-β gene expression following viral infection. To test this, allele-to-allele variability of interferon-β mRNA expression can be measured in virally-infected HeLa cells over-expressing opposite oriented ATF2-Jun heterodimers.

Two types of mRNA variability can be expected in this experimental system: cell-to-cell or "extrinsic" variability and within-cell or "intrinsic" variability. Extrinsic variability may reflect differences in the state of each cell or its surrounding environment, whereas intrinsic variability may stem from the inherently chaotic nature of biomolecular events—such as a chance collision between two randomly moving proteins or erratic fluctuations in the conformation of a stretch of DNA. Differences in the expression of the different alleles in the same cell can be assumed to be independent of extrinsic variability. For example, if bi-directional ATF2-Jun binding underlies intrinsic gene expression variability, you would expect to see more correlation between the levels of allele 1 and allele 2 mRNA in cells expressing favorably-oriented complexes compared to cells expressing unfavorably-oriented complexes [Fig. 5.5].

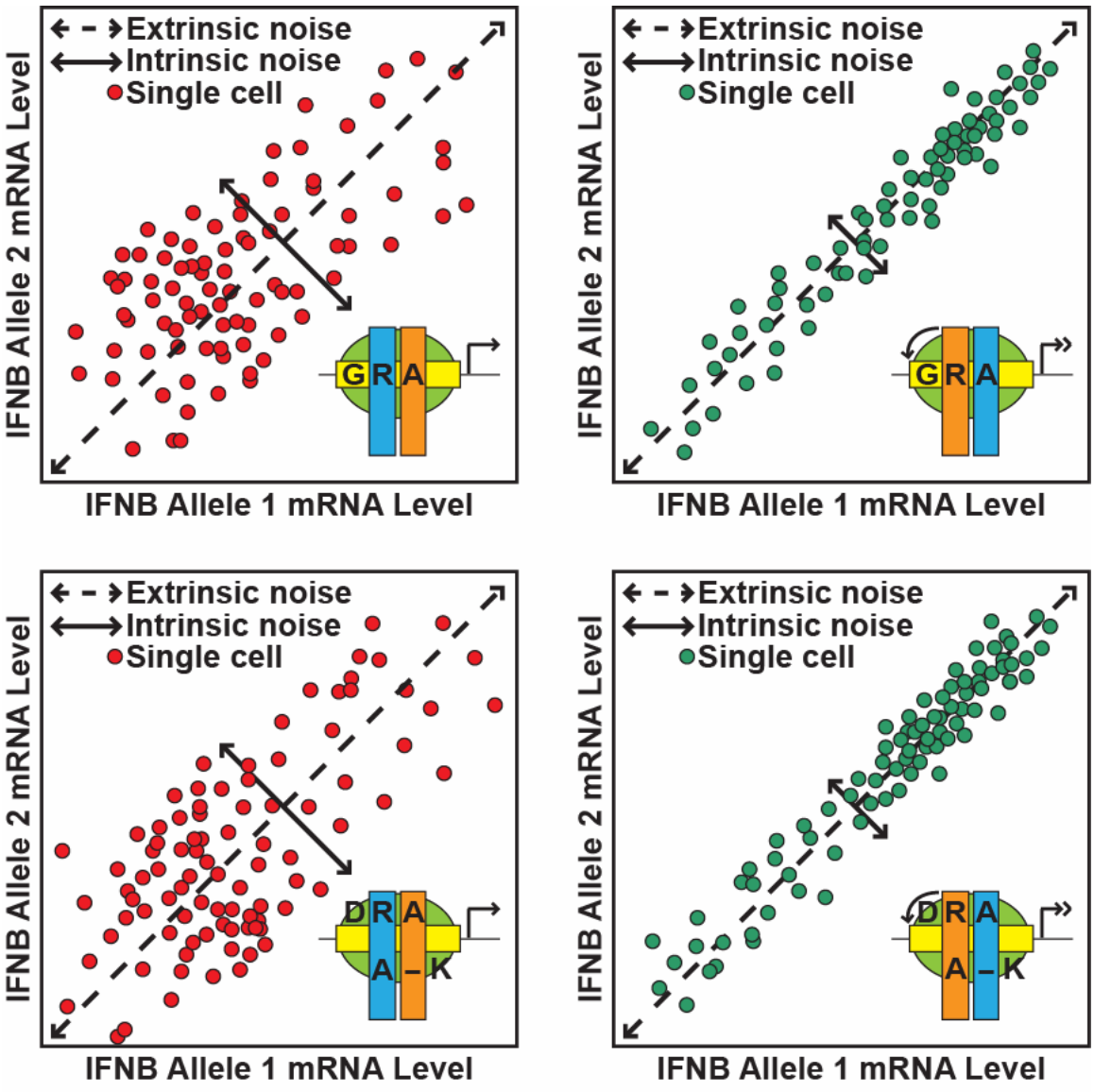

Figure 5.4. Proposed effect of conformational variability in transcription factor-DNA complexes on intrinsic gene expression noise. The expression of two different allelic variants of the interferon-β (IFNB) gene will be detected by qPCR in single cells isolated by flow cytometry. Extrinsic noise will be defined as the variation in expression of identical alleles due to differences between cells (this is represented by the total range of mRNA levels along the diagonal, dashed arrow), whereas the intrinsic noise will be defined as the variation in expression of two different alleles in the same cell (this is seen where data points for individual cells do not lie on the diagonal, solid arrow).

III.B Visualization of single mRNA transcripts

The textbook model of gene transcription that most students and educators have become accustomed to learning and teaching usually involves a scenario that is assumed to proceed smoothly and uniformly over time. However, recent work has revealed that many genes are expressed in a pulsating manner. That is, the period of time in which a gene is considered "on" can include bursts of transcriptional activity *and* intervals of inactivity. The most direct way to detect gene activation and inactivation is to directly monitor the mRNA produced from the gene at the resolution of single molecules. Since the stability of mRNA is typically much lower than that of proteins, mRNA levels tend to reflect more accurately the state of a gene. Pioneering work by the Singer laboratory has made possible the quantitation of mRNA expression at the single transcript level in living yeast. In this approach, the mRNA transcript of interest bears a repeated sequence motif which binds to an ectopically expressed protein tagged with green fluorescent protein (GFP). Then, the number of mRNA molecules can be reliably estimated by measuring the intensity of the fluorescent spots corresponding to mRNA-bound GFP molecules.

III.B.i. Role of heterodimer orientation in the kinetics of transcription

Interferon-β transcription has a strong stochastic element that results in large cell-to-cell variability. By observing the kinetics of mRNA expression in individual cells, the mechanism for how conformational variability in ATF2-Jun-IRF3 complexes contributes to the inherent randomness of gene activation can be elucidated. Many phenomena have been offered as potential mechanisms underlying "transcriptional bursting," however none have been critically tested. By quantitating mRNA expression at the single

molecule level in cells expressing the previously described conformation-trapping proteins, investigation of the role of conformational heterogeneity in transcription factor complexes on the dynamics of gene expression is possible.

This general strategy can be used to compare the dynamics of interferon-β mRNA expression in virally-infected human cells expressing ATF2-Jun-IRF3 complexes predicted to have different conformational variations. To do this, a previously established method for gene delivery in mammalian cells can be combined with the above-described mRNA detection method in yeast. Specifically, retroviral gene delivery can be used to integrate the entire enhancer-promoter region of interferon-β upstream of a reporter gene bearing binding sites for GFP-tagged proteins into the genomes of cultured human cells. These cells that stably express the reporter gene can then be transfected with plasmids expressing GFP-tagged proteins, ATF2, Jun, and IRF3 and virally infected.

It is predicted that if bursting is due to random fluctuations in interferon-β gene expression can be attributed to random changes in ATF2-Jun binding orientation, that cells transfected with heterodimers that only bind to DNA in the orientation that favors transcriptional activity will have a more uniform interferon-β expression pattern characterized by reduced frequencies of transcriptional bursting. Enhanceosome formation increases the rate of expression by an unknown mechanism. Many phenomena such as chromatin remodeling, the unbinding and binding of transcription factors, and changes in DNA conformation have been offered as potential mechanisms underlying "transcriptional bursting," however the subtle nature of these events has made critical testing of their roles impossible.

Several groups have reported new methods for temporally tracking mRNA levels in single cells through the use of fluorescent protein which binds to non-coding regions of mRNA. This technique can be used to determine the effect of different nucleoprotein conformations on the kinetics of interferon-β gene expression. Specifically, confocal microscopy and its associated quantification software can be used to visualize and measure increases in fluorescence due to allele-specific interferon-β gene expression in virally infected cells predicted to have either wild-type or conformationally-trapped ATF2-Jun-IRF3-HMGI complexes bound to the enhancer. It is predicted that, if oriented heterodimer binding is associated with a rate-limiting step in interferon-β transcription, the time it should take to achieve a particular level of mRNA expression will be decreased for gene loci bound by ATF2-Jun-IRF3-HMGI complexes that trap a particular conformation.

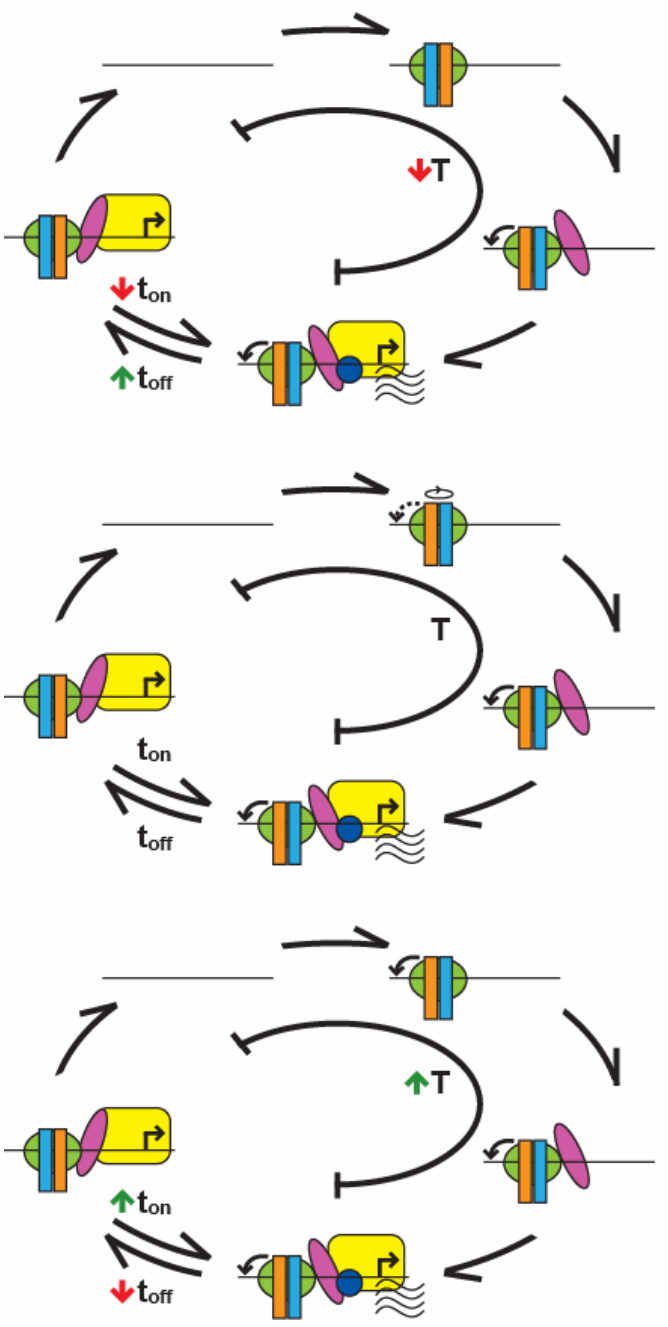

Figure 5.5. Proposed effect of orientation on the kinetics of interferon-beta transcription. Time required for the formation of the pre-initiation complexes is indicated by "T." Differences in the orientation preference of ATF2(orange)-Jun(cyan) heterodimers are predicted to increase (indicated by red arrow) or decrease (indicated by green arrow) the time is takes for de novo transcriptional activation. Heterodimer orientation preference can also influence the de-activation time (t_{off}) and the re-initiation time (t_{on}) which can influence the ratio of active versus inactive complexes.

IV. APPENDICES

Preliminary work

A method for the quantification of allele-to-allele variability in interferon-β mRNA expression in primary dendritic cells using real-time PCR has been previously reported (12). I have adapted this assay to the analysis of HeLa cells for the purpose of determining of the effect of transfected plasmids encoding ATF2 and Jun on allele-to-allele variability in interferon-β transcription.

In order to detect allele-to-allele variability, it is necessary to distinguish the expression of mRNA from one allele from the expression of mRNA from another allele. Single nucleotide polymorphisms (SNPs) are naturally occurring sequence variations in the genome that can occur in one but not the other allele of any given gene, and can be used in order to determine the allelic origins of gene transcripts. In order to determine the presence of SNPs in the coding region of the interferon-β gene, I PCR amplified the coding region of the interferon-β gene from either HeLa genomic DNA or cDNA synthesized from total mRNA isolated from virus infected HeLa cells and submitted the amplification products for DNA sequencing according to the following protocol:

Genomic DNA isolation from HeLa cells:

Washed HeLa cells twice in PBS and trypsinized. Centrifuged for 5 min. at 500 rpm. Harvested genomic DNA from 4.4 X 10^6 HeLa cells with DNeasy tissue kit; eluted with 400 μl buffer AE.

Purification of cDNA from virus-infected HeLa cells:

Purified cDNA from Sendai virus-infected HeLa cells with QiaQuick columns from gel elution kit using PCR purification protocol; eluted with 50 μl buffer TE

Amplification and Sequencing primers:
IFNB 5': 5'-ATGACCAACAAGTGTCTCCTCC-3'
IFNB 3': 5'-GATAGACATTAGCCAGGAGGTTC-3'

qPCR reaction buffer:
8.1 μl template DNA
1.5 μl 10X ThermoPol buffer
1.5 μl DMSO
0.6 μl dNTP
1.5 μl 10 μM For
1.5 μl 10 μM Rev
0.3 μl Vent polymerase

Cycling conditions:
94°C for 1 min. 30 sec.
94°C for 30 sec.
57°C for 30 sec.
72°C for 3 min.
go to 2, 39 times
72°C for 10 min.
4°C forever

Sequencing revealed a T/C SNP in the coding region of interferon-β. In order to determine the relative expression the interferon-β T allele from the interferon-β C allele in individual cells, I have applied adapted the previously described protocol (12) to the analysis of gene expression in individual virus-infected HeLa cells.

Virus-infection and cell-sorting:

Lysis buffer:
4 mM Magnesium acetate
0.05% NP-40
0.8 U/ml protector RNase inhibitor

Sorted 1 cell per well in round-bottom 96-well plates

Combined cDNA synthesis and qPCR

RT-qPCR primers:
GAPDH-Left 5'-AGCCACATCGCTCAGACAC-3'
GAPDH-Right 5'-GCCCAATACGACCAAATCC-3'

IFNB F 5'-GTCAGAAGCTCCTGTGGCAATTGAA-3'

IFNB R 3’-TTCTGGAACTGCTGCAGCTGCTTAA-3’

Combined reverse transcriptase and amplification buffer:
5 μl 2X SYBR mix containing Taq polymerase (Roche)
0.05 μl 100 mM primer 1
0.05 μl 100 mM primer 2
0.1 μl Transcriptor reverse transcriptase (Roche)

Cycling conditions (10 μl reaction volume, 50 cycles):
pre-incubation: 65°C for 30 min., 95°C for 10 min
amplification: 95°C for 30 sec., 60°C for 30 sec., 72°C for 15 sec.
melting curve: 95°C for 5 sec., 55°C for 30 sec., 95°C (continuous)
cooling: 40°C for 10 sec.

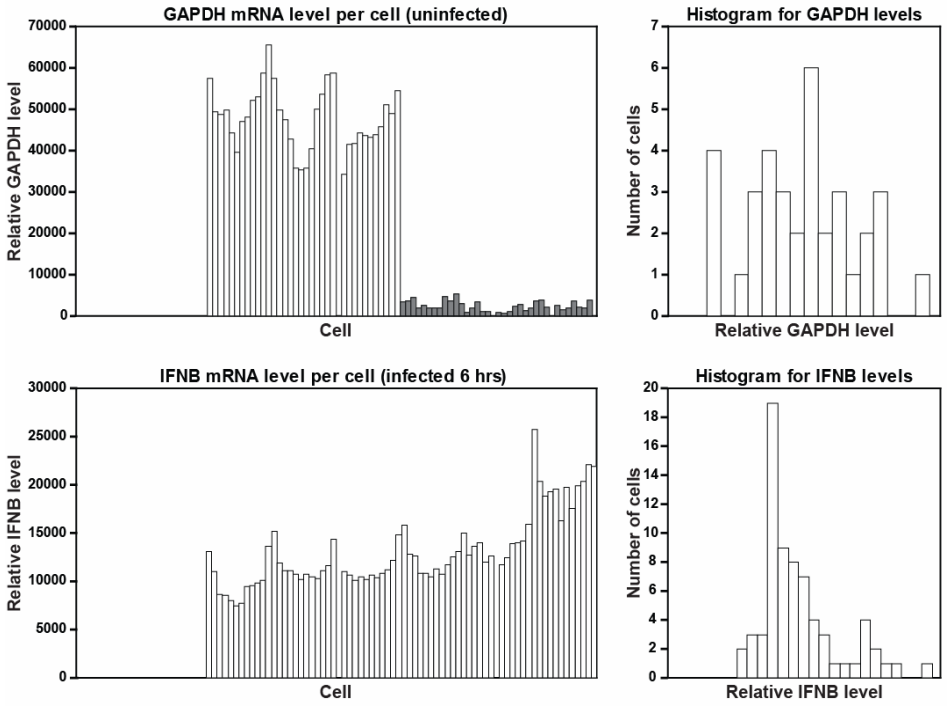

Figure 5.6. qPCR analysis of mRNA expression in individual virus-infected HeLa cells. HeLa cells were infected with Sendai virus for 6 hours and sorted by flow cytometry into individual wells of a 96-well round-bottom plate containing 5 μl lysis buffer. An equal volume of reaction mix containing reverse transcriptase, Taq polymerase, and gene-specific primers was added to each well. Following pre-incubation for 30 minutes at 65°C to allow conversion of the mRNA into cDNA, 50 cycles of amplification were carried out. *Upper left:* Relative GAPDH transcript level was plotted for each cell. Reactions containing the above described components (wells 25-60, white bars) produced amplified product. Reactions that did not include reverse transcriptase (wells 1-24) did not amplify, indicating that genomic DNA is not measured under these conditions. Reactions that included reverse transcriptase reaction buffer (well 61-96 well, dark bars) showed inhibited amplification. *Upper right:* Histogram of number of cells as a function of discrete ranges of GAPDH transcript levels for wells 25-60. *Bottom left:* Relative interferon-β (IFNB) transcript level was plotted for each cell. Reactions that did not include reverse transcriptase (wells 1-24) did not produce amplification. Reactions containing the above described components (wells 25-96, white bars) produced amplified product. *Bottom right:* Histogram of number of cells as a function of discrete ranges of IFNB transcript levels for wells 25-96.

V. BIBLIOGRAPHY

1. **Ambrosetti, D. C., C. Basilico, and L. Dailey.** 1997. Synergistic activation of the fibroblast growth factor 4 enhancer by Sox2 and Oct-3 depends on protein-protein interactions facilitated by a specific spatial arrangement of factor binding sites. Mol Cell Biol **17:**6321-9.
2. **Barelle, C. J., C. L. Manson, D. M. MacCallum, F. C. Odds, N. A. Gow, and A. J. Brown.** 2004. GFP as a quantitative reporter of gene regulation in Candida albicans. Yeast **21:**333-40.
3. **Blake, W. J., K. A. M, C. R. Cantor, and J. J. Collins.** 2003. Noise in eukaryotic gene expression. Nature **422:**633-7.
4. **Calado, D. P., T. Paixao, D. Holmberg, and M. Haury.** 2006. Stochastic monoallelic expression of IL-10 in T cells. J Immunol **177:**5358-64.
5. **Chytil, M., B. R. Peterson, D. A. Erlanson, and G. L. Verdine.** 1998. The orientation of the AP-1 heterodimer on DNA strongly affects transcriptional potency. Proc Natl Acad Sci U S A **95:**14076-81.
6. **Cleary, M. A., P. S. Pendergrast, and W. Herr.** 1997. Structural flexibility in transcription complex formation revealed by protein-DNA photocrosslinking. Proc Natl Acad Sci U S A **94:**8450-5.
7. **Du, W., D. Thanos, and T. Maniatis.** 1993. Mechanisms of transcriptional synergism between distinct virus-inducible enhancer elements. Cell **74:**887-98.
8. **Elowitz, M. B., A. J. Levine, E. D. Siggia, and P. S. Swain.** 2002. Stochastic gene expression in a single cell. Science **297:**1183-6.
9. **Falvo, J. V., B. S. Parekh, C. H. Lin, E. Fraenkel, and T. Maniatis.** 2000. Assembly of a functional beta interferon enhanceosome is dependent on ATF-2-c-jun heterodimer orientation. Mol Cell Biol **20:**4814-25.
10. **Giese, K., C. Kingsley, J. R. Kirshner, and R. Grosschedl.** 1995. Assembly and function of a TCR alpha enhancer complex is dependent on LEF-1-induced DNA bending and multiple protein-protein interactions. Genes Dev **9:**995-1008.
11. **Hall, J. M., D. P. McDonnell, and K. S. Korach.** 2002. Allosteric regulation of estrogen receptor structure, function, and coactivator recruitment by different estrogen response elements. Mol Endocrinol **16:**469-86.
12. **Hu, J., S. C. Sealfon, F. Hayot, C. Jayaprakash, M. Kumar, A. C. Pendleton, A. Ganee, A. Fernandez-Sesma, T. M. Moran, and J. G. Wetmur.** 2007. Chromosome-specific and noisy IFNB1 transcription in individual virus-infected human primary dendritic cells. Nucleic Acids Res **35:**5232-41.
13. **Karanam, B., L. Wang, D. Wang, X. Liu, R. Marmorstein, R. Cotter, and P. A. Cole.** 2007. Multiple roles for acetylation in the interaction of p300 HAT with ATF-2. Biochemistry **46:**8207-16.
14. **Kim, T. K., T. H. Kim, and T. Maniatis.** 1998. Efficient recruitment of TFIIB and CBP-RNA polymerase II holoenzyme by an interferon-beta enhanceosome in vitro. Proc Natl Acad Sci U S A **95:**12191-6.
15. **Kim, T. K., and T. Maniatis.** 1997. The mechanism of transcriptional synergy of an in vitro assembled interferon-beta enhanceosome. Mol Cell **1:**119-29.
16. **Kurokawa, R., V. C. Yu, A. Naar, S. Kyakumoto, Z. Han, S. Silverman, M. G. Rosenfeld, and C. K. Glass.** 1993. Differential orientations of the DNA-binding

domain and carboxy-terminal dimerization interface regulate binding site selection by nuclear receptor heterodimers. Genes Dev **7:**1423-35.

17. **Kutsch, O., E. N. Benveniste, G. M. Shaw, and D. N. Levy.** 2002. Direct and quantitative single-cell analysis of human immunodeficiency virus type 1 reactivation from latency. J Virol **76:**8776-86.
18. **Masumi, A.** 2011. Histone acetyltransferases as regulators of nonhistone proteins: the role of interferon regulatory factor acetylation on gene transcription. J Biomed Biotechnol **2011:**640610.
19. **Merika, M., A. J. Williams, G. Chen, T. Collins, and D. Thanos.** 1998. Recruitment of CBP/p300 by the IFN beta enhanceosome is required for synergistic activation of transcription. Mol Cell **1:**277-87.
20. **Mettenleiter, T. C., and W. Grawe.** 1996. Video imaging of firefly luciferase activity to identify and monitor herpesvirus infection in cell culture. J Virol Methods **59:**155-60.
21. **Misra, V., S. Walter, P. Yang, S. Hayes, and P. O'Hare.** 1996. Conformational alteration of Oct-1 upon DNA binding dictates selectivity in differential interactions with related transcriptional coactivators. Mol Cell Biol **16:**4404-13.
22. **Munshi, N., T. Agalioti, S. Lomvardas, M. Merika, G. Chen, and D. Thanos.** 2001. Coordination of a transcriptional switch by HMGI(Y) acetylation. Science **293:**1133-6.
23. **Panne, D., T. Maniatis, and S. C. Harrison.** 2004. Crystal structure of ATF-2/c-Jun and IRF-3 bound to the interferon-beta enhancer. Embo J **23:**4384-93.
24. **Ramirez-Carrozzi, V., and T. Kerppola.** 2003. Asymmetric recognition of nonconsensus AP-1 sites by Fos-Jun and Jun-Jun influences transcriptional cooperativity with NFAT1. Mol Cell Biol **23:**1737-49.
25. **Ramirez-Carrozzi, V., and T. Kerppola.** 2001. Gel-based fluorescence resonance energy transfer (gelFRET) analysis of nucleoprotein complex architecture. Methods **25:**31-43.
26. **Raser, J. M., and E. K. O'Shea.** 2004. Control of stochasticity in eukaryotic gene expression. Science **304:**1811-4.
27. **Raser, J. M., and E. K. O'Shea.** 2005. Noise in gene expression: origins, consequences, and control. Science **309:**2010-3.
28. **Remenyi, A., K. Lins, L. J. Nissen, R. Reinbold, H. R. Scholer, and M. Wilmanns.** 2003. Crystal structure of a POU/HMG/DNA ternary complex suggests differential assembly of Oct4 and Sox2 on two enhancers. Genes Dev **17:**2048-59.
29. **Rutter, G. A., M. R. White, and J. M. Tavare.** 1995. Involvement of MAP kinase in insulin signalling revealed by non-invasive imaging of luciferase gene expression in single living cells. Curr Biol **5:**890-9.
30. **Samoilov, M. S., G. Price, and A. P. Arkin.** 2006. From fluctuations to phenotypes: the physiology of noise. Sci STKE **2006:**re17.
31. **Schrader, M., K. M. Muller, S. Nayeri, J. P. Kahlen, and C. Carlberg.** 1994. Vitamin D3-thyroid hormone receptor heterodimer polarity directs ligand sensitivity of transactivation. Nature **370:**382-6.
32. **Schrader, M., S. Nayeri, J. P. Kahlen, K. M. Muller, and C. Carlberg.** 1995. Natural vitamin D3 response elements formed by inverted palindromes: polarity-

directed ligand sensitivity of vitamin D3 receptor-retinoid X receptor heterodimer-mediated transactivation. Mol Cell Biol **15:**1154-61.

33. **Schwabe, J. W., L. Chapman, J. T. Finch, and D. Rhodes.** 1993. The crystal structure of the estrogen receptor DNA-binding domain bound to DNA: how receptors discriminate between their response elements. Cell **75:**567-78.
34. **Scully, K. M., E. M. Jacobson, K. Jepsen, V. Lunyak, H. Viadiu, C. Carriere, D. W. Rose, F. Hooshmand, A. K. Aggarwal, and M. G. Rosenfeld.** 2000. Allosteric effects of Pit-1 DNA sites on long-term repression in cell type specification. Science **290:**1127-31.
35. **Sims, R. J., 3rd, and D. Reinberg.** 2008. Is there a code embedded in proteins that is based on post-translational modifications? Nat Rev Mol Cell Biol **9:**815-20.
36. **Staal, A., A. J. van Wijnen, J. C. Birkenhager, H. A. Pols, J. Prahl, H. DeLuca, M. P. Gaub, J. B. Lian, G. S. Stein, J. P. van Leeuwen, and J. L. Stein.** 1996. Distinct conformations of vitamin D receptor/retinoid X receptor-alpha heterodimers are specified by dinucleotide differences in the vitamin D-responsive elements of the osteocalcin and osteopontin genes. Mol Endocrinol **10:**1444-56.
37. **Thanos, D., and T. Maniatis.** 1995. Virus induction of human IFN beta gene expression requires the assembly of an enhanceosome. Cell **83:**1091-100.
38. **Tomilin, A., A. Remenyi, K. Lins, H. Bak, S. Leidel, G. Vriend, M. Wilmanns, and H. R. Scholer.** 2000. Synergism with the coactivator OBF-1 (OCA-B, BOB-1) is mediated by a specific POU dimer configuration. Cell **103:**853-64.
39. **Tsytsykova, A. V., and A. E. Goldfeld.** 2002. Inducer-specific enhanceosome formation controls tumor necrosis factor alpha gene expression in T lymphocytes. Mol Cell Biol **22:**2620-31.
40. **Voss, T. C., S. John, and G. L. Hager.** 2006. Single-cell analysis of glucocorticoid receptor action reveals that stochastic post-chromatin association mechanisms regulate ligand-specific transcription. Mol Endocrinol **20:**2641-55.
41. **Wathelet, M. G., C. H. Lin, B. S. Parekh, L. V. Ronco, P. M. Howley, and T. Maniatis.** 1998. Virus infection induces the assembly of coordinately activated transcription factors on the IFN-beta enhancer in vivo. Mol Cell **1:**507-18.
42. **White, M. R., M. Masuko, L. Amet, G. Elliott, M. Braddock, A. J. Kingsman, and S. M. Kingsman.** 1995. Real-time analysis of the transcriptional regulation of HIV and hCMV promoters in single mammalian cells. J Cell Sci **108 (Pt 2):**441-55.
43. **Xu, E. Y., K. A. Zawadzki, and J. R. Broach.** 2006. Single-cell observations reveal intermediate transcriptional silencing states. Mol Cell **23:**219-29.
44. **Yang, H., G. Ma, C. H. Lin, M. Orr, and M. G. Wathelet.** 2004. Mechanism for transcriptional synergy between interferon regulatory factor (IRF)-3 and IRF-7 in activation of the interferon-beta gene promoter. Eur J Biochem **271:**3693-703.
45. **Yie, J., K. Senger, and D. Thanos.** 1999. Mechanism by which the IFN-beta enhanceosome activates transcription. Proc Natl Acad Sci U S A **96:**13108-13.